Digital Ear Scanner:

Measuring the Compliance of the Ear

by

Daniel Hernandez-Stewart

B.S. Mechanical Engineering

Massachusetts Institute of Technology, 2007

SUBMITTED TO THE DEPARTMENT OF MECHANICAL ENGINEERING IN PARTIAL FULFILLMENT OF THE REQUIREMENTS FOR THE DEGREE OF

MASTER OF SCIENCE IN MECHANICAL ENGINEERING

AT THE

MASSACHUSETTS INSTITUTE OF TECHNOLOGY

FEBRUARY 2010

Signature of Author: .....

Department of Mechanical Engineering

January 28, 2010

Certified by: .....

Doug Hart

Professor of Mechanical Engineering

Thesis Supervisor

Accepted by: .....

David E. Hardt

Professor of Mechanical Engineering

Table of Contents

Listing of Figures and Tables

Nomenclature

$\alpha(\lambda)$	camera sensitivity to a given wavelength
C	effective two dye molar concentration
C_1	dye one molar concentration
C_2	dye two molar concentration
dV	differential volume of fluid
dI_f	differential element fluorescence
$\varepsilon(\lambda)$	molar absorption coefficient for a given dye and wavelength
I_e	excitation illumination intensity
I_o	excitation illumination intensity constant (intensity at x=0)
λ	wavelength of light
λ_{rmin}	smallest wavelength that passes through red filter of rgb camera
λ_{rmax}	largest wavelength that passes through red filter of rgb camera
λ_{gmin}	smallest wavelength that passes through green filter of rgb camera
λ_{gmax}	largest wavelength that passes through green filter of rgb camera
η	dye's relative emission at give wavelength
ξ	monitoring efficiency
Φ	quantum efficiency
R	intensity of red/green
x	fluid film thickness

Digital Ear Scanner:

Measuring the Compliance of the Ear

by

Daniel Hernandez-Stewart

Submitted to the Department of Mechanical Engineering

on January 28, 2010 in partial fulfillment of

the requirements for the degree of Master of Science in

Mechanical Engineering

Abstract

This paper seeks to resolve the biggest problem with hearing aids, their physical fit. By digitally scanning the ear canal and taking the dynamics of the ear into account the performance and comfort of a hearing aid can be greatly improved. Current optical techniques for 3-D imaging are too expensive to be implemented in the ear canal for the purpose of custom fitted hearing aids. A new absorption based optical technique is introduced, which is capable of generating three dimensional maps of an ear subjected to a varying pressure. Specifically a hearing aid can be constructed with allowances for the compliance of the ear and the distortions associated with jaw movement. It is shown that the information that can be captured with this new technique will be of value toward improving hearing aids, and that the hearing aid industry is ready to take advantage of a digital scanner. A one dimensional calibration was made, and qualitative 3-D data is shown. The imaging technique was implemented with much lower cost equipment then would be needed by other 3-D techniques such as interferometry. A technique for the laboratory manufacture of brushed on fluorescent balloons was presented that are suitable to be used by this imaging technique to measure the dynamics of the ear. The bulk compliance of a human ear in vitro was measured with a laboratory fabricated balloon.

Thesis Supervisor: Doug Hart

Title: Professor Mechanical Engineering

1. Introduction

This paper seeks to resolve the biggest problem with hearing aids, their physical fit. By digitally scanning the ear canal and taking the dynamics of the ear into account the performance and comfort of a hearing aid can be greatly improved. Current optical techniques for 3-D imaging are too expensive to be implemented in the ear canal for the purpose of custom fitted hearing aids. A new absorption based optical technique is introduced, which is capable of generating three dimensional maps of an ear subjected to a varying pressure. It is possible to capture the dynamics of the ear in 3-D video and design a hearing aid that takes them into account. Specifically a hearing aid can be constructed with allowances for the compliance of the ear and the distortions associated with jaw movement. Additionally the development of a balloon fabrication methodology, which is necessary to implement the optical technique, is described as well as a simple method for measuring the bulk compliance of an ear. It is shown that the information that can be captured with this new technique will be of value toward improving hearing aids, and that the hearing aid industry is ready to take advantage of a digital scanner.

1.1 Motivation

Unlike glasses and contact lenses hearing aids have a social stigma attached to them. The problem with hearing aids is that they do not provide as robust a solution to hearing problems as exists for vision problems. Contacts, glasses, and laser eye surgery can restore almost perfect sight to all but the most visually impaired. These solutions have comfort, aesthetic, convenience, and cost tradeoffs that can fulfill the most demanding

of customers. Future fighter pilots, embarrassed teenagers, and aging retirees can all be satisfied by existing vision correction options.

In contrast hearing aids do not restore perfect hearing, run out of batteries, are considered unsightly, can be uncomfortable, fall out, and have a multitude of other issues. They are not main stream enough to be covered by most insurance even though hearing trouble is more prevalent than vision trouble. According to the National Center for Health Statistics [1], the percentage of American adults with hearing trouble, 17%, is significantly more than that than the percentage of adults with vision trouble, 11%. This percentage is likely to continue to rise because of noise induced hearing loss and an aging population.

In his "Hearing Aid Physical Fit: The Next Revolution," David Fabry [2] outlines the potential benefit of a digital scanner.

> The most obvious way that digital technology may shift the paradigm is by ultimately eliminating the need for earmold impressions via direct ear scanning. The use of the 3D scanner may permit earmold/shell characteristics to be transmitted electronically to the manufacturer. Digital mechanics may be used to quantify and compensate for dynamic properties of the cartilaginous portion of the ear canal; this, in turn, will improve user comfort and reduce hearing aid feedback. Direct ear scanning may eliminate the need for earmold impressions. Digital mechanics may permit hearing aid acoustic characteristics to be assessed, modified, and optimized for individual ears. [2]

Other professionals are making similar hopeful statements, such as the editor of the Hearing Journal, David H. Kirkwood [3], in his article, "The Bright Promise of Direct Ear Scanning." Professionals in the hearing aid industry are eager to replace impression with direct ear scanning.

1.2 Current Problems with Hearing Aids

In order to ensure that a digital scanner could improve hearing aids it is necessary to examine the current issues with hearing aids. The various issues with hearing aids, most importantly performance, comfort, and background noise, have led to an all time low market penetration of 20.4% [4]. This low number arises from the fact that hearing aids are not effectively meeting the needs of the hearing impaired, and have not gained enough status to be widely covered by insurance. Kochkin's survey of 2720 hearing aid owners seeks the answer to the problem why "hearing aids are in the drawer." [4] His content analysis of the 348 letters received from owners of hearing aids who do not use them is shown in table 1.1.

Rank	Stated reason for not wearing hearing aids	Number of mentions	Percent of respondents	Estimated number of hearing aid owners
1	Poor benefit from hearing aids	103	29.6%	268,510
2	Background noise/noisy situations	88	25.3%	229,407
3	Fit & comfort	65	18.7%	169,448
4	Negative side effects of H.A.	38	10.9%	99,062
5	Price & cost of repairs	36	10.3%	93,848
6	Don't need help	28	8.0%	72,993
7	Hearing aid is broken	27	7.8%	70,386
8	Sound quality is poor	22	6.3%	57,352
9	Unspecified - do not wear	21	6.0%	54,745
10	Volume control adjustment	17	4.9%	44,317
11	Whistling and feedback	15	4.3%	39,103
12	Nuisance/hassle/annoying	14	4.0%	36,497
13	Poor service from dispenser	11	3.2%	28,676
14	High-frequency loss not helped	10	2.9%	26,069
15	Stigma of wearing hearing aids	10	2.9%	26,069
16	Work in limited situations	9	2.6%	23,462
17	Profound hearing loss not helped	9	2.6%	23,462
18	Too loud	8	2.3%	20,855
19	Battery life too short	7	2.0%	18,248
20	Forget to use	4	1.1%	10,428
21	Does not work on phone	4	1.1%	10,428
22	Monaural aids inadequate	3	0.9%	7,821
23	Oversold expectations	3	0.9%	7,821
24	Have tinnitus	3	0.9%	7,821
25	Family pressure led to purchase	3	0.9%	7,821
26	Manual dexterity	2	0.6%	5,214
27	Rare social user	2	0.6%	5,214
28	Feel like earplugs	1	0.3%	2,607
29	Poor directivity	1	0.3%	2,607
30	Gain is too low	1	0.3%	2,607
31	Can not find them	1	0.3%	2,607
32	Ear wax problem	1	0.3%	2,607

Table 1.1: Tabulated content analysis of the 348 letters received from owners of hearing aids who do not use them. Most complaints can divided up into poor performance, comfort, and increased background noise. [4]

A majority of complaints are related to performance or comfort. The most common complaint given is that the hearing aid has little benefit (29.6%). Additional performance related complaints included poor sound quality (6.3%) and feedback (4.3%). The second most prevalent issue for consumers, comfort, is the chief complaint for over a quarter of the population: 18.7% of consumers said fit and comfort specifically is their biggest issue with their hearing aid, and 10.9% cited negative side effects including blisters, rashes, itching, headaches, infections, problems chewing or swallowing, too much pressure. [4] It is not hard to see why hearing aid owners discontinue use given either poor performance of discomfort.

Comfort and performance are coupled are coupled by physical fit. To prevent leaking and feedback hearing aids need to create a seal in the ear canal. The correct amount of uniform pressure needs to be put on the surrounding tissues to create a seal and anchor the hearing aid to the ear without causing discomfort. A bad seal allows sound to leak past the hearing aid and mix out of phase, which degrades sound quality. Degrading sound quality requires higher amplification which requires more power and can decrease the efficacy of the hearing aid in background noise. The two most egregious problems consumers have with hearing aids ultimately are the result of a poorly fitting physical shell.

Complaints of increased background noise (25.3%), which are largely dependent on the users cognitive processing of sound, cannot be solved completely by improving fit. [4] Without a very large improvement in signal processing, hearing aids cannot hope to replace the brain's sound signal processing abilities. This problem is very frustrating for the hearing impaired, as the hearing aid amplifies both the signal and the background noise leaving them unable to hear in noisy environments.

This noteworthy difficulty is not addressed by the methods developed in this paper, but much progress can be made in improving hearing aids before this more complex problem is resolved. The most important problem with hearing aids is physical fit, which the new scanning technique is capable of solving. The next section explores the size and the makeup of the hearing loss problem.

1.3 Demographics and Market

In order to understand the magnitude and composition of the hearing loss problem a brief study of demographics of hearing loss and the hearing aid market will be made in this section. In this study the following information will be considered: demographics, noise induced hearing loss, hearing aid adoption rates, hearing aid costs, number of hearing aids sold annually, growth, severity distribution, and types of hearing aids. A breakdown of hearing loss by sex, age, marital status, and education take from the National Center for Health Statistics is given in the table 1.2.

Total		16.8	**Sex**	Male	19.4
Income	Less than $20,000	20.9		Female	14.6
	$20,000 or more	16	**Age**	18–44	7.6
	$20,000–$34,999	18.7		45–64	19.4
	$35,000–$54,999	17.5		65–74	31.9
	$55,000–$74,999	16		over 75	50.4
	$75,000 or more	14.2	**Marital Status**	Married	17.8
Education	Less than a high school diploma	22		Widowed	39
	High school diploma or GED	19.3		Divorced Or Separated	18.7
	Some college	19.6		Never Married	8.3
	Bachelor's degree or higher	14.7		Living With a Partner	12.3

Table 2.2: 2006 hearing loss statistics by sex, age, marital status, and education taken from NCHS (National Center for Health Statistics). [1]

Many are aware that hearing worsens with age, but are unaware that over 50% percent of those over seventy five suffer from hearing loss. The effects of marital status can most likely be explained by correlation with age. For example, the group of widowed people is made up of older people on average than the married group. The effects of

sex, income, and education are smaller, but not negligible. Males with a poor education, and low income are the most prone to hearing loss.

The trends that are independent of age can be explained in part by noise induced hearing loss. According to the National Institute of Deafness and other Communication Disorders [5], NIDCD, "15 percent of Americans between the ages of 20 and 69 or 26 million Americans have high frequency hearing loss that may have been caused by exposure to loud sounds or noise at work or in leisure activities." Industrial hearing loss and lack of education concerning recreational noise is likely to be responsible for the trends of increased hearing loss in males and those with lower income or poor education. Many jobs that involved operating heavy noisy industrial equipment are held by poorly educated males. Noise induced hearing loss has gained more notoriety, which has recently led industry to respond to it with increased hearing protection. According to David H. Kirkwood [6], the military is associated with a large portion of hearing loss, with the Department of Veterans Affairs (VA) purchasing 16% of hearing aids in 2008. Additionally the number of VA purchased hearing aids went up by 9.2% between the third quarter of 2008 and 2007, while total hearing aid purchases declined 1.2%.

A very important characteristic of the hearing aid market is the market penetration, or the adoption rates. The overall adoption rate of approximately one fifth is indicative of hearing aids providing a poor solution to hearing impairment. Historical data for hearing instrument adoption rates broken down by sex, age, education, household income, employment status, metro size, and life stage is shown in the table below taken from Sergei Kochkin's [7] "MarkeTrak VII report. : Hearing Loss Population Tops 31 Million."

	Hearing Instrument Adoption Rates (%)						
	1984	1989	1991	1994	1997	2000	2004
	(n=1,206)	(n=7,340)	(n=13,487)	(n=11,996)	(n=14,931)	(n=16,681)	(15,497)
By Sex							
Male	24.5%	19.5%	22.4%	21.4%	21.3%	22.3%	22.2%
Female	22.7%	22.0%	22.7%	21.3%	19.3%	21.1%	23.8%
By Age group							
<18 yrs				9.1%	13.9%	12.8%	12.5%
18-34 yrs	10.7%	9.6%	6.5%	5.3%	5.8%	6.7%	10.9%
35-44 yrs	6.1%	6.3%	7.5%	7.9%	5.5%	8.2%	6.7%
45-54 yrs	12.4%	9.9%	12.8%	11.6%	9.8%	9.5%	9.7%
55-64 yrs	22.4%	16.3%	20.9%	21.0%	18.7%	17.2%	16.7%
65-74 yrs	34.0%	32.7%	34.4%	35.3%	33.2%	32.6%	31.3%
75-84 yrs	45.6%	45.0%	47.1%	44.0%	45.6%	45.7%	44.1%
85 + yrs	58.6%	51.9%	56.1%	45.6%	56.3%	59.4%	60.6%
By Household income							
Less than $10K	32.6%	27.7%	28.2%	25.1%	25.4%	24.7%	24.0%
$10-19k	26.3%	25.5%	27.6%	27.1%	26.3%	26.4%	26.8%
$20-29k	19.5%	25.4%	24.1%	23.3%	22.3%	25.9%	25.9%
$30-39k	16.1%	19.6%	19.5%	20.0%	16.8%	22.4%	25.2%
$40-49k	20.4%	19.5%	17.4%	16.3%	15.1%	18.7%	23.6%
$50-59k	20.2%	17.9%	19.5%	17.4%	17.2%	20.1%	23.5%
$60k +	19.5%	19.3%	19.0%	16.3%	17.7%	18.7%	20.3%
By Educational level*							
Some elementary				33.7%	34.8%	33.4%	25.7%
Elementary degree	36.8%	31.9%	35.1%	27.4%	26.2%	24.2%	23.4%
High school (some)	32.0%	25.9%	26.8%	22.1%	21.0%	23.1%	23.8%
High school degree	21.0%	20.4%	22.6%	18.5%	18.9%	21.2%	22.6%
College (some)	20.9%	17.4%	19.3%	18.0%	15.7%	14.8%	17.5%
College degree	22.5%	19.9%	19.6%	19.2%	20.0%	21.5%	21.9%
College (post graduate)	21.4%	19.4%	23.5%	20.8%	18.9%	23.8%	24.5%
By Employment category*							
Full time employment	13.4%	10.6%	11.3%	10.5%	9.8%	10.4%	10.1%
Part time employment	21.2%	16.8%	18.8%	18.4%	17.9%	18.5%	20.2%
Unemployed	20.2%	17.0%	15.2%	15.1%	14.2%	14.2%	16.2%
Retired	36.3%	36.2%	37.2%	37.4%	37.4%	37.6%	37.7%
By Metro size							
Less than 50k	24.2%	22.9%	21.4%	19.6%	18.7%	20.4%	20.0%
50k-499k	22.3%	21.6%	22.2%	20.2%	19.5%	21.1%	21.0%
500k-1.99 mil.	25.2%	24.0%	22.3%	23.7%	21.0%	22.2%	25.2%
2 mil. and above	23.2%	24.8%	24.0%	22.1%	21.8%	23.7%	24.8%
By Lifestage							
Roomates	18.5%	16.6%	18.9%	15.7%	11.2%	21.1%	18.8%
Singles - young	12.4%	16.4%	14.3%	11.6%	12.5%	13.4%	17.4%
- middle	13.5%	19.2%	20.9%	16.3%	15.7%	17.6%	17.7%
- older	41.2%	45.8%	45.7%	43.2%	44.2%	44.9%	47.0%
Couples - young	7.0%	19.0%	13.0%	11.6%	10.8%	13.2%	11.3%
- working older	23.6%	23.7%	25.7%	24.0%	21.7%	20.3%	21.3%
- retired	35.7%	36.6%	37.0%	36.0%	35.7%	37.0%	36.2%
Parents - young	10.3%	9.8%	7.5%	7.6%	6.9%	7.8%	8.9%
- middle	7.7%	13.1%	8.9%	7.7%	6.4%	8.2%	9.4%
- older	19.6%	19.6%	17.8%	15.7%	15.0%	15.1%	17.5%

Table 3.3: Hearing aid adoption rate statistics from MarkeTrak VII. [7] Overall adoption rates have held steady at approximately one fifth of the impaired population.

The overall adoption rate has held steady over this time span at approximately twenty percent of the hearing impaired population. Adoption rates increase dramatically with age. This trend is most likely a result of the severity of the hearing loss. Besides age related effects life stage and employment status appear to have little effect on adoption rates. Adoption rates also appear independent of the size of the metro area. The effect of income and education are becoming less important factors in hearing aid adoption. However the adoption rates among the poorest and worst educated have fallen from

over 30% to only slightly higher than average at approximately 25%. Higher than average past adoption rates among the poor and uneducated and are not normal for a well functioning expensive medical device. This oddity might be explained by changes in hearing aid benefit coverage, increased hearing aid cost, or improved access to hearing testing.

Given the lack of widely available insurance coverage for hearing aids, cost might be expected to be more of an issue. The wealthy could be more sensitive to the social stigma associated with hearing aids. If current hearing aids were a good solution to the hearing loss problem one would expect significantly more overall market penetration, especially for those whom money was not an issue. Even though the price of a hearing aid does not seem central to adoption rates, it is important in characterizing the hearing aid market. The out of pocket expense of hearing aids as well as the percent covered by third parties is shown in the table 1.4, taken from Kochkin's report.

	1984	1989	1991	1994	1997	2000	2004
Price of hearing aids (retail)	*(n=428)*	*(n=417)*	*(n=493)*	*(n=557)*	*(n=498)*	*(n=561)*	*(n=518)*
Third-party payments (%) - w/o VA	22.2%	19.4%	17.7%	20.8%	24.7%	24.8%	21.9%
Third-party payments (%) - with VA		23.5%	21.7%	25.6%	30.2%	34.0%	37.3%
Average out-of-pocket price to consumer *(Exluding VA fittings)*	$501	$623	$680	$735	$917	$1,276	$1,369
By type of hearing aid----------							
BTE		$557	$581	$779	$852	$1,215	$1,514
ITC		$742	$810	$790	$1,040	$1,434	$1,361
ITE		$621	$681	$673	$768	$1,097	$1,306
Hearing instrument distribution (Purchases this period)	*(n=428)*	*(n=356)*	*(n=493)*	*(n=653)*	*(n=537)*	*(n=593)*	*(n=503)*
By perceived profession----------							
Audiologist	22.0%	48.4%	46.1%	49.3%	53.6%	65.0%	55.0%
Hearing aid specialist	66.4%	46.6%	49.8%	44.7%	43.4%	28.8%	35.9%
Medical doctor	4.8%	1.5%	1.2%	1.9%	1.3%	2.1%	2.0%
Other	6.9%	3.6%	2.9%	4.1%	1.7%	4.1%	7.1%
By Source of distribution----------							
Hearing aid specialist office*	48.7%	30.0%	35.5%	31.1%	30.5%	22.2%	37.0%
Audiologist's office	21.3%	35.8%	36.5%	40.9%	41.3%	47.2%	24.9%
Clinic		5.2%	1.4%	1.9%	2.0%	3.0%	1.6%
Hospital		2.1%	2.2%	2.2%	2.6%	1.5%	1.4%
Ear doctor's office	5.0%	14.5%	5.5%	7.6%	7.1%	7.1%	8.6%
Family doctor's office	0.3%	1.3%	0.2%	0.6%	4.0%	0.2%	0.6%
Veterans Administration		1.8%	2.4%	3.4%	4.5%	8.4%	14.9%
Mail order	2.1%	3.0%	0.8%	2.5%	0.9%	3.5%	5.4%
Department store	2.4%	3.2%	4.7%	2.2%	2.4%	2.4%	0.6%
Home	6.3%	8.4%	7.3%	4.4%	3.7%	2.0%	0.8%
Military installation		2.5%	1.4%	1.4%	1.1%	1.0%	1.0%
Wholesale club							2.0%
Other	15.0%	1.7%	2.0%	1.9%	3.4%	1.5%	1.4%

Table 4.4: The out of pocket price per hearing aid and point of purchase from 1984-2004 The price has been rising steadily. [7]

The out of pocket price of a hearing aid has been on the rise. While the percent paid for by third parties excluding veterans' affairs has been steady, the percent Veteran's Affairs (VA) has been responsible for has had a dramatic increase. VA is now responsible for 14.9% of the hearing aids distributed. Most hearing aids are purchased from audiologists and hearing aid specialists, but new sources such as whole sale clubs have begun to distribute them.

Another important piece of the hearing aid market is the number of units sold. The size of the hearing aid market in terms of units is shown in the figure 1.1 that comes from David H. Kirkwood's [6] report, "Economic turmoil threatens to reverse recent growth in the hearing aid market."

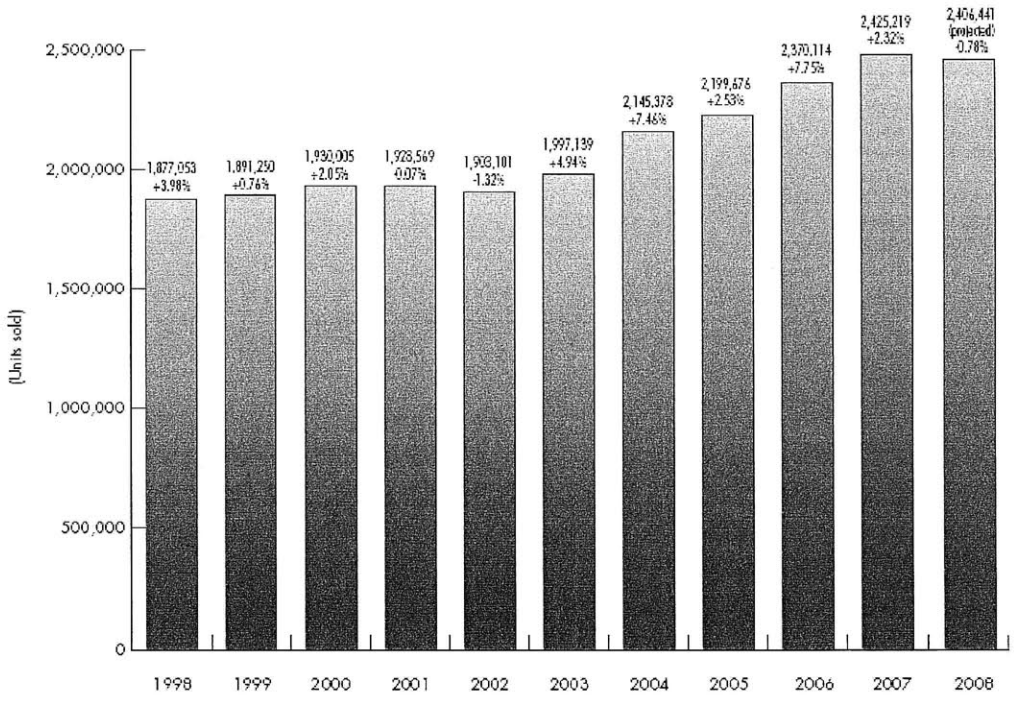

Figure 1.1: The units of hearing aids sold per year. [6]

The number sold was fairly steady from 1998 through 2003 at approximately 1.9 million units. From 2004-2008 this number grew to 2.4 million units. Current hearing aid market projections include significant growth, because the number of people affected by hearing loss is expected to rise. Projections for the growth of the incidence of hearing loss are shown in figure 1.2, taken from Kochkin's report.

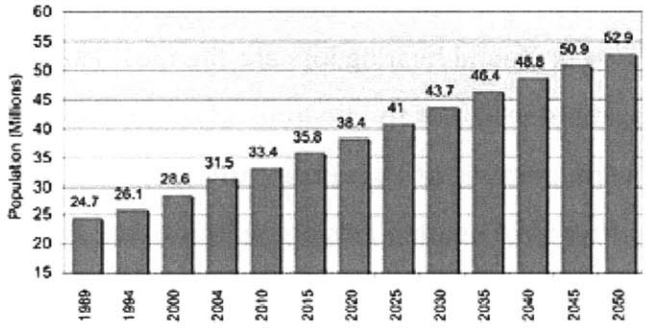

Figure 1.2: Number of hearing impaired, includes future projection based on US census population projections coupled with hearing loss by age group. [7]

The US census projects a steadily aging population. The hearing aid market is expected to grow significantly, because of this projection combined with the correlation between healing loss and age. The expected growth of the problem makes improving hearing aids even more important. As the population ages, severe hearing loss will also increase.

The severity of hearing impairment determines the reduction in quality of life, and the likelihood that an individual will seek out a solution. In the table below taken from Karl E. Strom's [9] "HR 2006 Dispenser Survey" statistics concerning hearing aid clients' level of hearing loss are shown.

	HIS	DA	Average
Mild (<40 dBHL)	14% (12%)	18% (15%)	16% (14%)
Moderate (40-70 dBHL)	52% (50%)	54% (55%)	53% (52%)
Severe (70-90 dBHL)	25% (30%)	21% (23%)	23% (26%)
Profound (>90 dBHL)	9% (8%)	7% (7%)	8% (8%)

Table 1.5: Hearing loss levels from Hearing Instrument Specialists (HIS) and Dispensing Audiologists (DA) clients in 2005 and (2004). [8]

People with severe and profound hearing loss are the most likely to seek out a solution, and make up approximately 30% of the hearing impaired. Mild and moderate hearing loss is often coped with, because of the current utility of hearing aids. Given a level of hearing loss different types of hearing aids are appropriate. Breaking the market down by hearing aid type gives insight into the needs of the hearing impaired. The main types are shown in the figure below, taken from National Institute on Deafness and Other Communication Disorders NIDCD [9].

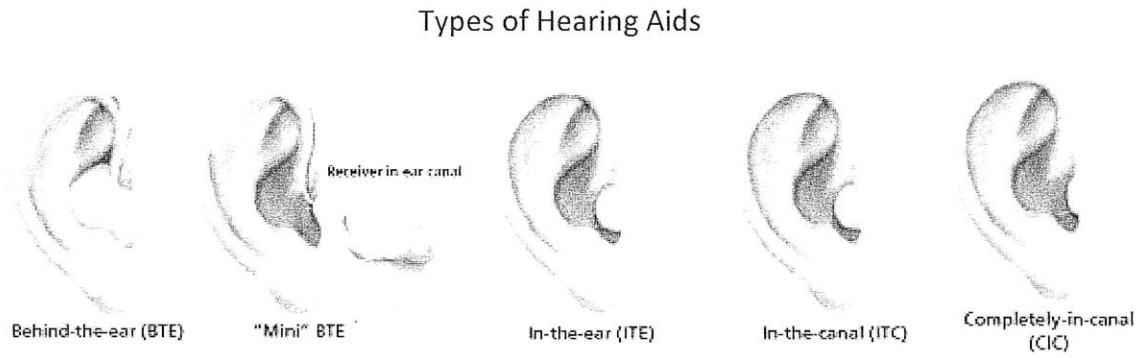

Figure 1.3: 5 main types of Hearing Aids [9].

Behind the ear hearing aids are best suited for those with severe hearing loss or low price needs, as they can provide large batteries and gains or economic electronics. In general as the hearing aids become smaller and deeper in the canal, they become more expensive, as the electronics need to be higher end. However, these hearing aids can have more problems with feedback because they have a shorter distance and as such time delay between input and output. In addition, the deeper impressions and shells go

into the sensitive bony region of the ear, which requires tighter tolerances to assure comfort without allowing sound to leak. An improved fitting technique could make deeper fitting impressions higher performance and more comfortable. Deeper in the canal sound transmission can be done more efficiently, reducing power requirements.

Studies like "The Hearing Aid Effect 2005: A Rigorous Test of the Visibility of New Hearing Aid Styles" by Johnson et all, [10] have studied the stigma against hearing aids in depth. The more noticeable the hearing aid the worse the stigma attached to it. The low visibility of smaller deeper fitting hearing aids is valuable to consumers. As hearing aid technology improves it is expected that the footprint of the electronics will continue to decrease. However, the progression to smaller deeper fitting hearing aids could be held up by the current impression based fitting process

An alternative to these four types of custom fit hearing aids, all of which require a custom impression, is the "mini" BTE or open fit hearing aid. The open fit hearing aids have been gaining popularity. In a survey by Earl E. Johnson [11] of 418 audiologists, 41.6% of hearing aids sold were mini open fit behind the ear devices. Customers like open fit hearing aids because they can walk out of the audiologist's office with one after their first visit, and they mitigate problems like occlusion, jaw movement, and poor retention (problems which will be explained further later). Additionally, open fit hearing aids save audiologist times by not requiring an impression, but are only suitable for minor and moderate hearing loss (less than 65 DB), because of the open path for feedback. The demand for hearing aids by type is taken from Kirkwood [6] and shown in table 1.6.

TYPE	UNITS SOLD 2008 (Jan.-Sept.)	% OF ALL INSTRUMENTS SOLI 2008	2007	2006
Completely-in-the-canal (CIC) analog	4053	0.2%	0.9%	0.6%
CIC digital signal processing (DSP)	158,784	8.6%	8.9%	10.2%
All CIC	**162,837**	**8.8%**	**9.8%**	**10.8%**
In-the-canal analog	7905	0.4%	1.1%	1.1%
In-the-canal DSP	186,842	10.1%	11.3%	13.3%
All in-the-canal	**194,747**	**10.6%**	**12.4%**	**14.4%**
Half-shell in-the-ear (ITE) analog	3221	0.2%	0.5%	0.3%
Half-shell ITE DSP	132,318	7.2%	7.0%	8.4%
All half-shell ITE	**135,539**	**7.3%**	**7.5%**	**8.7%**
Full-shell analog ITE	23,671	1.3%	2.4%	2.4%
Full-shell DSP ITE	266,342	14.4%	15.0%	17.9%
All full-shell ITE	**290,013**	**15.7%**	**17.4%**	**20.3%**
Other ITE analog	5073	0.3%	0.7%	0.8%
Other ITE DSP	14,362	0.8%	0.8%	1.1%
All other ITE	**19,435**	**1.1%**	**1.5%**	**1.9%**
Total ITE analog	**43,923**	**2.4%**	**5.6%**	**5.2%**
Total ITE DSP	**758,648**	**41.0%**	**43.0%**	**50.9%**
All ITEs	**802,571**	**43.5%**	**48.6%**	**56.1%**
Behind-the-ear (BTE) analog	21,213	1.1%	2.5%	3.1%
BTE DSP	1,021,084	55.3%	48.9%	40.8%
Total BTE	**1,042,297**	**56.5%**	**51.4%**	**43.8%**
Total all styles analog	**65,136**	**3.5%**	**8.1%**	**8.3%**
Total all styles digital	**1,779,732**	**96.5%**	**91.9%**	**91.7%**
Total all styles	**1,844,868**	**100.0%**	**100.0%**	**100%**

Table 1.6: Relative demand for various types of hearing aids 2006 -2008. [6]

The most important trend illustrated in the figure above is a rise in BTE demand, which comes mostly from growth in the market for open fit hearing aids. The number of open fit versus regular fit can be tracked by evaluating the batteries the BTE's were equipped with. In 2007 they made up 37.2% of the BTE hearing aids sold, and in Q1-Q3 of 2008 they made up 42.2% of the BTE hearing aids. [6] Open fit hearing aids were responsible for 2.5% growth in the total market on their own. They have lead to a reduction in the market share of all the other hearing aids. The hearing aid that has lost the most ground is the ITE, in the trend towards miniaturization. Hearing aids are also becoming increasing digital, with analog devices down by more than a 50% is just a single year.

To help finish quantifying the market presence of these different styles the average price of low end, middle end, and high end BTE (behind the ear), mBTE(mini behind the ear), ITE (in the ear), ITC (in the canal), and CIC (completely in the canal) are shown in the figure below taken from Earl E. Johnson's [12] dispenser survey report, "Despite having more advanced features, hearing aids hold line on retail price."

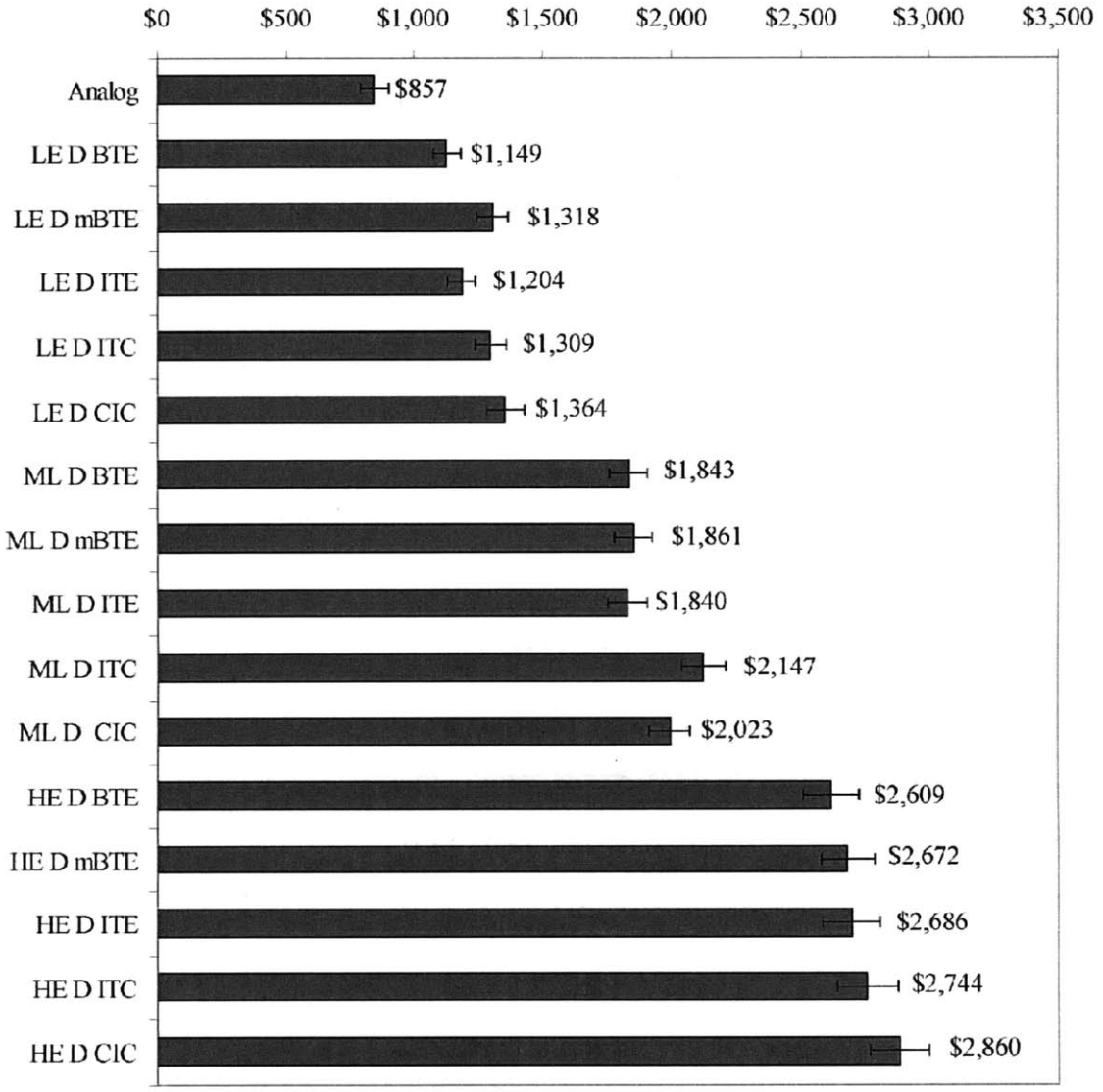

Figure 1.4: 2007 average reported prices of BTE (behind the ear), mBTE(mini behind the ear), ITE (in the ear), ITC (in the canal), and CIC (completely in the canal) by low end (LED), middle end (MLD) and high end (HED) with 95% confidence intervals. [12]

In general as shown above smaller hearing aids are more expensive, with CIC being the smallest and most expensive and the BTE being the largest and cheapest. The gap between low and high end is nearly a factor of 3 for a given type of hearing aid.

The most important point to take away from this section is that the hearing loss problem is big and growing. The existing solutions are unsatisfactory to a larger percentage of the affected population. Open fit hearing aids provide a good solution for many who have moderate hearing loss and their introduction has caused a lot growth. An improvement to fitted hearing aids would most likely lead to similar growth, and pave the way towards less visible, more comfortable, better performing hearing aids. Those who have purchased open fitted hearing aids will eventually need a custom fitted one that is just as functional. It is not just Fabry [2] and Kirkwood [3] calling for an improvement in fitting techniques, the market is as well. Now that the market has been characterized and shown favorable to the proposed technology, the next section will turn its attention to the traditional fitting technique of hearing aids.

1.4 Traditional Manufacturing Procedure

The current approach to fitting for both traditional and digital manufacture is based on injecting a deformable setting substance, often silicone based into the ear. It is a process that requires significant skill, thirty minutes of an audiologist's time, can cause significant discomfort to the patient, and is shown below in figure 1.5.

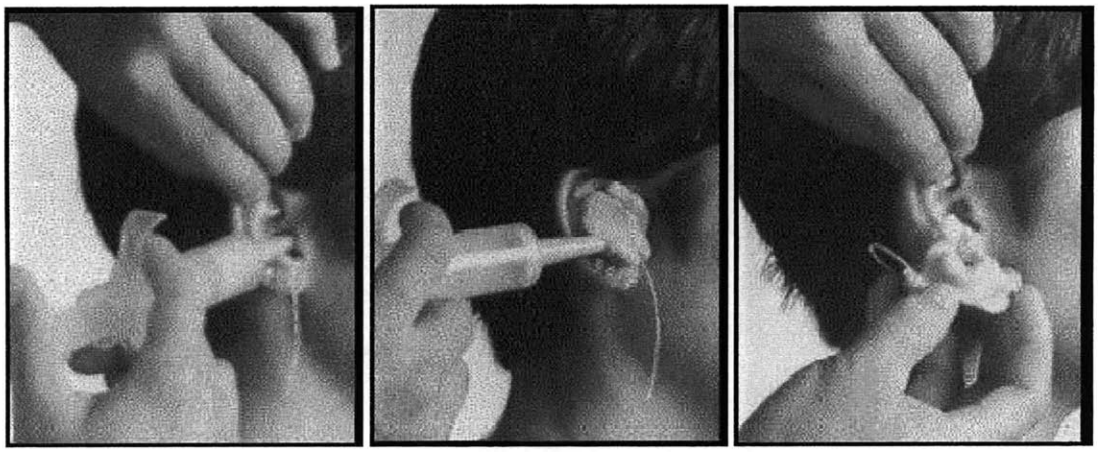

Figure 1.5: The injection of impression material into an ear, and the removal of the impression.

Before the silicone can be injected any excess hair must be removed and the ear must be cleaned of wax. A foam plug is then placed deep in canal to protect ear drum. The impression material is mixed and put in large syringe. The syringe is used to skillfully fill the ear with resin in order to make a good impression. Ten minutes later, after the material has hardened the impression is popped out, sometimes painfully. The whole process is sometimes uncomfortable for the patient. Every audiologist has their own methodology, concerning what type of silicone to use, how to fill the ear with resin, and what position to put the patient's mouth in.

This complicated manual procedure has a poor track record with quality control. In discussions with manufacturers it was learned that as many as 30% of hearing aids need to be remade, because they do not fit the user properly. The impression process is variable, but even when the impression is made well the hearing aid can fit poorly because of un-captured dynamics. Too tight of a fit can be painful, while too loose of a fit will lead the hearing aid to fall out and add undesired acoustic effects.

Creating a hearing aid from this impression traditionally requires significant post processing. The impression is coated with wax to reduce surface imperfection and to give the extra material needed for a seal, a reverse mold is produced (investment

casting) and in this mold the final shell material is poured. The detailed steps in traditional manufacture are outlined by Richard Corte et all, [13] in figure 1.6.

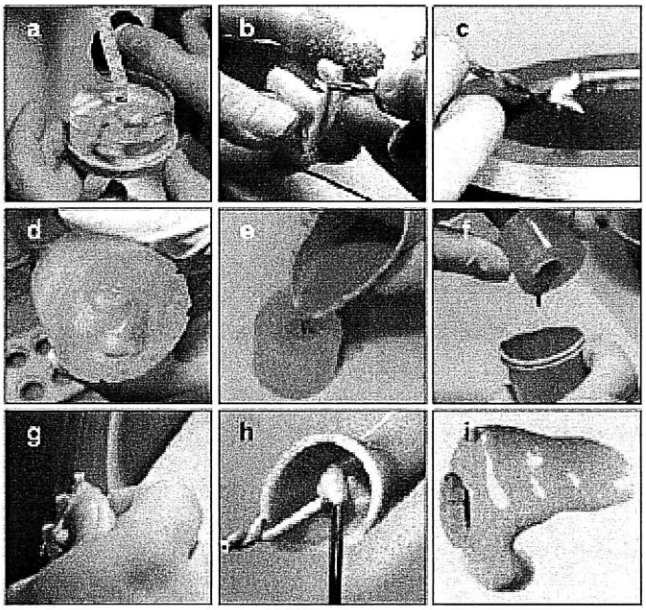

Figures 1.6a-i. The 9 steps in making a conventional hearing aid shell (prior to assembling electronic components): a) A cast of the impression is made; b) The ear impression is trimmed to the model size; c) The impression is dipped in wax; d) A hydrocolloid cast of the impression; e) Acrylic resin is poured into the hydrocolloid cast; f) Excess acrylic resin is drained from the hydrocolloid cast; g) The faceplate end of the shell is trimmed; h) The vent is laid into the shell; i) The finished shell is ready for electronics. [13]

The majority of shells are made by this fully manual process, and as a result the quality of the fit depends largely on the skill of the technician who acts almost as an artisan. This process is time, labor and therefore cost intensive.

Hearing aids often include vents to allow moisture to escape the ear and reduce low frequency booming. A loose fit acts as a vent, but of an uncontrolled, sometimes very large size. In an 8mm canal an uncontrolled vent can be quite large compared to a normal vent, 1-2 mm in diameter. The frequency response of different size vents in figure 1.7 illustrates the effect an uncontrolled vent could have, taken from Stuart et all,

[14] "The effect of venting on in-the-ear, in-the-canal, and completely in-the-canal hearing aid shell frequency responses: real-ear measures."

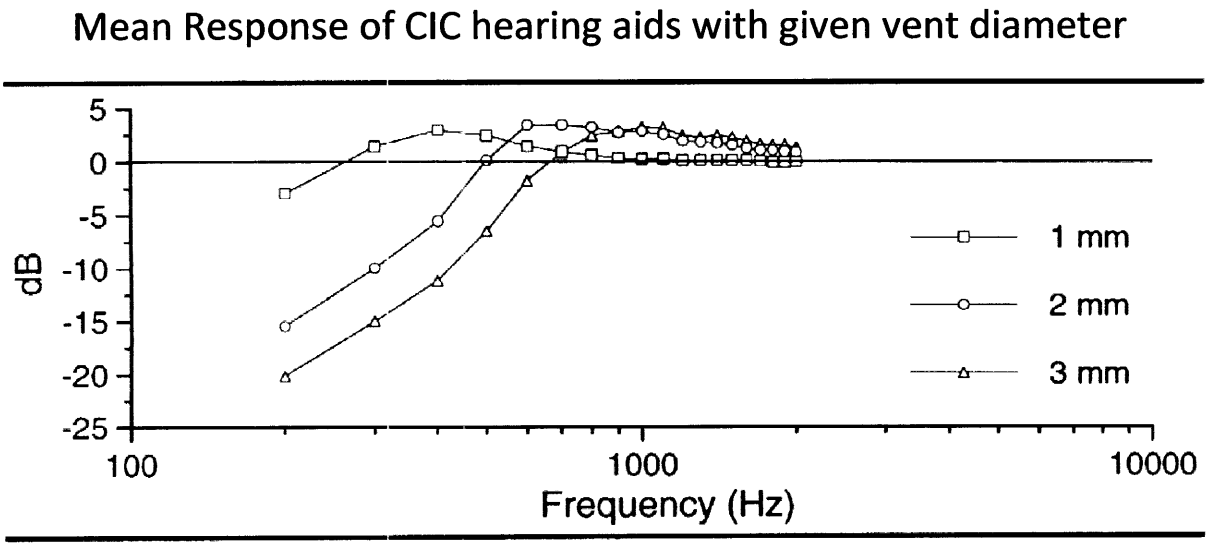

Figure 1.7 The mean response of a sample of 12 CIC hearing aids with a given vent diameter is shown above. [14]

As shown above, increasing the area of the vent in an uncontrolled manner due to poor fit can have a dramatic effect of the frequency response of the hearing aid. The expense of the remakes led the hearing aid industry to respond to the fit problem with a new technology. Laser scanning of the impressions has been introduced which will be discussed in the next section.

1.5 Laser Scanning

The hearing aid industry has begun regularly using what are called laser shell or digital shell technologies. The process begins by taking a scan of the impression using a desktop machine shown in figure 1.8 in the images taken from Sullivan's [15] paper, "Scan/print vs. invest/pour shell-making technologies for CIC hearing aid fitting"

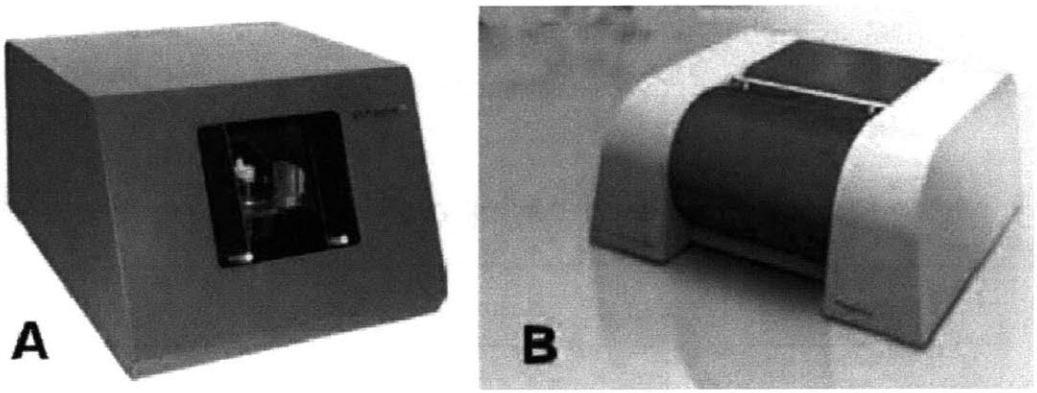

Figure 1.8: Desktop Laser Scanners [15]

Selected Laser Sintering (SLS), Stereo Lithographic Apparatus (SLA), and Digital Light Processing (DLP) are the three technologies used for producing hearing aids. The scanning is highly accurate and can measure the impression to 50 micron accuracy. They are expensive to produce and are often provided to audiologists by hearing aid companies, such as Siemens. The scanner generates a point cloud such as the one shown below from the impression also taken from Sullivan's paper.

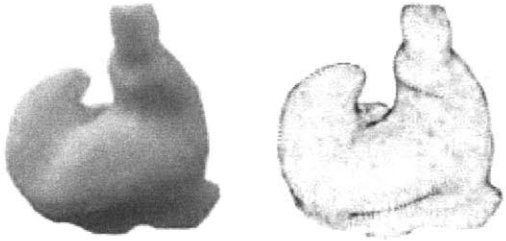

Figure 1.9: Point cloud (right) generated from this impression (left). [15]

When laser scanning began, the hearing aids created were the exact replicas of the impression. The manufacturers were confused because at first more remakes were necessary than have been previously by the traditional method of manufacture. As a result, manufacturers brought parts of the manual process in to the digital one to improve it. Wax of slightly varying thickness was replaced with a perfect digital offset. Trimming of the impression was replaced with virtual trimming. However, after these

steps the gains in the quality of hearing aids coming out of digital methods in terms of physical fit were not as large as the manufactures had hoped.

The recent trend towards scanning and printing of hearing aids has led the industry to be ready to print hearing aids from digital data. 3-D systems made a press release on May 14, 2009, announcing a new hearing aid manufacturing system the V-Flash HA 230 Manufacturing System. The V-Flash platform is the first commercially available 3-D printer under $10,000. The existence of a cheap desktop platform for making hearing aid from digital data was a crucial step in making the market ready to benefit from a direct ear scanner.

Now that the digital scan/print process has reached a plateau, it is safe to say that while it may have improved repeatability, lead times, and cost, it has not drastically improved physical fit though there was room for radical improvement. The laser scan's tolerances are very good, but it is probably much more accurate than the ear impression. Measuring the ear impression in a highly accurate fashion is not worthwhile if the impression itself is inaccurate. If this was the only problem a more accurate single digital in ear scan might be sufficient to solve the physical fit problem. However, there are two other important issues, jaw induced canal distortion and ear compliance. No single 3-D model or impression can capture the data needed to make a hearing aid that accounts for these phenomena.

1.6 Jaw Movement and Compliance

The process of capturing jaw movement and compliance is similar in that both require multiple sets of three dimensional data to be fully captured. Currently, the only way that such data has been captured experimentally is by taking two impressions with the mouth opened and closed (for jaw movement) and with high-viscosity and low-viscosity

silicone (for compliance). The high-viscosity silicone pushes harder against the ear and makes a slightly larger impression.

This multiple impression technique is reasonable to carry out experimentally, but not in general practice because of the added cost of the extra impressions. The study by Chester Pirzanski [16] titled "Ear canal dynamics: Facts versus perception," shows that both jaw movement and compliance can lead to large distortions of the ear, up to 2 mm, (ear canals are on the order of 10mm), and that the size of the effects cannot be predicted accurately by trained audiologist. In figure 1.10 the growth in the canal associated with the jaw's temporomandibular joint (TMJ) is shown.

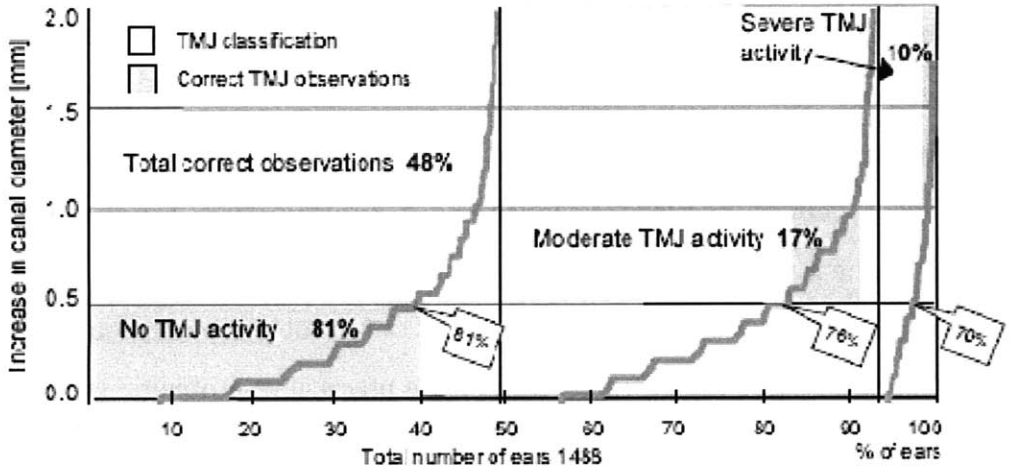

Figure 1.10: The increase in canal diameter between an open mouth low viscosity silicone and a closed mouth high viscosity silicone. [16]

Approximately 80% of ears have less than a .5 mm increase in canal diameter, but other 20% are likely to have problems with fit if there TMJ activity isn't accounted for. 1 mm of growth on a ten millimeter canal can easily cause an uncontrolled vent or a loose fitting hearing aid. Either one of these issues will probably lead to a remake of the hearing aid or discontinued use. One question addressed in Pirzanski's paper was whether or not audiologists could categorize the mouth dynamics without additional

impressions. This solution would be cost effective, but audiologists could only correctly categorize the mouth dynamics into these three categories 48% of the time. Data for an equally important hearing aid fit problem, compliance, is shown in figure 11, taken from Pirzanski [16].

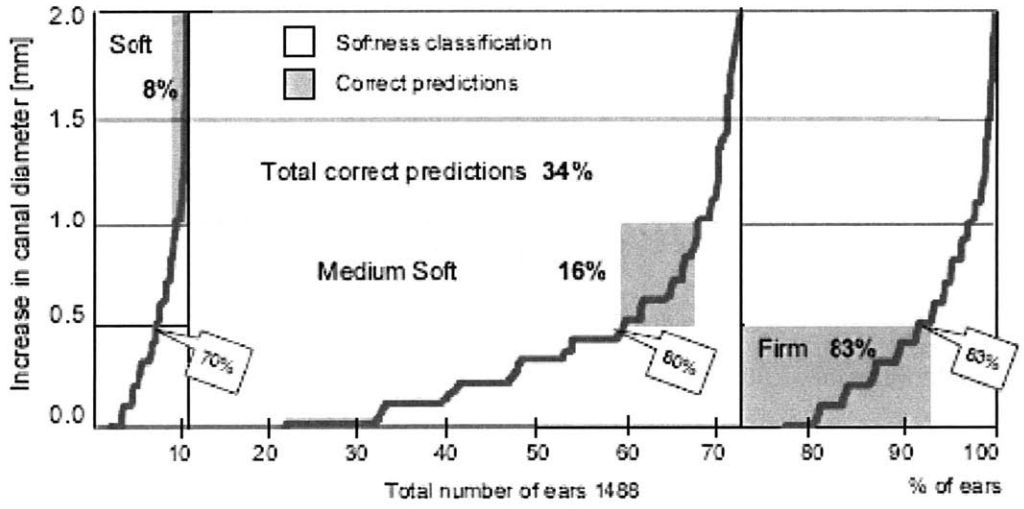

Figure 1.11: The increase in canal diameter between a closed mouth high viscosity silicone and a closed mouth low viscosity silicone. [16]

If the compliance of the ear is not taken into account, serious problems with fit may arise. A soft ear could easily lead to a loose fit and bad seal, and a firm ear can easily lead to pain and discomfort, especially when combined with TMJ activity. Audiologists could only correctly categorize the compliance into these three categories 34% of the time.

Given these two data sets, it becomes clear why the impression/scan and traditional manufacturing methods often lead to problems with fit. Hearing aids will regularly be too tight on some people with very firm ears, too loose on some people with very soft ears, or lose performance or comfort while opening the mouth to talk or chew. An important goal of this paper is to introduce a method of scanning ears that would cost

effectively allow for the manufacturers to gain access to information about the compliance and TMJ distortions of an ear. It may not be immediately clear how to use the additional 3-D data to improve hearing aid fit, but when it can be effectively utilized it should put an end to the issues with hearing aid fit that laser scan/print has failed to solve. A recently introduced hearing aid technology that attempts to address some of these problems with fit, compliant tipped hearing aids; the limitations of this solution are discussed in the next section.

1.7 New Types of Hearing Aids

Compliant tipped hearing aids are quite new and have only recently come into the literature in February 2008. Compliant tipped hearing aids make use of slow recovery foam with the goal of mitigating fit problems like jaw movement, poor retention, and comfort. Compliant tipped hearing aids have done well in studies, but are subject to the limitation of being for moderate hearing loss. As a result they only solve a problem that for the most part has been solved by open fit hearing aids.

The tips need to be changed every 10-14 days, but may still be cost effective since they have a low initial cost and reduce the time needed for fitting with an audiologist. They are currently manufactured by one manufacturer, Hearing Components Inc, and have only published data for one small trial with 30 patients. The user-factor results are promising and are shown in figure 1.7 taken from Smith et all [17] paper, "Study finds compliant eartips can be used instead of custom earmolds."

Percentage scores, mean, (and SD)	Earmolds	Compliant eartips
Use	82.2, (22.3)	83.0, (24.0)
Benefit	56.7, (12.5)	55.0, (11.6)
Residual disability	26.3, (10.1)	26.5, (10.8)
Satisfaction	57.3, (12.2)	58.1, (10.2)

Table 1.7: In the figure above it is clear that in their small trial compliant tipped hearing aids did quite well in terms of user-factors. [17]

They are similar to open fit hearing aids in that they save audiologist times by not needing an impression, and are only suitable for moderate hearing loss. However, open fit hearing aids are already providing a good solution for this subset of the hearing impaired. Given their performance limitations compliant tipped hearing aids do not reduce the need to improve the physical fit of custom hearing aids.

1.8 Existing 3-D Approaches

3-D imaging is a vast and varied field. For the most part 3-D imaging solutions are very expensive. Good literature reviews of the work in 3-D imaging can be found in the following three papers. [18, 19, 20] Despite the vast amount of research devoted to machine vision, not very much work has been put into measuring objects dimensionally similar to the ear canal from the inside. The earliest 3-D measuring instruments required contact with the surface. However, physical measurement is impractical with certain fragile materials. The two standard non-contact approaches rely on either triangulation or time of flight.

Non-contact optical scanners fall into the categories of passive and active. Passive scanners use triangulation between two or more cameras, resolving depth in the same manner as the human visual system [18]. The biggest technical hurdle of stereo and multi-view systems is the correspondence problem. Daniel Scharstein evaluates several algorithms performance in this field [21]. Another major goal for a 3-D system is to be able to measure in real time. Recently real time stereo correlation has been implemented on ATI Radeon 9800 GPU [22]. Correspondence algorithms make use of local and global matching of textures, shapes, and shadows. Stereo systems need too much space to fit in the ear canal, because a stereo system requires two cameras separated by an appropriate distance.

Active non-contact scanners can bypass the correspondence problem by using active illumination. Active methods, like passive methods, rely on triangulation. The first active scanner used a camera to track a moving single laser point. This process mirrored the physical coordinate measuring machine by building up the model one point at a time. A similar but faster approach was invented that relied on a plane of laser light. This technique removed a dimension of the scan and is widely used today. Another method that makes use of lasers is interferometry, which combines two lasers offset by a distance.

The newest non-contact method uses a digital projector instead of a laser and is known as structured light. Digital projectors can make complex depth dependant patterns that can be picked up on the camera. A lot of work has been put into the problem of optimizing the projected patterns. [23] Like passive methods, active methods require more space than is available in the ear canal because of the need for a light source, camera, and triangulation. Additionally active methods are currently too expensive for fabricating custom fit hearing aids.

The time of flight method is based on measuring the time it takes for the emitted pulse to be reflected back to the sensor. The accuracy is limited by how well time can be resolved. For example an accuracy of one centimeter requires a time resolution of 66 picoseconds. [19] Time of flight is typically used to measure large objects like buildings because it is inexpensive and is relatively inaccurate.

None of the current 3-D imaging methods are appropriate for measuring the ear canal. Triangulation methods take up too much space and are too expensive. Time of flight is not accurate enough. MRI's were used by Olivera [24] scan ear canals, but are too expensive to be suitable for making hearing aids. Given the goal of making a cheap, robust system that could scan an ear canal, none of the existing technologies were suitable.

1.9 Approach

In order to push development forward the problem of taking three dimensional data on the ear, it was decomposed into two main problems: measuring the compliance of an ear and developing a technique capable of imaging the ear. These two issues are discussed in their own sections. They were split up in order to allow concurrent work on the two, with the hope that both solutions could eventually be combined. Another sub problem is the stitching of 3-D data, which is also treated on its own briefly in the imaging section. In the subsequent imaging section ERLIF (emission reabsorbtion laser induced fluorescence) and an absorption based imaging technique inspired by it will be introduced and described mathematically.

2. Imaging with ERLIF and Absorption

When the goal of 3-dimensionally scanning the ear was first being pursued, the planned technique was ERLIF (emission reabsorption laser induced fluorescence), which can be used to measure a film thickness. This technique was introduced by Coppeta, J., et. al. [25] in 1998 under the name of DELIF (dual emission laser induced fluorescence) and expanded upon by Carlos Hidrovo and Doug Hart in a series of papers between 2000 and 2004. This section will develop the equations to explain ERLIF and the absorption based imaging technique it inspired, as well as show the resulting calibration curves. The fundamentals of this technique are explained in the next section.

2.1 ERLIF Fundamentals

ERLIF is an extension of Laser Induced Fluorescence (LIF). In LIF a light source is used to excite fluorescent tracers. LIF has been used as a qualitative tool used to visualize particles of interest by Ayala et al [26] and Joffe et al [27], and as a flow tracer by Georgiev and Alden [28], Kovacs [29], and Thirouard and Hart [30]. It is difficult to use as a quantitive tool, because of variation in illumination, surface reflectivity, color, and translucency as well as vignetting effects from tracer emission. The core idea behind ERLIF is to cancel out these variations taking a ratio of measured intensities between two fluorescent frequencies. The mathematics that show it to be a variation free approach are developed in Hidrovo and Hart's papers, and will be treated briefly in this section. Hidrovo [31] begins with the differential fluid element shown in figure 2.1.

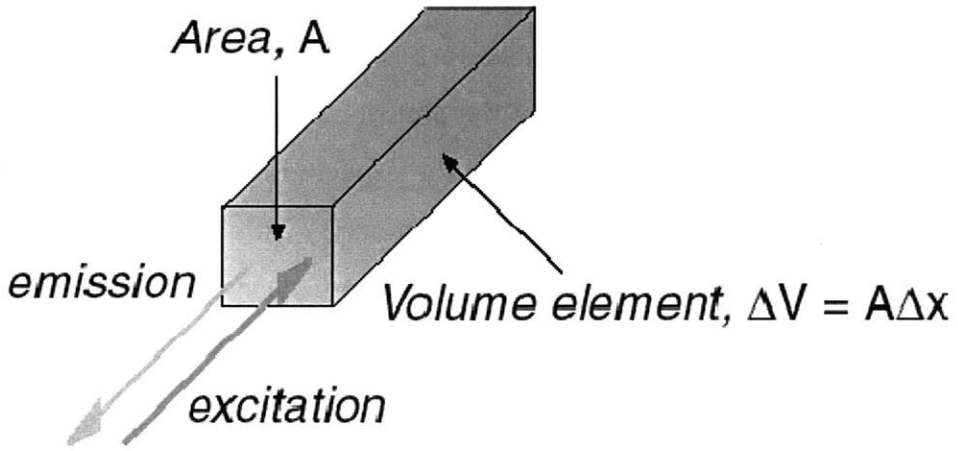

Figure 2.1: A differential fluorescent element. [25]

Given this fluid element of concentration C, volume dV, molar absorption coefficient $\varepsilon(\lambda)$, quantum efficiency Φ, illuminated by a uniform intensity I_e, the amount of light captured by a camera pixel with monitoring efficiency, ξ, from this differential volume, dI_f, is given by:

$$dI_f = \xi I_e \varepsilon(\lambda) C \Phi dV. \quad (1)$$

Monitoring efficiency, the percentage of light that is captured by the camera, remains essentially constant over the area of interest. The first modification that needs to be made is to consider the absorption of light by other elements of fluid, by including the Beer-Lambert's Law of Absorption [32]. I_e is modeled to exponentially decay with, x, with I_o as the strength or illumination at $x=0$,

$$I_e = I_o e\text{^}[-\varepsilon(\lambda) C x]. \quad (2)$$

This modification is critical to the success of the ratiometric approach as it used absorbance to make the intensity seen at the CCD depend of the depth of the fluid in a predictable manner. If a pair of dyes is used in which the absorption spectrum of dye 2 overlaps the emission spectrum of dye one, a thickness dependent behavior between

the ratio of the intensities of their emissions will emerge. The expected intensity at the peak fluorescence for dye 1 and 2 needs to take into account absorption of the laser frequency by dye one and dye two and the emission of the first dye by the second dye Once these modifications have been made the expected intensity for both peaks is the result of integrating modified versions of equation (1) with respect to x. This process leads to the following equations developed in Hidrovo and Harts [31] on DELIF film measurement, with an addition in nomenclature η_{dye}, (dye's relative emission at give wavelength)

$$I_{f1} = \frac{\xi I_o \varepsilon_1(\lambda) C_1 \Phi_1 \eta_1(\lambda_{filter1})(1-\exp\{-[\varepsilon(\lambda_{laser})C+\varepsilon(\lambda_{filter1})C_2]x\}}{\varepsilon(\lambda_{laser})C+\varepsilon(\lambda_{filter1})C_2}. \quad (3)$$

$$I_{f2} = \frac{\xi I_o \varepsilon_2(\lambda) C_2 \Phi_2 \eta_2(\lambda_{filter2})(1-\exp\{-[\varepsilon(\lambda_{laser})C]t\}}{\varepsilon(\lambda_{laser})C}. \quad (4)$$

The ratio of the two intensities is calculated below and can be seen to be thickness dependent, but not excitation dependent

$$R = \frac{\varepsilon_1(\lambda) C_1 \Phi_1 \eta_1(\lambda_{filter1})(1-\exp\{-[\varepsilon(\lambda_{laser})C+\varepsilon(\lambda_{filter1})C_2]x\}}{\varepsilon_2(\lambda) C_2 \Phi_2 \eta_2(\lambda_{filter2})(1-\exp\{-[\varepsilon(\lambda_{laser})C]x\}}. \quad (5)$$

It is hard to predict the behavior of this ratio by inspection. The quantities in equations 3-5 were graphed as a function of film thickness in figure 2.1 taken from Hidrovo and Hart's [33] paper on ERLIF in 2001.

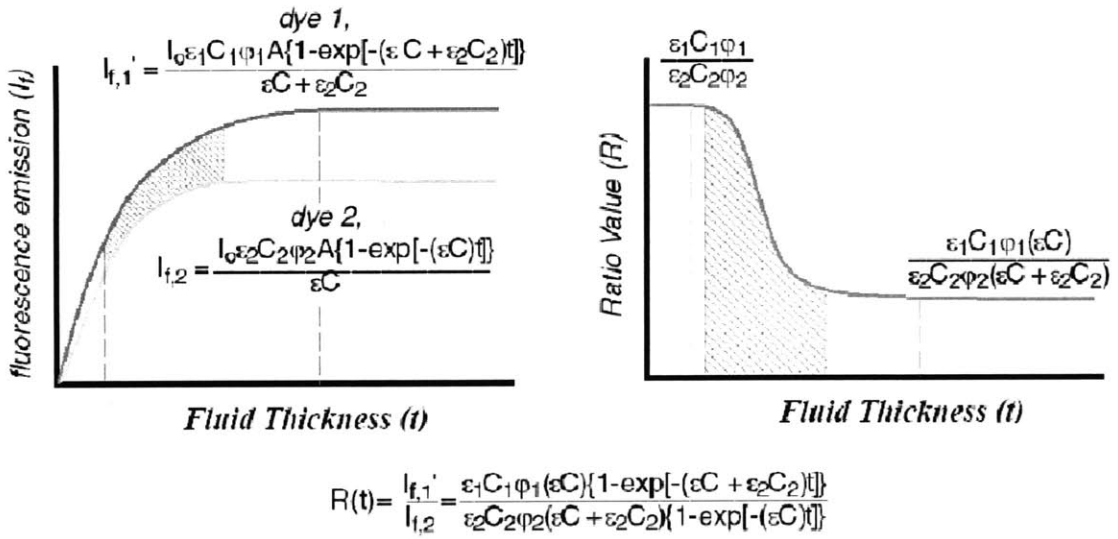

Figure 2.2: Graph shows the intensity of the fluorescent emission of dye 1 and 2, as well as the ratio between them. [26]

The first flat region on the graph is the area where there the film is too thin for reabsorption to make a quantitative difference in the ratio. In the second flat region the majority of the excitation light has been absorbed. Additional fluid is shielded and as such cannot contribute to the behavior of the system. This approach was verified experimentally by Hidrovo and Hart. They used the following optical setup in order to measure the output fluorescence in two distinct bands.

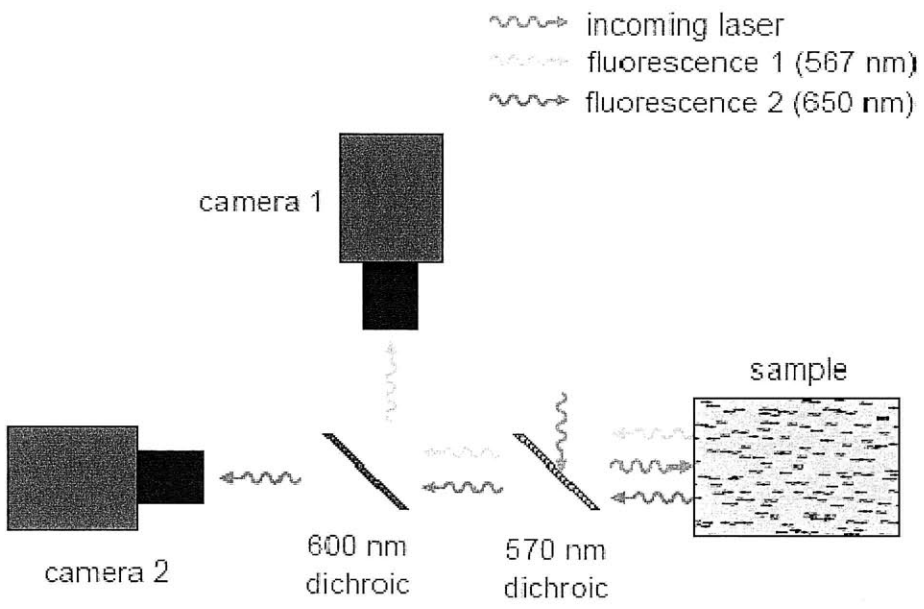

Figure 2.3: Experimental setup that can separate light into two small bands of wavelengths of interest. [25]

The exciting light is reflected off of the first dicroic mirror into the sample. Two frequencies of fluorescence are excited and can pass through the first dicroic mirror. The second dicroic mirror splits the two fluorescence frequencies between the two CCD's allowing there intensities to be measured separately. Utilizing this setup they took 3-D measurements of the coin shown in figure 2.4 taken from Hidrovo's Ph.D thesis [33] to validate the approach.

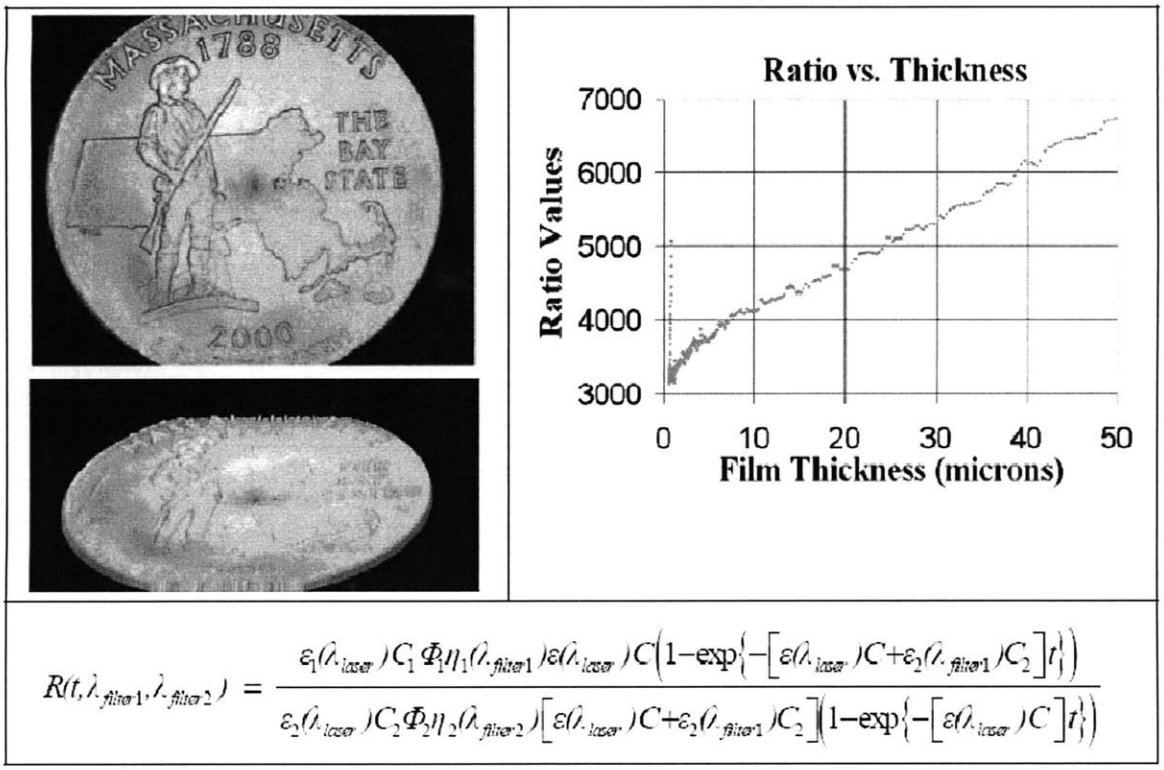

$$R(t,\lambda_{filter1},\lambda_{filter2}) = \frac{\varepsilon_1(\lambda_{laser})C_1\Phi_1\eta_1(\lambda_{filter1})\varepsilon(\lambda_{laser})C\left(1-\exp\left\{-\left[\varepsilon(\lambda_{laser})C+\varepsilon_2(\lambda_{filter1})C_2\right]t\right\}\right)}{\varepsilon_2(\lambda_{laser})C_2\Phi_2\eta_2(\lambda_{filter2})\left[\varepsilon(\lambda_{laser})C+\varepsilon_2(\lambda_{filter1})C_2\right]\left(1-\exp\left\{-\left[\varepsilon(\lambda_{laser})C\right]t\right\}\right)}$$

Figure 2.4: 3-D of coin scanned with ERLIF methods, and ERLIF calibration curve.

One problem with the above data is that it was generated with a pair of very toxic dyes. The first step to modifying the approach to be appropriate to scanning ears was to find a non-toxic fluorescent dye pair or a single self reabsorbing dye.

After an extended search the best option that was found was Fluorescein. Fluorescein is a very safe self-reabsorbing fluorescent dye. It is regularly used to dye the Chicago River on St. Patrick's Day. The same dye is also FDA approved to stain people eyes in Fluorescein Angiography. In order to validate self reabsorbing emission/absorption profile found in the literature two fluorimeters were used to take this data show in the figure 2.5.

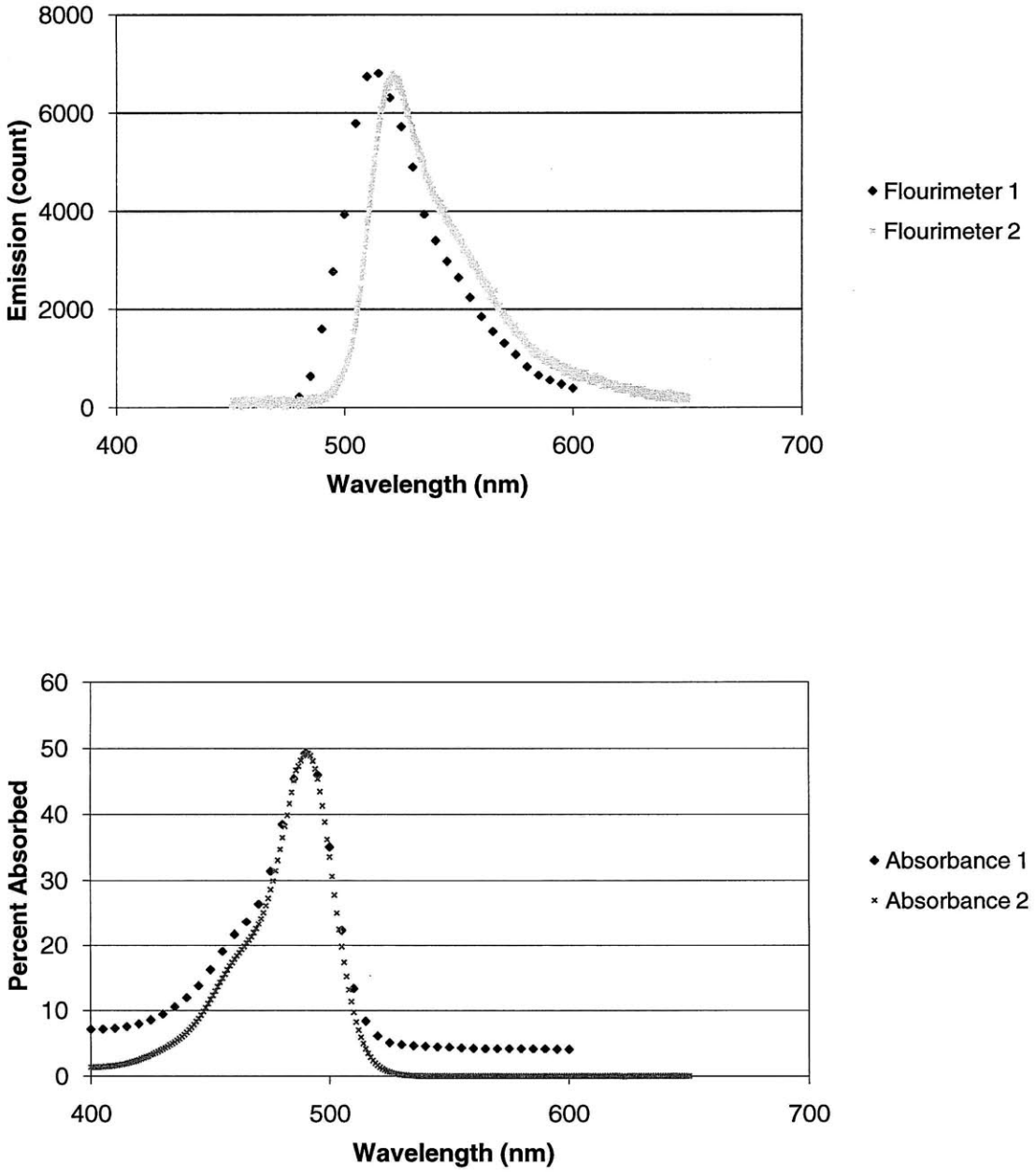

Figure 2.5: Quantitative absorption/emission profiles of Fluorescein as measured by two distinct fluorimeter instruments.

The self-reabsorbing nature of Fluorescein was validated by these results. Some preliminary data 3-D was taken with Fluorescein, but it was found that a self

reabsorbing dye is not ideal. In a two dye pair there is an additional degree of freedom, the amount of reabsorbance, available to tune the system. Another approach that required a fluorescent surface instead of a dye was invented by a colleague Federico Frigerio, which could use a single color camera. That approach is the subject of the next section.

2.2 Extension to Absorption Methods

ERLIF has some important weaknesses when applied to scanning ears. ERLIF requires quite a lot of hardware, two cameras, filters, dicroic mirrors, alignment, and as a result might be too expensive for the hearing aid application. Additionally, for ERLIF, there was only a single non-toxic self-reabsorbing dye, Fluorescein. While ERLIF is possible with a single self-reabsorbing fluorescent dye such as Fluorescein, it is not optimal. In a solution with just Fluorescein the amount of reabsorbtion is coupled to the amount of fluorescence. The question that arose was could a single RGB camera be used to do something similar to ERLIF. The basic idea behind absorption based methods is illustrated in figure 2.6.

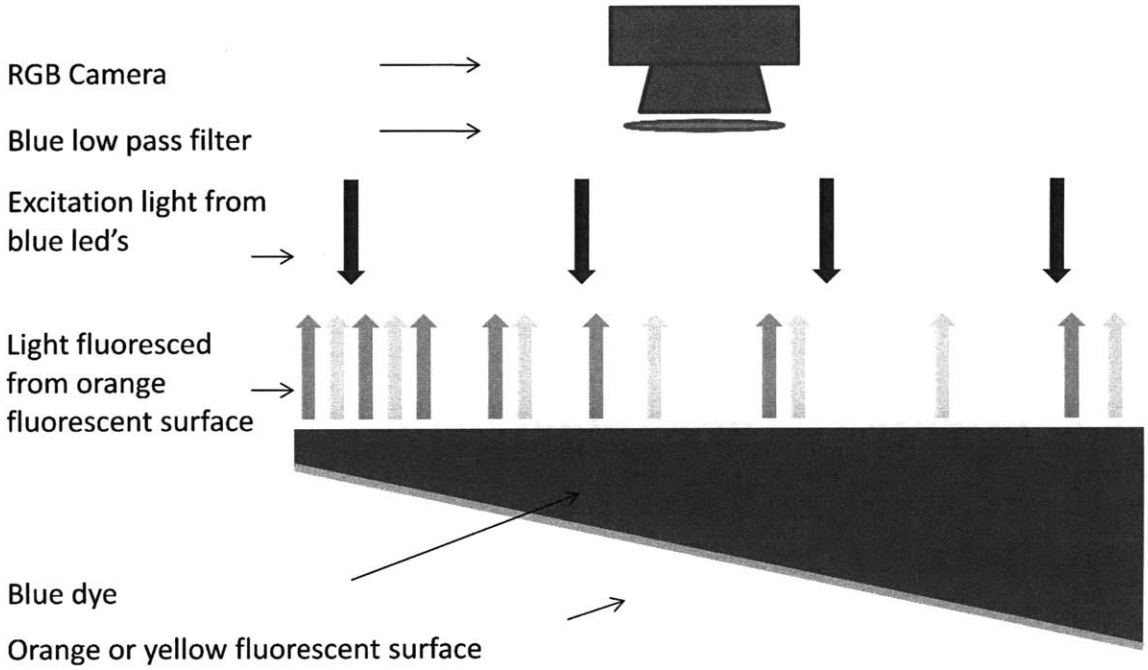

Figure 2.6: A representation of an absorption based depth scan setup. Blue excitation light passes through blue food coloring where it hits an orange or yellow fluorescent surface. When it hits the fluorescent surface orange or yellow fluorescence is given off. This light passes through a blue low pass filter into the camera.

The figure above shows the basic setup for an absorption based depth scan. Blue excitation light passes through blue food coloring where it hits an orange or yellow fluorescent surface. As the light travels through the medium more and the more of the excitation light is absorbed. When it hits the fluorescent surface orange or yellow fluorescence is given off, and the remaining excitation light is reflected. The reflected blue light can be ignored, because there is a blue low pass filter downstream. The medium continues to absorb light on the return path where it hits a blue low pass filter, allowing lower frequency light through. This filtered light goes to an RGB camera where the red and green components used to make ratio that is related to depth in a quantifiable way. The red to green ratio decreases with depth as will be developed in the set of equations to follow.

The math needed for absorption based techniques is very similar to that for ERLIF. The Intensity of the excitation light at the fluorescent surface, I_{efs}, is given by the Beer-Lambert Law of Absorption [32]

$$I_{efs} = I_o e\text{^}[-\varepsilon(\lambda_{excitation})Cx]. \quad (6)$$

This excitation light will cause fluorescence, generating a light profile proportional to this intensity. The spectrum of light generated needs to be taken into account, because the red and green camera filters are not are not as narrow as the filters used to isolate the fluorescent peaks in ERLIF methods. The intensity of light generated at a given wavelength, $I(\lambda)$, is given by the following relation

$$I_{emmitted}(\lambda) = \Phi\eta I_{efs}(\lambda). \quad (7)$$

The emitted light will be subject to absorption as it travels back up through the optical medium. The light at the filter will have the following intensity

$$I_{filter}(\lambda_{emmitted}) = \xi\Phi\eta(\lambda_{emmitted})I_o e\text{^}[-\{\varepsilon(\lambda_{excitation}) + \varepsilon(\lambda_{emmission})\}Cx. \quad (8)$$

At this stage the systems fluorescence, absorption, and monitoring efficiency have been taken into account. The final step is to integrate intensity seen by the red and green pixels of the camera and take their ratio, R. These red and green intensity integrals will integrated over the wavelengths of interest λ_{rmin}- λ_{rmax} for red and λ_{gmin}- λ_{gmax} for green. In order to take into account the camera sensitivity to a given wavelength the new parameter, $\alpha(\lambda)$, has been introduced into the ratio equation below.

$$R = \frac{\int_{\lambda_{rmin}}^{\lambda_{rmax}} \xi\Phi\alpha(\lambda_{emmitted})\eta(\lambda_{emmitted})I_o e\text{^}[-\{\varepsilon(\lambda_{excitation})+\varepsilon(\lambda_{emmitted})\}Cx]d\lambda_{emmitted}}{\int_{\lambda_{gmin}}^{\lambda_{gmax}} \xi\Phi\alpha(\lambda_{emmitted})\eta(\lambda_{emmitted})I_o e\text{^}[-\{\varepsilon(\lambda_{excitation})+\varepsilon(\lambda_{emmitted})\}Cx]d\lambda_{emmitted}} \quad (9)$$

The ratio of interest should be related to depth and independent of lighting conditions when simplified by canceling equal constants.

$$R = \frac{\int_{\lambda_{rmin}}^{\lambda_{rmax}} \{\alpha(\lambda_{emmitted})\eta(\lambda_{emmitted})e\text{^}[-\varepsilon(\lambda_{emmitted})Cx]\}d\lambda_{emmitted}}{\int_{\lambda_{gmin}}^{\lambda_{gmax}} \{\alpha(\lambda_{emmitted})\eta(\lambda_{emmitted})e\text{^}[-\varepsilon(\lambda_{emmitted})Cx]\}d\lambda_{emmitted}} \quad (10)$$

This ratio is the heart of absorption based imaging methods. It is not immediately obvious how this ratio should vary with depth. The most intuitive way to approach it is to consider two representative frequencies. These frequencies will have different molar absorption coefficients, ε, and so they will decay at different rates. In this simplification the ratio, R, will decay exponentially. The overall ratio will consist of the sum of a continuum of exponential decaying functions divided by the sum of another continuum of functions.

2.3 1-D Absorption Calibration

Given good quality data on the emission spectrum of the dye, the absorption spectrum of the food coloring, the behavior of the filters, and the camera sensitivity the dependence of the ratio on film thickness could be modeled analytically. However, pieces of this data are of insufficient accuracy for an analytical model to be more useful than an experimental calibration given the purpose of measuring an ear. For simplicity a 1-D calibration setup was used, and is shown in figure 2.7.

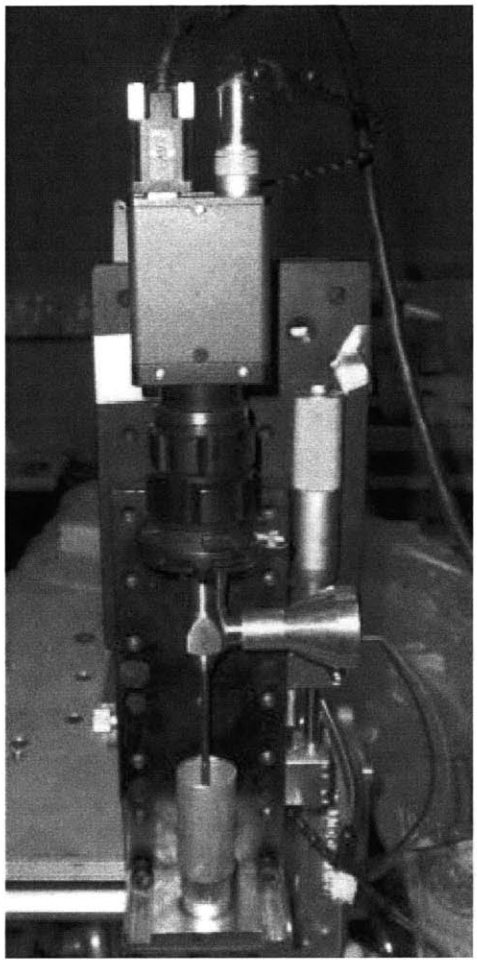

Figure 2.7: 1-D depth calibration experimental setup.

A micrometer was used to change the distance between the fluorescent surface and the probe. An AVT Stingray F-033c color CCD camera was used to take the optical data. A set of powerful blue LEDs was used as the excitation light and was triggered by the camera. A 500 nm long pass filter was used to prevent the blue excitation light from entering the camera. Preliminary data was taken with the orange fluorescent paint in which depth was varied at an unknown concentration of blue food coloring number one to investigate the basic behavior of the system. This calibration curve is shown in figure 2.8.

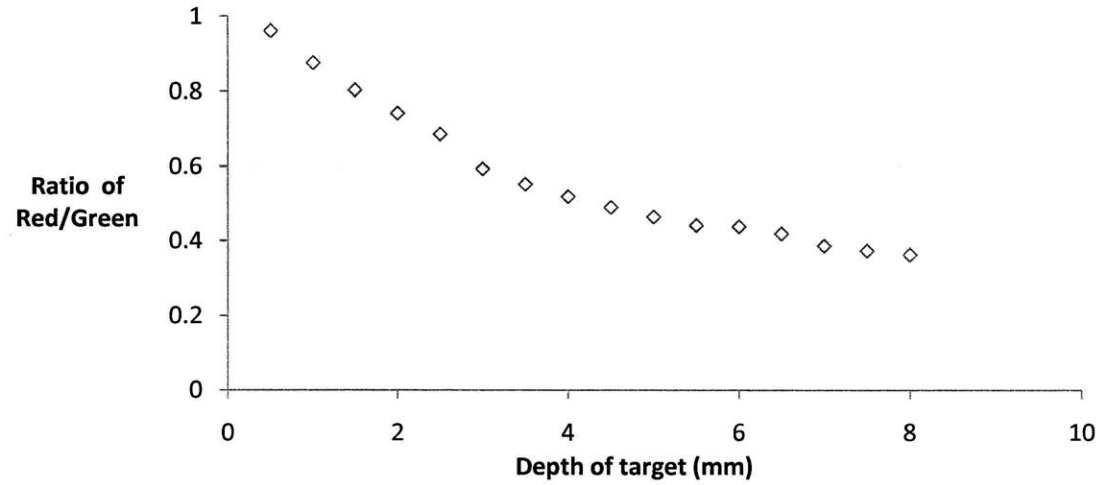

Figure 2.8: Preliminary 1-D depth calibration with flat, orange fluorescent target.

This data was very encouraging as it is reasonably well behaved. There are some kinks in it that look like noise, but could be small non linearities. As the depth increases the signal to noise ratio decreases, decreasing the effective resolution. The next step was to do another 1-D calibration with a known concentration and a fluorescent membrane. Since orange fluorescent paint could not be used on a balloon Coumarin 153 was put into a urethane membrane and used to provide the fluorescent surface for this calibration. This calibration curve is shown in figure 2.9.

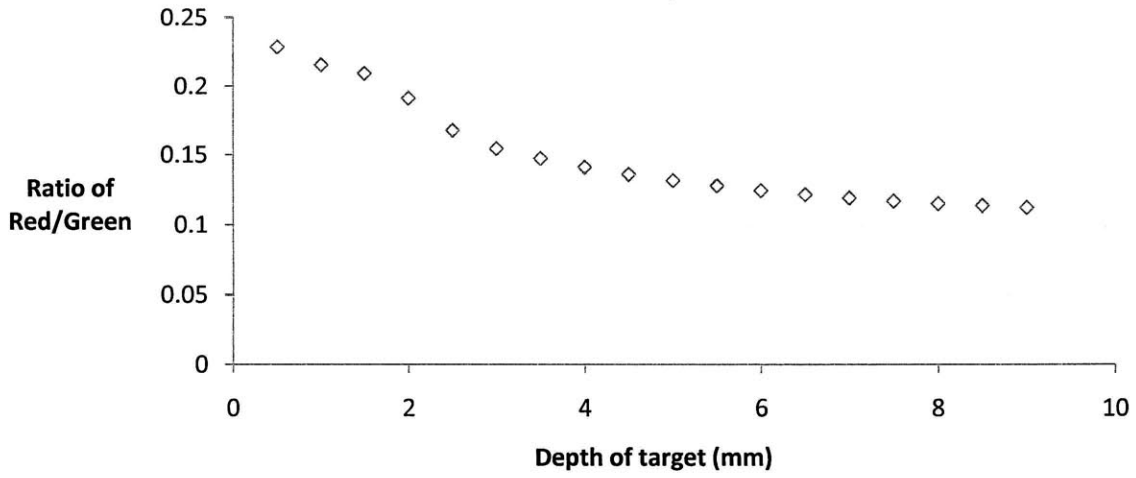

Figure 2.9: 1-D depth calibration with flat, Coumarin 153 impregnated membrane.

The main differences between the calibration curves with Coumarin and the paint are a more pronounced kink and the magnitude of the ratio. The data is still well behaved, but the ratio is reduced by approximately a factor of 4. Using the same setup the concentration was also varied, the resultant calibration curve is shown in figure 2.10.

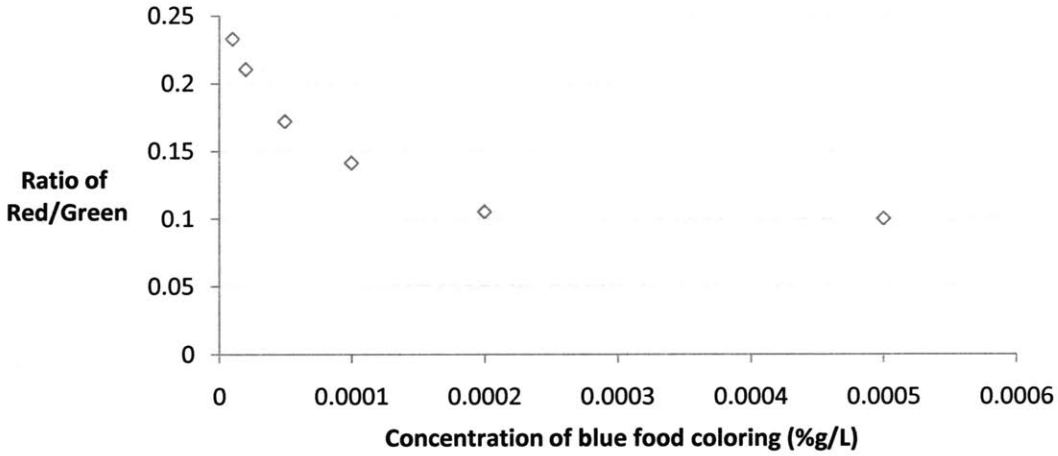

Figure 2.10: 1-D concentration calibration with flat, Coumarin 153 impregnated membrane.

The behavior of the concentration calibration curve is as expected. Increasing concentration for a given depth is equivalent to increasing the depth. Lighting may be different, but that should be canceled out by the ratiometric nature of absorption based imaging. In the ratio equation, (10) it is the product of concentration and depth that determines the amount of light absorbed. The potential of this imaging system is discussed in the next section.

2.4 Discussion of Imaging Potential

For absorption methods to improve the physical fit of hearing aids, they will need to meet certain specifications. Currently effects from compliance and TMJ motion as large as 2 mm in a 10 mm canal are not captured by current methods. Capturing these effects alone with the same accuracy as impressions could provide great improvement. On a 10

mm canal an accuracy of 100 microns would be good, and 50 microns might be near the bleeding edge of accuracy's utility. By tailoring the concentration to the film thickness range of interest these types of accuracies can be attained with ERLIF and absorption methods. One way to achieve high accuracy is to use different concentration of dye in different parts of the ear. A concept solid modeled in figure 2.11 has regions with different concentrations.

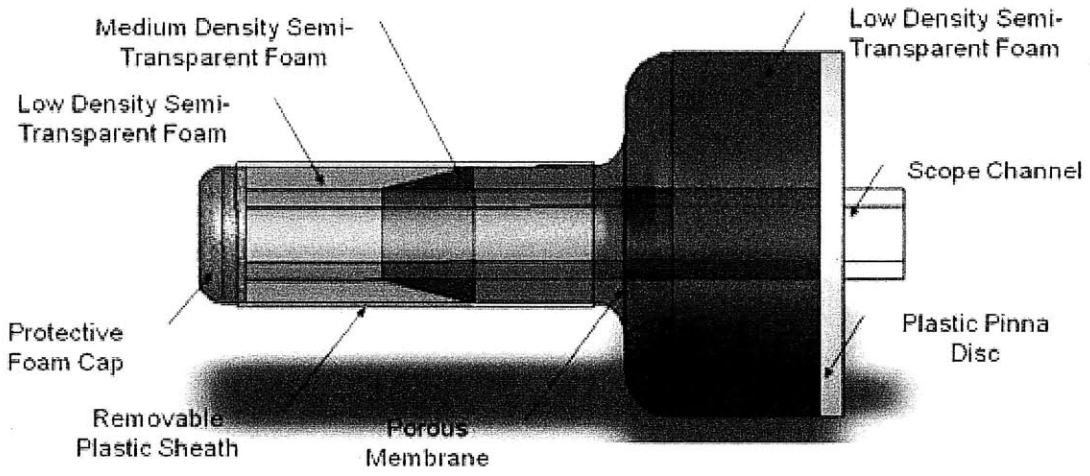

Figure 2.10: Solid model of foam assisted multiple region balloon concept.

Different regions of the ear would be measured with different dye concentrations. Appropriate pressures could be applied regionally by varying the density of the foam. The idea behind utilizing foam was make applying pressure to the ear simple and safe for the audiologist.

Another way to improve accuracy is to compare take multiple sets of data stitched together. In this manner the model can be assured to be of good quality, and the noise can be canceled out. A brief 3-D stitching simulation was done with ear data to assure the feasibility of this approach.

2.5 3-D Stitching Simulation

One problem that arises in machine vision and 3-D techniques is the problem of stitching. In this paper stitching will be treated briefly in this section to demonstrate that the stitching needs of this project are easily within the capabilities of existing techniques. If the requirements were near the maximum potential of stitching techniques a lot of engineering work would be required to get that last bit of performance out of current standards. The specifications that an algorithm would need to meet: stitch together three to ten 3-D shapes in the presence of a low level of noise and aberrations.

An ICP (iterative closest point) algorithm based on a paper by [34] Paul J. Bed was tested in simulation and found to be suitable for the needs of absorption based imaging of the ear. The algorithm minimizes the least squares distance between each point from one section and the closest point in the other section in an iterative manner. The result is a matrix that translates and rotates the sections so that the overlapping parts are stitched back together. For the simulation the data from a real 3-D ear impression laser scan were provided courtesy of 3-Shape Inc. The point cloud was divided into six sections along one axis, and those sections were modified by translation, rotation, and noise. The original and the divided up ear are shown in the figure below.

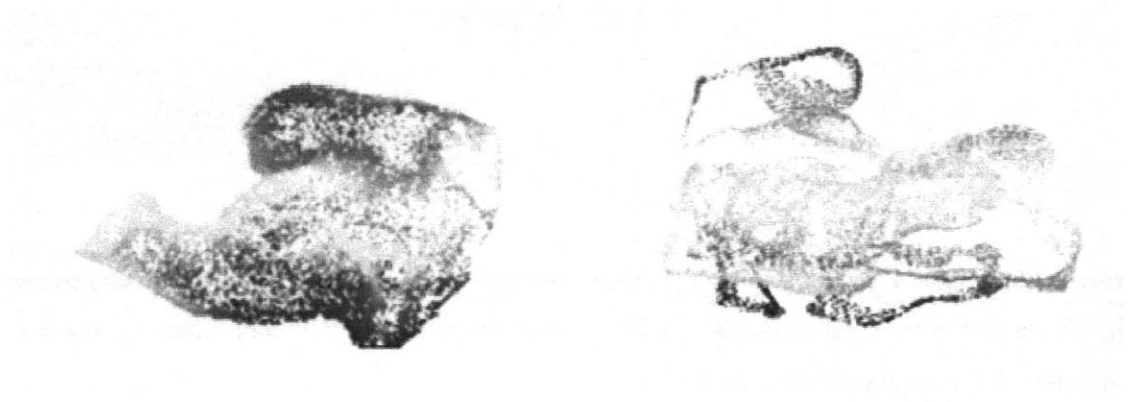

Figure 2.11: 3-D point cloud of ear (left). Same 3-D point cloud cut up into six sections and then rotated, translated, and with xyz noise (right). The restitched point cloud is visually indistinguishable from the original and as such is not shown. The error between the two is shown in the next figure.

In order to put the cut up ear back together with minimal knowledge of its original shape an ICP algorithm was used. In order to put the ear back together the second section was stitched to the first, and the third to the first two, and the fourth to the first three and so on. The only knowledge of the shape that was used was which sections fit together. In a more rigorous simulation even this would not have been necessary. All of the combinations could have been tried and the combination that produced the best results would almost certainly be the correct one. The performance of the algorithm in the simulation is shown in the figure below.

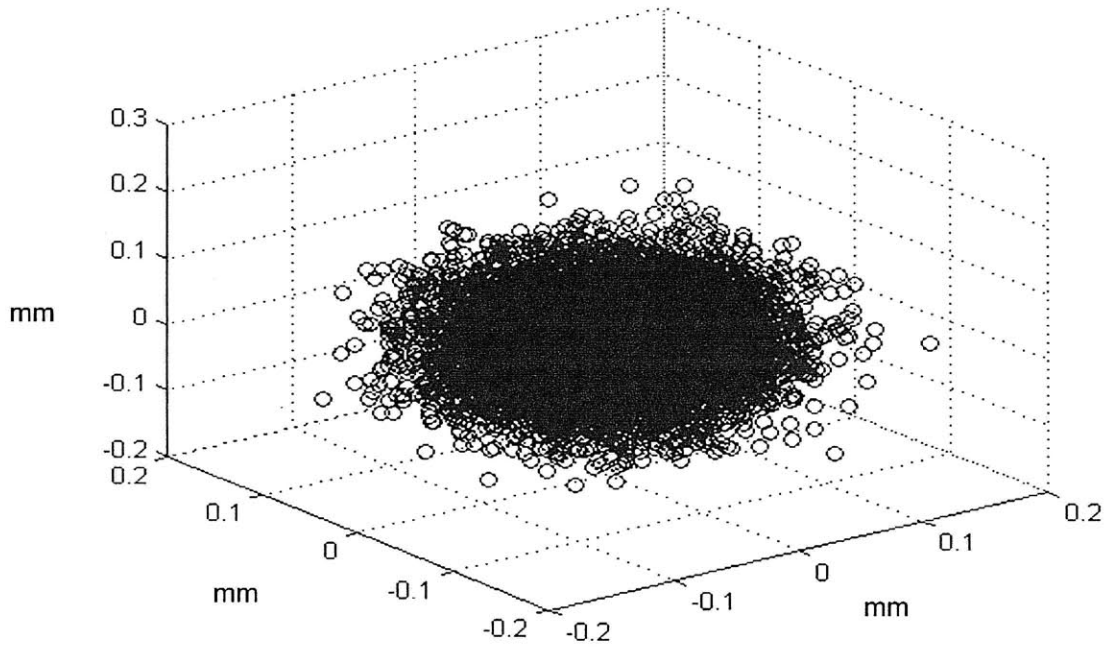

Figure 2.12: Original 3-D point cloud minus stitched 3-D point cloud. Characteristic length was 40 mm, xyz noise was .05 mm. Stitching was as success, as residual differences were concentrated in the same magnitude as the noise a (.05 mm) sphere.

The simulation validated the assumption that current techniques were sufficient. The residual distances were small and on the order of the noise. Given an appropriate system for imaging the ear, the next problem to be discussed is that of fabricating the balloon.

3. Balloon Fabrication

The need for a balloon arose from a desire to measure compliance. In order to measure compliance, an adjustable uniform pressure needs to be placed on the ear, for which a balloon is ideally suited. Additionally, for the optical scan the balloon serves two critical functions: it allows the device to retain the optical fluid and provides a fluorescent surface. Both ERLIF and absorption based methods require optical fluids, but absorption methods have the additional requirement of a fluorescent surface. In this chapter the main problems associated with making the balloon and the steps taken to get to a successful prototype will be discussed. In the next section the requirements for the balloon needed will be discussed.

3.1 Requirements

A balloon suitable for imaging the ear must fulfill certain constraints: it must be appropriately compliant, conform well to the ear, and have the appropriate ports. In order to measure bulk compliance the additional constraint that the balloon cannot expand freely anywhere must also be met.

The balloon's compliance will need to lie in a certain range. The upper bound comes from the amount of pressure that is safe and comfortable in the ear. The lower bound arises from the need to get a good amount of signal to noise in the bulk compliance measuring experimental setup. After a significant number of satisfactory balloons were made and tested, this range was determined experimentally as to require the balloon to be fully inflated at between 1 and 4 psig.

The conformity of a balloon to the ear canal is also important. A gap between the balloon and the ear will introduce error into the measurement. The conformity requirement makes the uniformity of the balloon important. Additionally, unmeasured variations in the thickness of the balloon will be measured as changes in the profile of the ear canal, adding noise to the optical data. Thick parts of the balloon will conform poorly and thin parts limit the strength of the balloon. For all of the above reasons the balloon will need to have a uniform appropriate thickness. A compliant cylindrical balloon was unlikely to conform sufficiently, which is why an ear shaped balloon is desired. It may be that in order to conform to the variety of ear canals to be measured, a plurality of balloon shapes will eventually be needed. It was thus expected that eventually the balloon would need to be more ear shaped, and so a variety of hearing aid shells were acquired to be used as molds.

The experiments that follow have their own set of additional requirements. The bulk compliance of an ear measurement requires that the portions of the balloon that are not up against the ear are stiff. These stiff portions will improve the accuracy of a simple model of the system, springs in parallel, by removing areas where the balloon can freely expand while not touching the ear. A pressure tap will be the only port needed for the bulk compliance measurements. The optical measurements will require a port for the otoscope as well as a pressure tap.

A final requirement for the balloon comes from cost. Despite the technical complexity of the custom balloons available from the medical balloon industry as shown in figure 3.1 below, for this research's purposes the balloon will need to be fabricated in the laboratory.

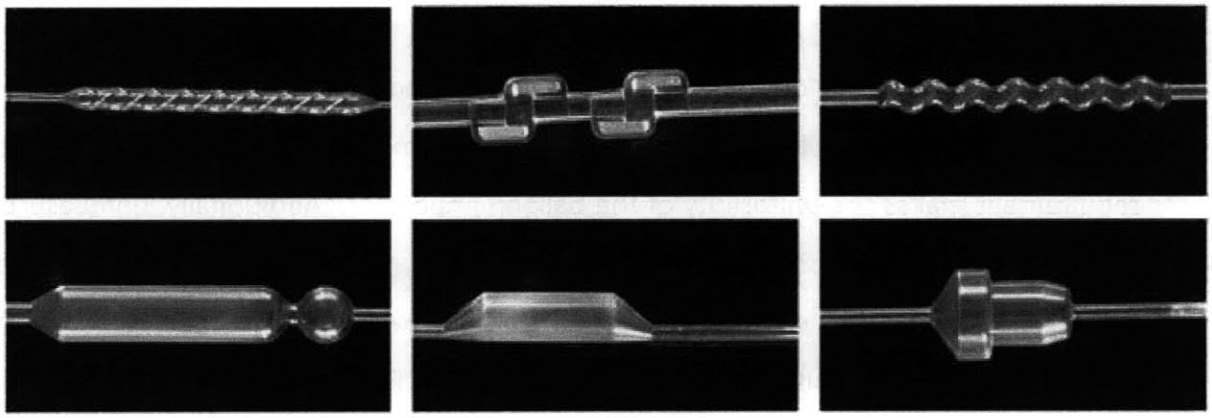

Figure 3.1: Sample producible balloon geometries from Advanced Polymers [29].

The cost to purchase existing medical balloons for experimentation would be been in the hundreds of dollars. For bulk compliance testing an ear-shaped balloon was needed. No ear-shaped balloons are being made as stock balloons, and moreover for optical scanning a set of custom ear-shaped, fluorescent inside coating, was needed. This set would have had a setup cost upwards of ten thousand dollars. As such, the balloon needs to be made in the laboratory to make costs reasonable. The next section deals with what material to use, and how to manufacture the balloon.

3.2 Material and Manufacturing Method Selection

The first question to be answered was concerning from what material to make the balloon. The majority of balloons are traditionally made out of latex. While the material properties would be acceptable for the balloons needed, its allergenic properties may eventually pose a serious problem. In a paper, Tilak M. Shaw [36] discusses, the allergenic issues concerning latex, which affect approximately 7% of the US population, as well as the medical device industries response of switching to urethanes and silicones.

A search of the materials used by large medical balloon manufacturing firms, including Advanced Polymers Incorporated, showed that many of the compliant balloons were

urethane based. Urethane can be used to make balloons in a low volume laboratory setting with a two part mix and dip molding. Other possible materials include silicone and nylon. Nylon based balloons were typically used for non compliant balloons, and therefore were not suitable. Silicone based balloons would be a reasonable alternative. They can be harder to seal, but if the urethane manufacturing path had proved unsuccessful, silicone would have been explored.

Once it had been decided to make use of urethane, the production method needed to be decided. For mass production, blow molding is currently being used by the medical balloon industry. The basic steps of blow molding are illustrated in figure 3.2.

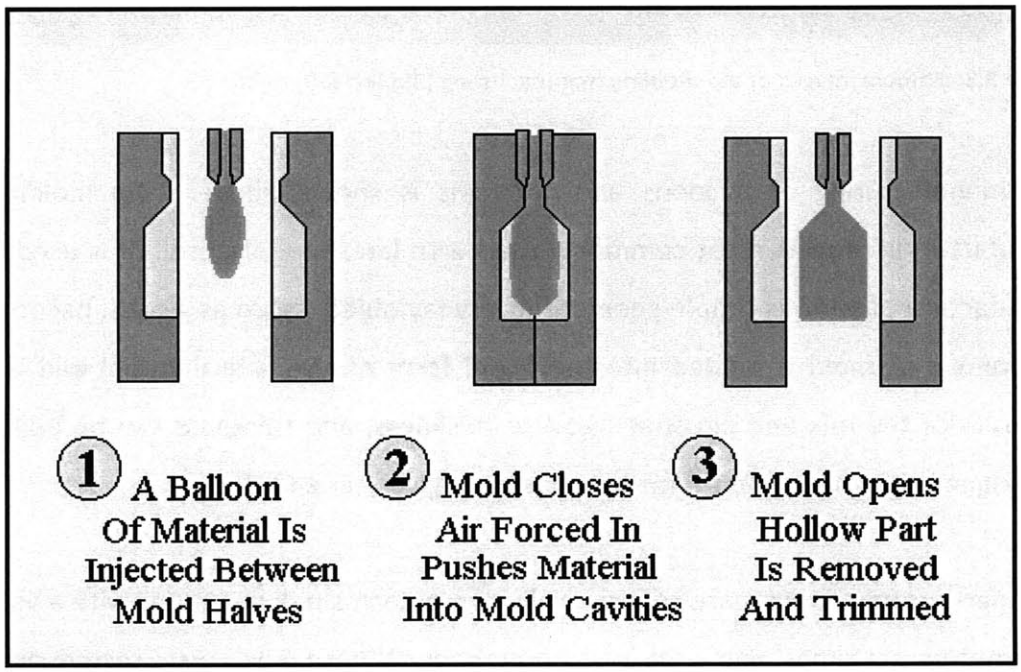

Figure 3.2: Steps involved in blow molding. [37]

Blow molding begins with a balloon of material and makes use of pressurized air to push the material up against the mold. Blow molding offers high accuracies, low cost per balloon, and complex geometries and the basics of it are shown in figure 3.1. However blow molding like injection molding has a large setup cost and as such is less suited to

prototypes than dip molding. Dip molding is also suited for mass production as shown in the figure below.

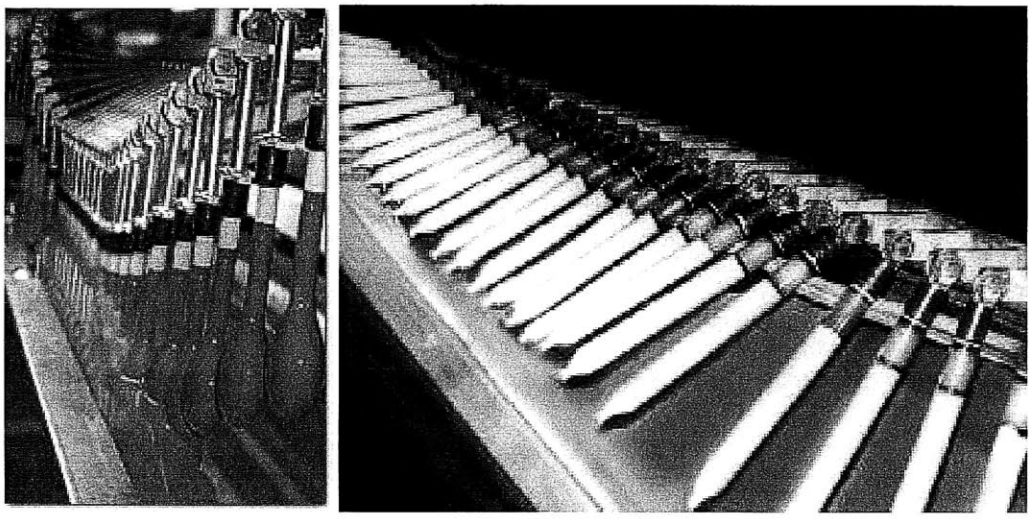

Figure 3.3: Sample images of dip molding manufacturing [38] left [39] right.

The manufacturing of balloons and condoms is shown above. Dip molding is a manufacturing process most commonly used with latex and plastisol. It is used for the manufacture of various simple geometry everyday objects such as gloves, balloons, and condoms. A mold is dipped into the liquid form of the final material and is dried. Viscosity of the mix and dip speed govern thickness, and thickness can be built up by dipping multiple times after it mixture has been given time to dry.

Two-part urethane mixes are commercially available in small quantities with a variety of durometers, set times, and viscosities. A number of these mixes were tested, and given the thickness and compliance of the desired balloons, the urethane that worked best was Polytek 74-30, mixed viscosity 2000 cP, Durometer 30 shore A . The early attempts of making a balloon with this urethane are discussed in the next section.

3.3 Early Attempts

In the beginning, to determine feasibility a very geometrically simple mold was used, a glass rod. Polished glass is suitable as a mold, because it is more difficult for the urethane to stick to then other surfaces like metals and plastics. The two-part polytek 30 was combined and mixed, and the glass rod was dipped into it and slowly pulled up. The rod was then hung up and allowed to drip. An illustrative early balloon is shown in figure 3.4

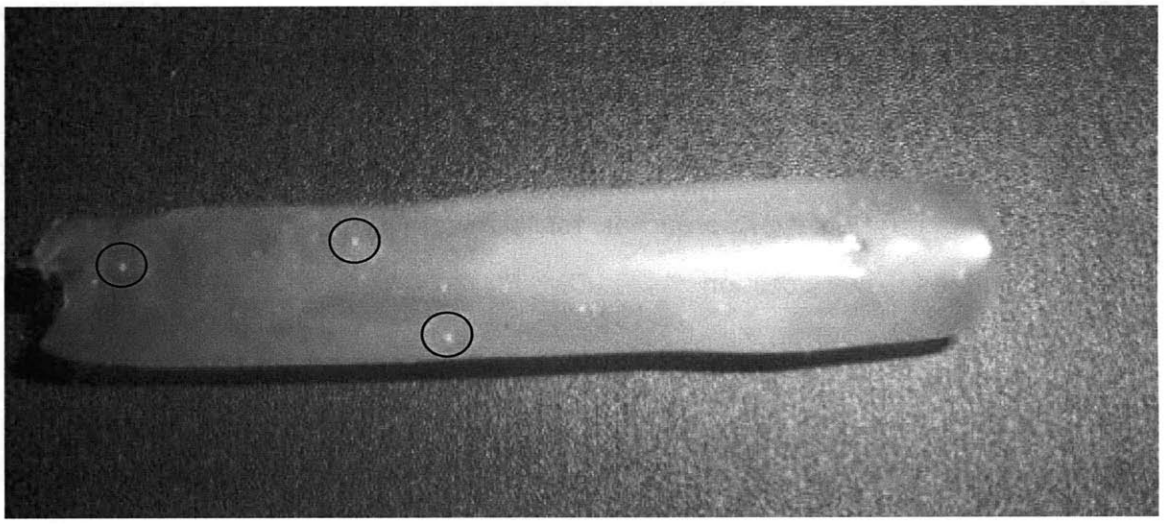

Figure 3.4: Early attempt at producing urethane balloons. Air bubbles are circled in black.

This balloon was somewhat encouraging, but it does have obvious defects. Regions of it were of an appropriate thickness for the desired compliance. It has air bubbles throughout the balloon some of which are pin holes that destroy the integrity of the balloon, and there are large gradients in wall thickness. Another type of defect, a nub, is shown in figure 3.5.

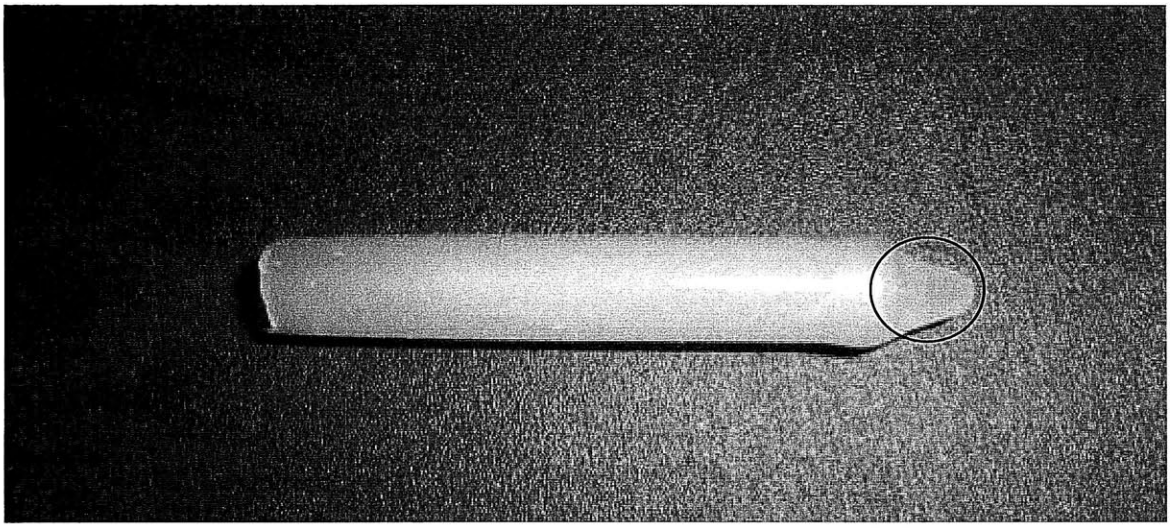

Figure 3.5: Early attempt at producing urethane balloons. Nub is circled in black.

This defect is the result of the slow dripping of excess urethane downwards from the vertical drying position. Approaches for eliminating the mentioned defects are explained in the following section.

3.4 Balloon Improvement

The balloons manufactured had several issues. Balloons are fragile and could tear during the removal process. They had air bubbles, which in thin balloons could become pin holes. The balloons average thickness was too large, and thickness gradients were present in addition to nubs.

The first problem that was solved concerned urethane binding strongly to its mold. The removal process was very delicate, as the balloon could easily tear. The use of a release agent was expedited removal and prevented the balloon from sticking to the mold and tearing.

The most critical defect to eliminate was air bubbles. Air bubbles reduce the integrity of the balloon and can cause pinholes which render the balloon useless. Given the sensitivity of the balloon quality to pin holes, air bubbles were more of a concern then in most applications of this urethane mix. This defect was the easiest to decouple from other defects.

A vacuum oven was used to remove some of the air bubbles. When the urethane is subject to a vacuum the air bubbles trapped inside expand, causing the mix to foam up. The mixture slowly expands until 29 inHg are reached during which it rapidly expands to 5-10 times its initial size. The 29 inHg is critical to ensure that the bubbles collapse instead of simply expanding and worsening the problem [40]. At the height of the rapid expansion bubbles quickly pop and the mixture settles back down to its original height. However, all of the bubbles have not yet been eliminated. The number of air bubbles has been significantly reduced, but all of the remaining bubbles are at the top of mixture.

These lingering bubbles pose a serious problem as they will definitely be picked up by dipping. To further reduce these bubbles an additional two cycles of vacuum between 25 and 29 inHg were utilized. These extra cycles are not as effective as the initial cycle, as there is not enough air trapped in the mixture for another episode of foaming and collapsing. The additional cycles proved to be more helpful than merely subjecting the mixture to a constant high vacuum. At this point the number of bubbles is still too great to achieve a good yield for dipped cylindrical balloons, and the bubbles are still all on the top of the mixture where they would be picked up by the mold. The final step taken to eliminate air bubbles was to scrape the top of the urethane mixture. After all of these steps were taken a thinly dipped balloon had an approximately 50% chance of being free of a pinhole defect. A simple cylindrical balloon free of air bubbles is shown in figure 3.6

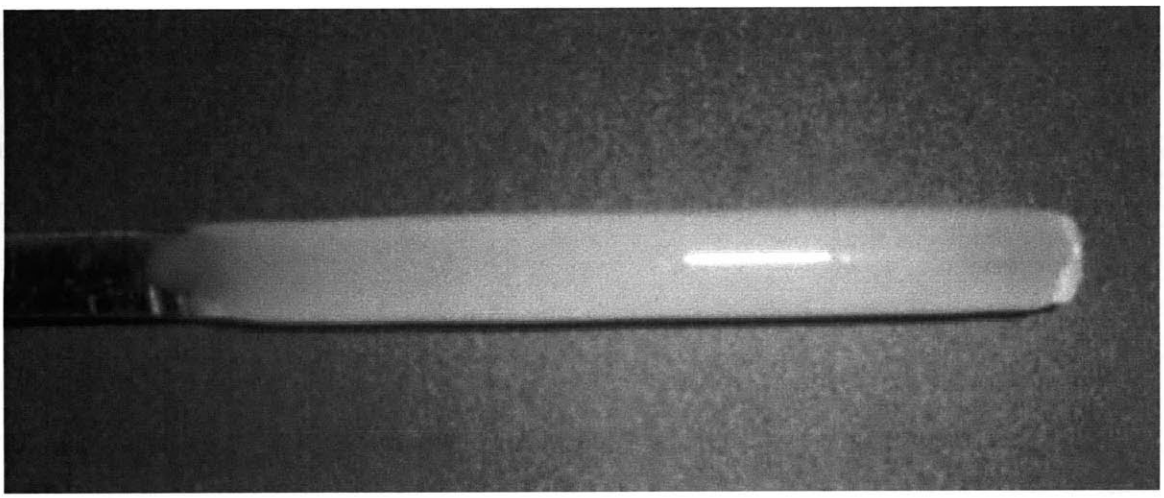

Figure 3.6: Air bubble free urethane balloon.

In order to eliminate the other types of defects, an understanding of the relevant forces on the urethane was required. The urethane is under gravitational, viscous, and surface tension forces. Surface tension is very helpful for balloon production purposes; it pushes the balloon thickness to a constant. Viscous forces are more neutral, they inhibit the flow of material. The gravitational force hinders balloon production as it causes nubs and thickness gradients. In order to make high quality ear-shaped balloons, the disruptive effect of the gravitational force needs to be mitigated. An ear shaped mold used for making balloons is shown in figure 3.7.

Figure 3.7: Hard plastic hearing aid shell to be used for mold as balloon.

For the purpose of balloon making the expense of achieving zero-g or reduced-g is not feasible. The first solution attempted was repeated flipping of the balloons during the drying phase. Through this manual mechanism the balloon thickness was made more even, and the nubs were reduced in size. The idea of using rotation to counteract gravity was attempted, and was found to be reasonable for cylindrical shaped balloons. However for ear-shaped balloons, the eventual goal, rotation caused additional surface gradients.

After the flipping steps was implemented the surface gradients were still unacceptably high, and the balloons were too thick. The traditional ways to decrease thickness in dip molding are to increase dipping speed and decrease viscosity. A good way to get an intuitive feel for this is to imagine dipping something in honey and water. The honey is very viscous, and a lot of honey can be gathered on a rod, especially when dipped slowly. The viscosity of the urethane mix being used can be reduced up to some limit by changing the ratio of the two part mix, but the manual dipping process cannot be sped up without losing repeatability.

A non traditional method that proved to be very helpful was to pull extra material off of the nub by spinning a glass cylinder. Before this technique was utilized the excess urethane would slowly drip off in an uncontrolled manner. Controlled removal of excess material it afforded much better regulation over the average thickness and further reduced nubs. A nub-free balloon produced utilizing this technique is shown in figure 3.8.

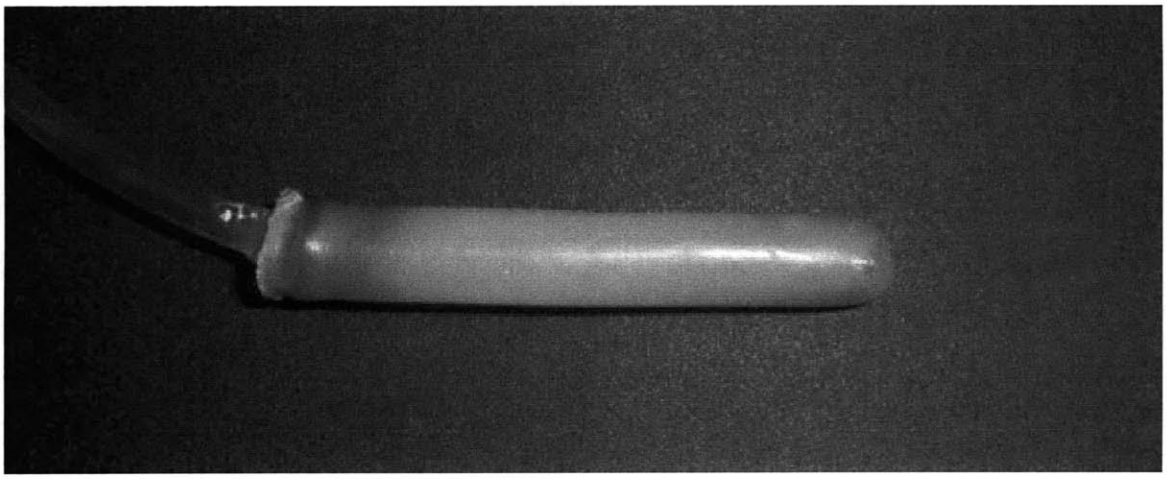

Figure 3.8: A nub free balloon is shown in the picture above.

In addition to improving control over and reducing average thickness, it illustrated that a more uniform thickness could be achieved with thinner balloons. The reduction in the mass of urethane decreased the force of gravity, while not affecting the strength of surface tension forces. This improved the ratio of helpful forces to disruptive forces, reducing thickness gradients and nubs. This knowledge also led to subsequent improvements by switching from dipped balloons to brushed-on balloons.

At first the brush was used simply as a tool to even out the balloon as it dried. Eventually it replaced dipping entirely, as it provided more control. Brushed on balloons could be made to be thinner than was needed. A very thin brushed on ear shaped balloon in which nubs were not mitigated is shown in figure 3.9.

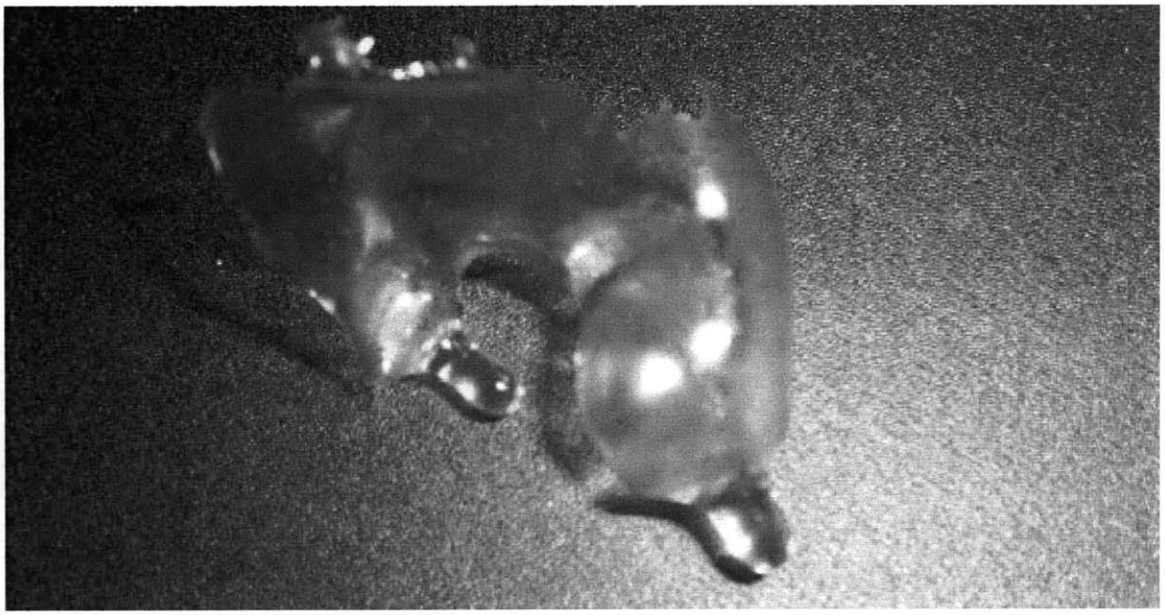

Figure 3.9: Thin brushed on balloon.

This balloon is very uniform aside from the edge effects at the top of the balloon and the nub at the bottom. Additionally there was very good uniformity, that would be sacrificed if a thicker coat was painted on. At this thickness a single reasonable sized bubble would cause a pinhole, so to increase the reliability while retaining the uniform thickness; it was decided to attempt to build up a balloon in 2-4 layers of very thin urethane. These balloons had very good properties and could be accurately make uniform balloons on complex ear shaped molds as show below. These balloons were also resilient to air bubbles, as a pinhole in a single layer would be covered up by the additional layers. A defect-free brushed-on balloon is shown in figure

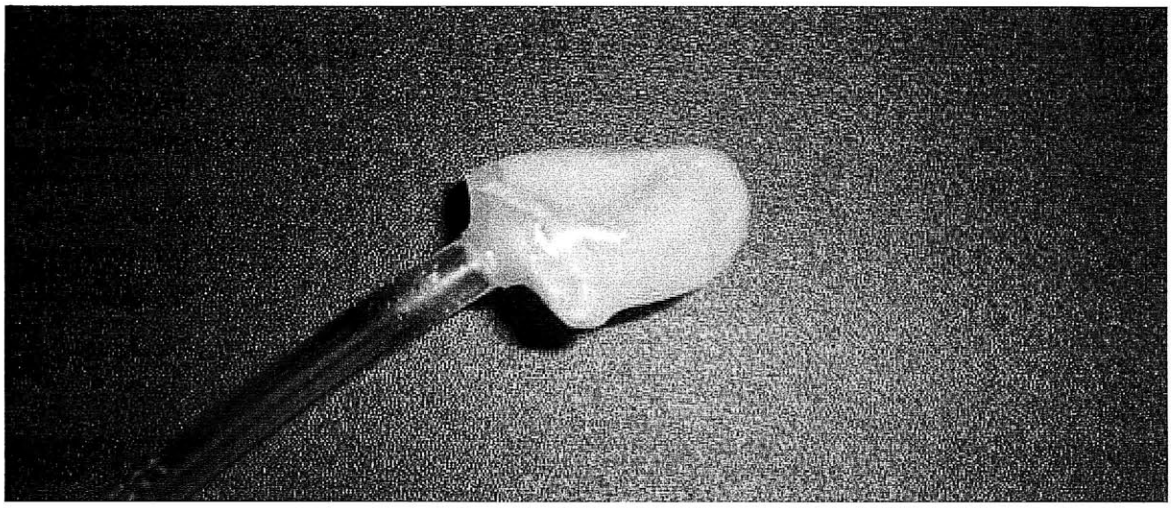

Figure 3.10: Successful, multiple brushed on layer, uniform ear shaped balloon.

This balloon is brushed-on, defect-free, ear-shaped balloon with a urethane base and an inflation port. In the next section it will be discussed how to finish the balloons that come off of the ear mold by adding ports, seals, and plastic backings.

3.5 Adding Seals, Ports, and Rigid Plastic Backings

Dipping and painting balloons onto molds leaves an opening, which requires additional work in order to produce a usable balloon for imaging or compliance testing. A variety of methods were used to try and create robust ports with seals. Early attempts using O-rings and cyanoacrylate are shown in figure 3.11 . The caps of the first balloons produced were not satisfactory, so they were cut off. The remaining cylindrical balloon was placed between the O-rings and the ports and glued in place. Extra O-rings were added in an attempt to create better seals.

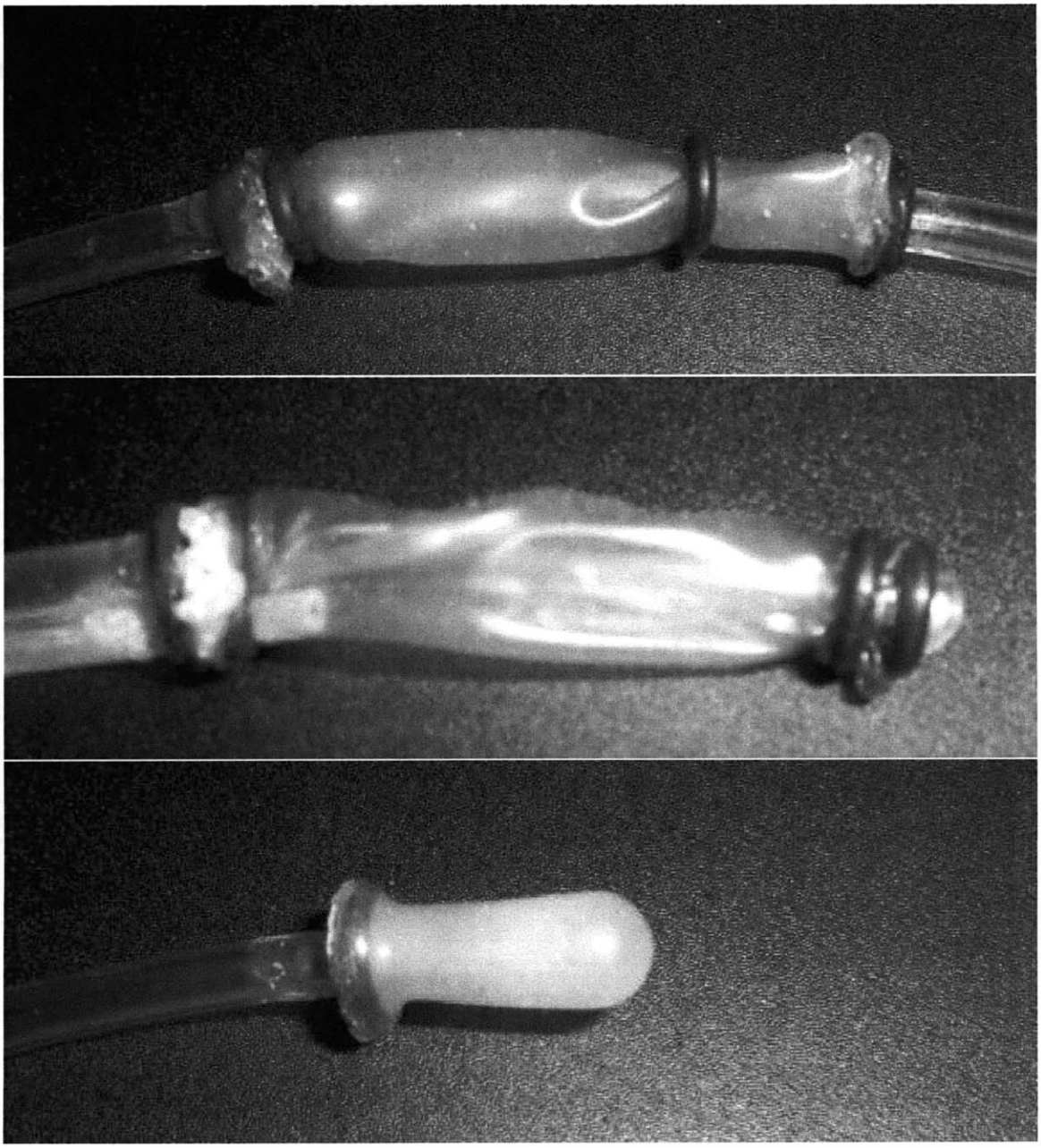

Figure 3.11: Balloons sealed with O-rings and super glue.

In the top image of figure 3.11 a balloon was constructed for use in a model ear. This balloon made use of the fact that a better seal could be made when only one port was needed per side. The seals were more robust because they had smaller gaps to fill. Even the more viscous gel forms of cyanoacrylate contract upon dying, filling gaps poorly. The balloon in the middle of the figure 3.11 was made with two ports on one

side, and had a somewhat satisfactory cap. The O-rings were small enough to fit in an ear canal, and they were also safe and soft as they prevented the balloon from going past a certain distance in the canal. They were still unappealing when compared to a balloon with a urethane cap that could eventually be made with brush on methods and an improved mold, such as the one at the bottom of figure 3.11. This balloon was only suitable for compliance testing, as it had no pressure tap. Another problem with these O-ring and glue ports is that they cannot be extended to non cylindrical balloons.

The first attempt at adding a port and base to an ear shaped balloon involved gluing a fitted piece of urethane cut out from a thin sheet. A sample sheet and base cutout are shown in figure 3.12.

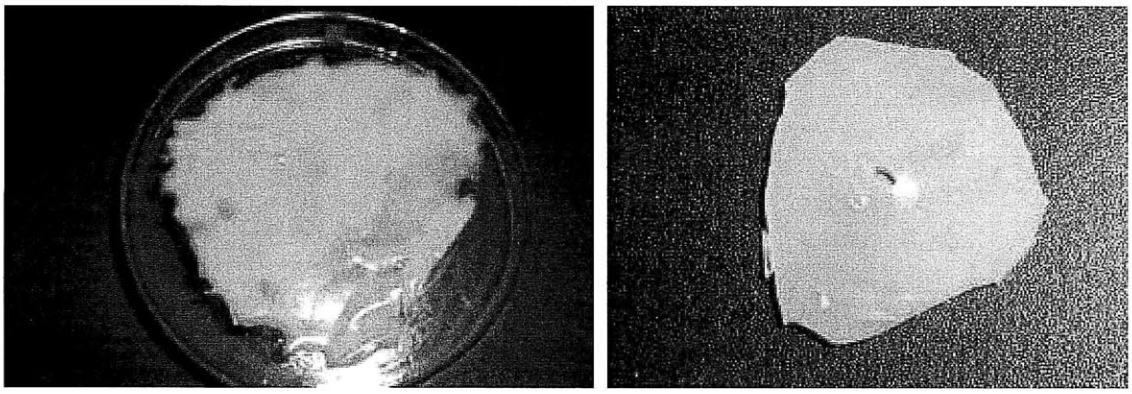

Figure 3.12 Sheet of orange urethane for making balloon bases (left), and sample cutout base (right).

Silicone and cyanoacrylate glues were both tested. The base needs to be attached to the existing balloon. An image of an assembled balloon in which silicone sealant was used is shown in figure 3.13.

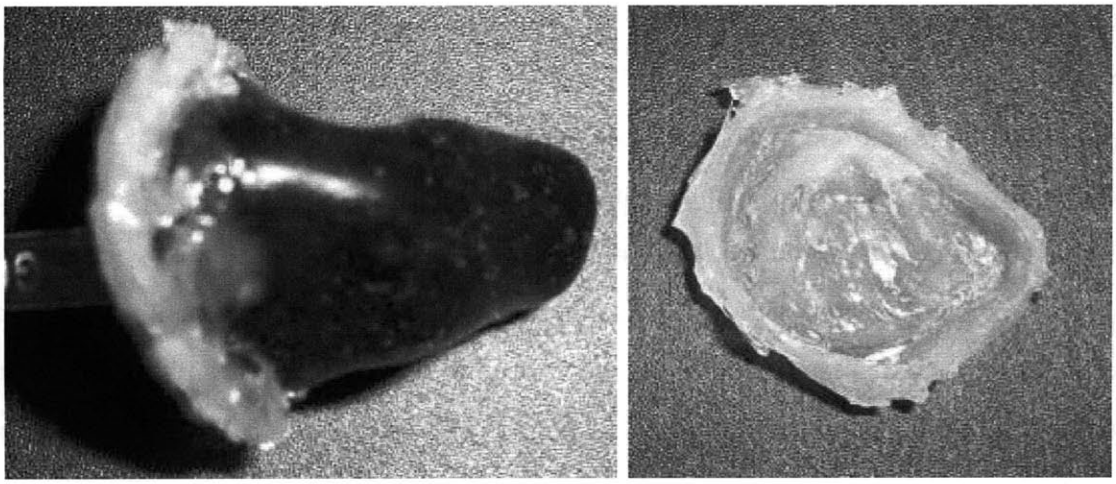

Figure 3.13: Base attached with silicone and removed

The seal made with silicone was for the most part a failure. The seal is not elegant, and it does not stick to the urethane well. The base could be easily removed from the balloon as show on the right image of figure 3.13

Cyanoacrylate based seals worked considerably better. They were worse at gap filling but, adhered well to the urethane. A cutaway of a seal between a clear base and an orange balloon is shown in figure 3.14.

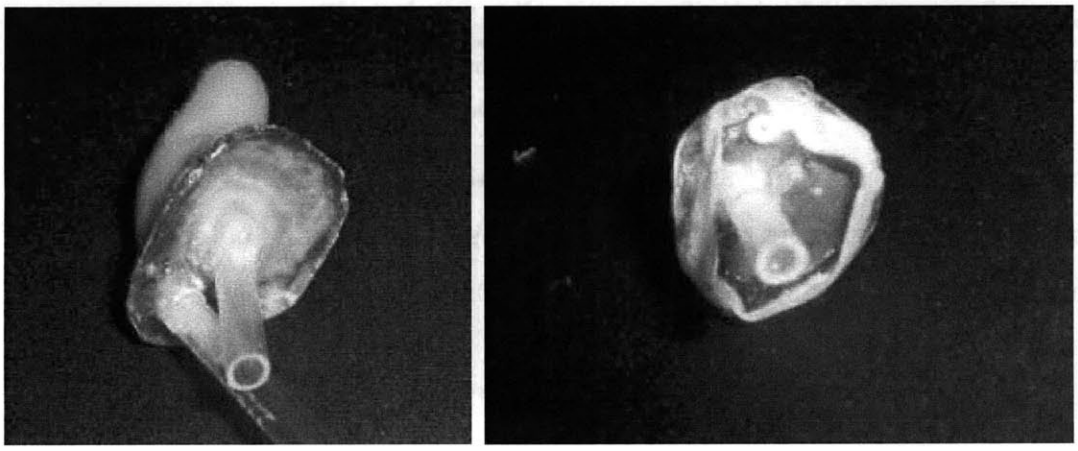

Figure 3.14: Cyanoacrylate based method of adding base. Full balloon is shown on left, balloon is cutaway to show seal on right.

The cyanoacrylate seals were functional. The main issue with the cyanoacrylate was that once it dried it became totally inflexible. A large improvement in functionality and appearance of the added bases wash achieved through the use of completely urethane-based approach was used. To make a urethane base, an entire coat of urethane needed to be painted on the existing balloon and it was allowed to dry sitting on top of a wet layer of urethane on a glass dish. This solution was seamless and robust. Ports could be added by cutting small holes in the urethane base to insert the tubes and seals could be made with cyanoacrylate based glue. The balloon shown in figure 3.15 was made in this manner.

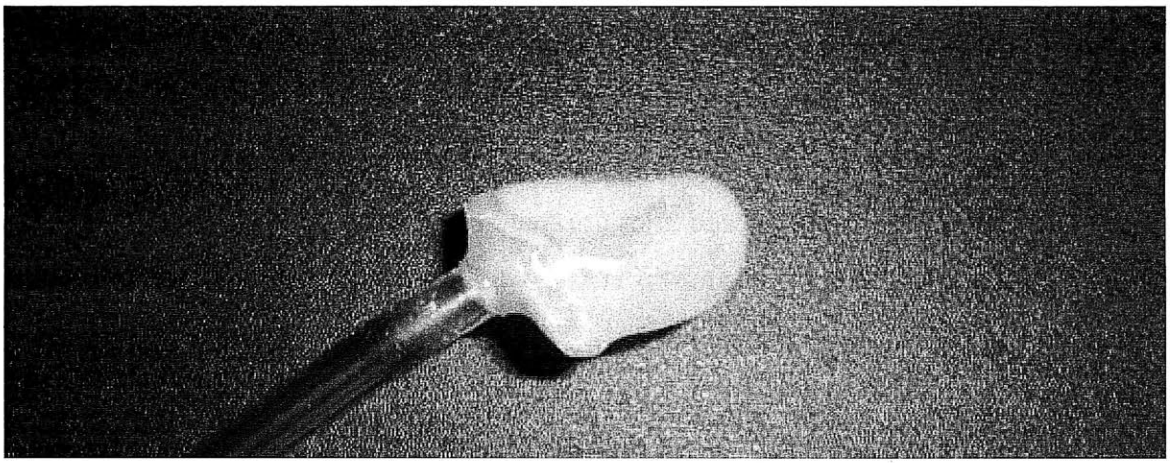

Figure 3.15: Balloon base attached entirely with urethane

The last modification that was made to this method to produce a balloon suited for compliance testing was to glue a rigid plastic base to the bottom before adding the final coat of urethane. A balloon with a rigid plastic base is shown in figure 3.16.

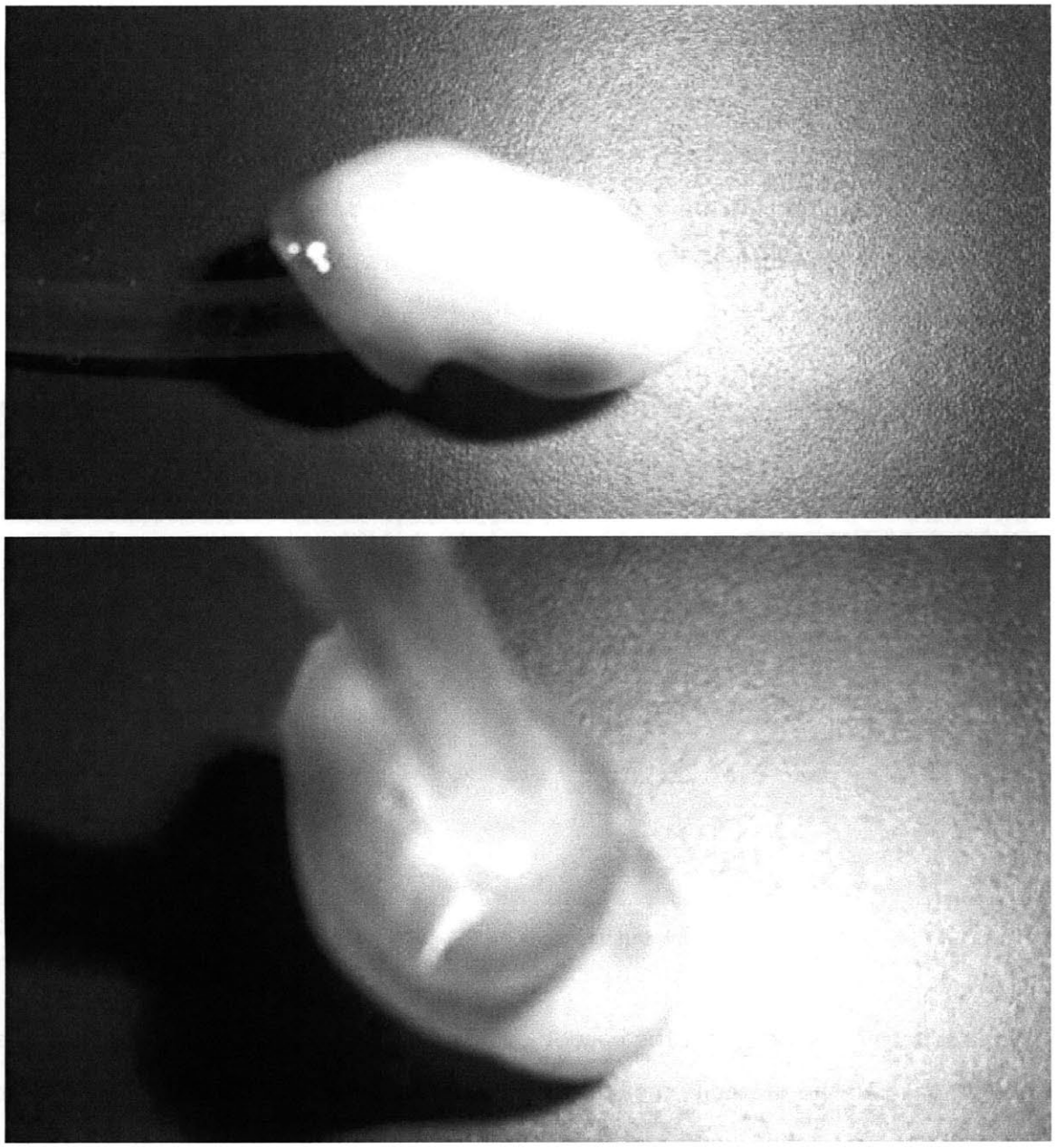

Figure 3.16: Balloon base with rigid plastic base.

The rigid base prevents free-expansion of the base of the balloon, so that the compliance of the balloon can be more accurately measured. At this stage all of the physical aspects of the balloon have been finalized and all that is left is to add fluorescence.

3.6 Adding Fluorescence

The process of adding fluorescence to a balloon to meet our imaging needs was more difficult then it first appeared to be. For calibration and other experiments a fluorescent paint was used to provide the fluorescent surface needed for absorption based imaging. Simply painting the outside of the balloon was not an option, because the paint would crack subject to strain, as shown below.

Figure 3.17: Paint flaking off of a painted balloon

When it became obvious that the balloon could not be painted an attempt was made at adding paint to the urethane mix, but it caused severe amounts of bubble nucleation. Air bubbles were still unacceptable, so another method of adding fluorescence was needed.

One potential solution to the problem of paint drying was be to capture paint between two layers of urethane and have the paint never dry. By adding linseed oil balloons could be created that had a shelf life of about two weeks, before they dried out and became less suitable for use. What had been accomplished was delaying the onset of the drying out. Such a balloon is shown in figure 3.18.

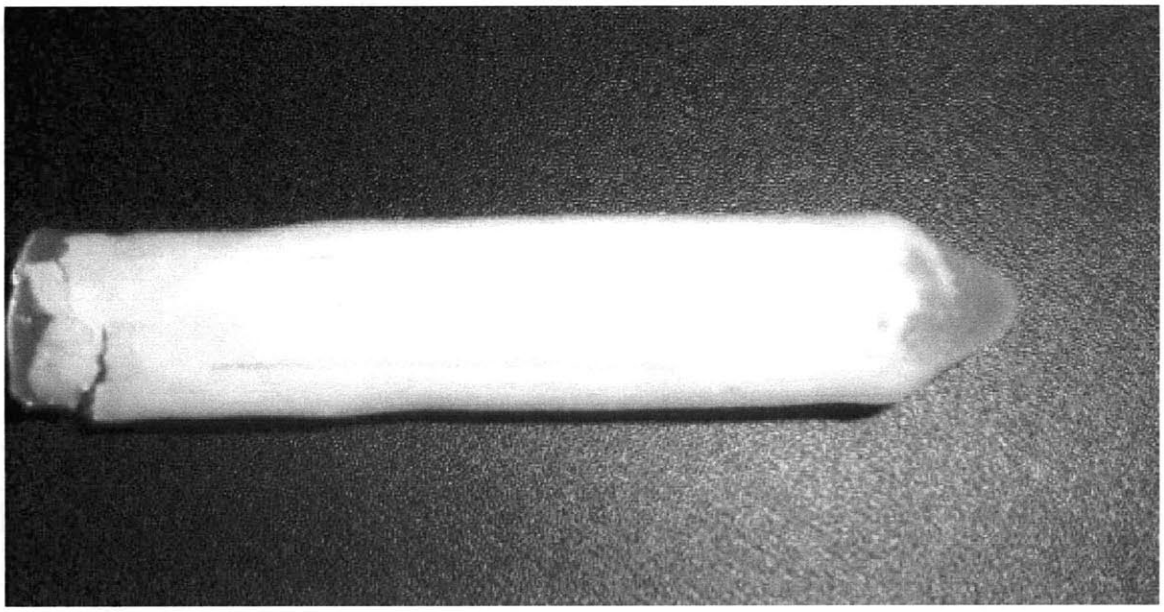

Figure 3.18: Balloon made with layer of fluorescent paint trapped between two layers of urethane

This was a great improvement, but was still not a robust solution. A closer inspection of the balloon under load reveals a zebra stripe pattern.

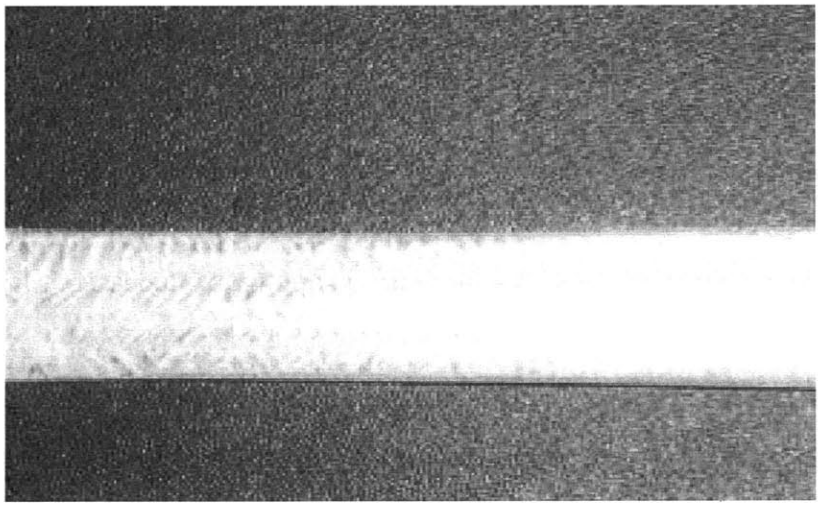

Figure 3.19: Zebra striped pattern on stretched balloon made up of two layers of urethane with layer of fluorescent paint in between.

The final attempt to make use of this orange fluorescent paint involved grinding up dried paint. A mortar and pestle was used to produce orange fluorescent powder, which was put into the urethane mix. The results are shown in figure 3.20.

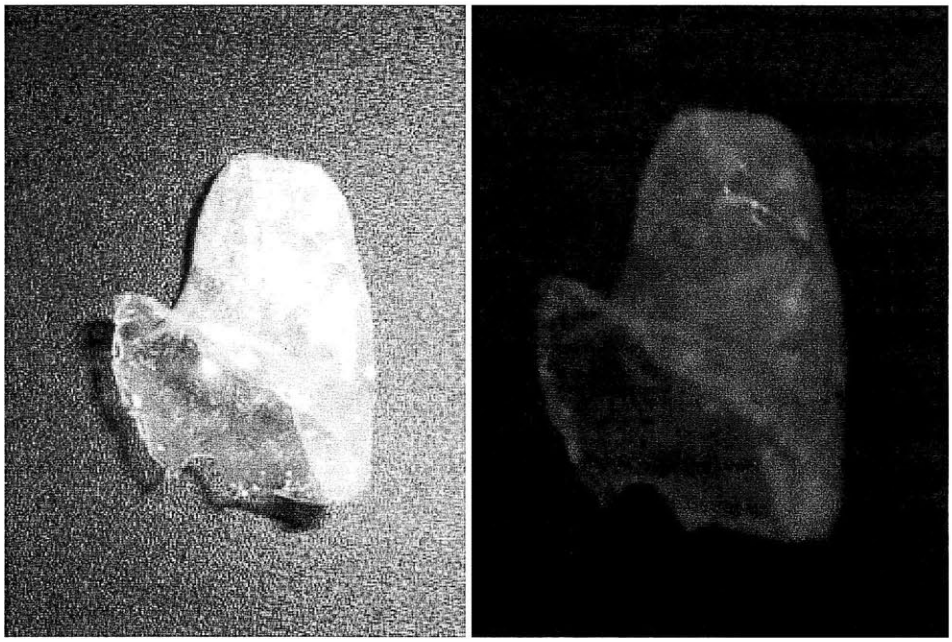

Figure 3.20: Balloon mad with ground up fluorescent paint. Photographed with flash (left), and without flash (right)

These results were quite promising. The ground paint had little effect on the production of the balloons. These results lead to further inquiry into industrial balloon manufacturing techniques, during which it was found that balloons were often colored with pigments rather than dyes. A search for a supplier of fluorescent pigment powder quickly lead to acquiring a selection of finely ground uniform powders. Such powders were available cheaply and could be easily integrated into the existing balloon production framework. A balloon made with orange fluorescent powder is shown below.

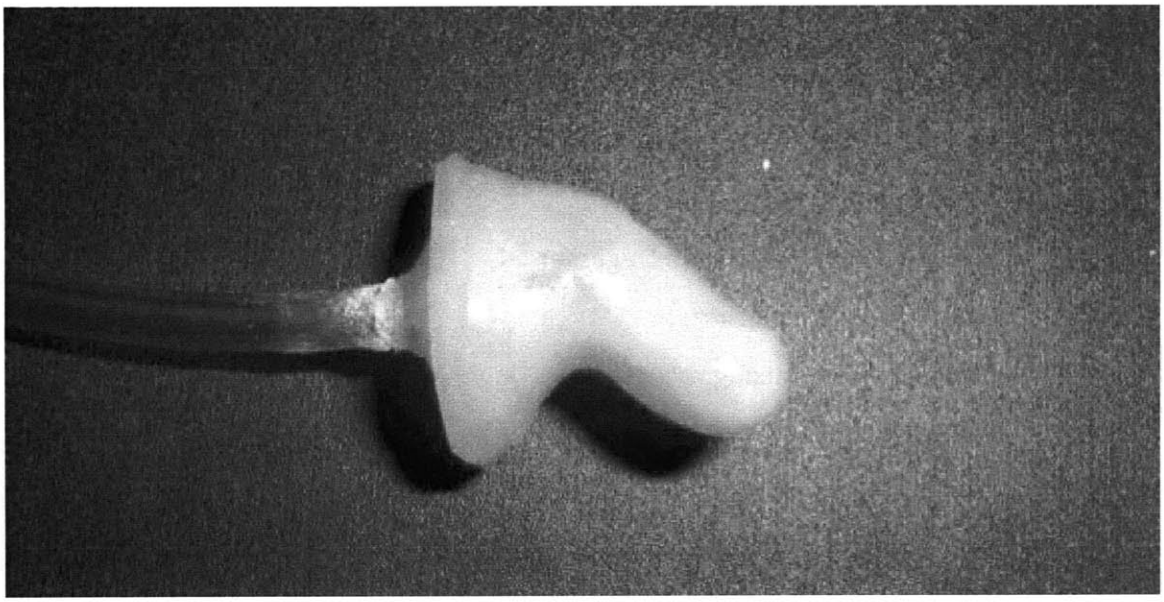

Figure 3.21: Balloon made with fluorescent orange powder.

At first it seemed like this was the final solution to adding fluorescence to the balloon. However, when balloons like this were used for imaging they produced a lot of unexpected noise, because they were self-reabsorbing. Their fluorescent emissions were reabsorbed by neighboring regions leading to cross-talk and noise. The self reabsorbtion made uniformity of balloon thickness very critical from an optical standpoint. The tolerances necessary for surface conformity were much easier to attain in the laboratory. To solve this final problem, a more expensive well behaved fluorescent powder was used, Coumarin 153. With the techniques described earlier and this powder, the problem of adding fluorescence to the balloon was solved.

3.7 Step by Step Procedures

A system by which acceptable quality balloons could be manufactured in the laboratory was developed. In order that others may be able to do the same a list of the procedure used to manufacture the balloons is given below.

Supplies and Equipment needed:

1. Polytek 74-30 Urethane Rubber two part mixture
2. Mold Release
3. Vacuum Oven or Vacuum Degasser
4. Small flat paint brush
5. Plastic or glass mixing receptacle
6. Balloon Mold
7. Work area where balloons can be hung to dry
8. Flat glass sheet, slide, or dish
9. Gloves

Figure 3.22: Equipment needed.

Steps for making multi layer balloon with plastic base:

Painting the First Coat

1. Prepare all molds by cleaning and spraying with mold release.
2. Mix equal parts 74-30 Polytek Urethane Rubber in plastic or glass receptacle. Do not fill above 20% the height of the container to allow for expansion during the vacuum oven. Add fluorescent pigment if desired.
3. Use vacuum oven or degasser to subject mixture to 29 in Hg
4. Cycle between 25 and 29 in Hg two additional times, and remove mixture from vacuum oven after 15 total minutes.
5. Use spoon to scoop off top of mix where remaining air bubbles are.
6. Paint mixture on evenly with paint brush.
7. Continue to handle mold, moving around making additional brush strokes as necessary for the next 15 minutes until right before mixture becomes tacky and stroke do more harm than good. Can test tackiness of mixture still in receptacle.
8. Hang up to dry. If possible to flip vertically after 15 minutes.

Adding a base layer of urethane

9. Add an additional layer repeat steps 2-8.
10. After two layers have been made, remove balloon carefully from mold. Cut to desired shape.
11. Repeat steps 2-5 to prepare another batch of urethane.
12. Spray glass sheet, slide, or dish with urethane.
13. Paint urethane layer on glass.
14. Paint thin urethane layer on balloon

15. Stick balloon into urethane layer on glass
16. Allow to dry
17. Remove balloon from glass slide and clean off mold release

Adding a rigid plastic base and ports

18. Prepare rigid plastic base by tracing balloon base on it, cutting, and punching holes for ports.
19. Use cyanoacrylate based glue to attach rigid plastic base to balloon base
20. Poke holes in urethane and put in tubing where desired.
21. Slide tubing in and make seal with glue.
22. Allow to dry
23. Repeat steps 2-8 to finish balloon.

4. Compliance

Compliance is a critical factor in hearing aid fit that is the entirely left out of the current impression methodology. In order for a hearing aid to fit comfortably the amount of pressure it is exuding needs to be appropriate in all the areas in which it makes contact with the ear. A simple over sizing of the hearing aid will only satisfy some subset of people's who by chance have ears suited to the current method.

The compliance of the ear as a mechanical system is pretty complex. It is made up of bones, cartilage, and skin, assembled into a compound system. Each ear is unique in its shape and the properties of its components. The 3-D compliance of the ear, which is the eventual goal of this work, can be forwarded by a simpler measurement, the bulk compliance. In order to inform the data from bulk compliance measurements, a simple model for the compliance of an ear is needed, to give some basis of comparison to existing data. This model is developed in the next section.

4.1 Infinite Cylinder of Skin Model of the Ear

A mechanical model of the ear as a compound system made up of bones, cartilage, and skin is too complex to be fitted to data from bulk compliance measurements. It might be reasonable to make such a model with 3-D compliance measurements, or bulk compliance measurements aided by X-rays or MRI's. A company using 3-D compliance measurements to manufacture hearing aids would certainly need a model that takes into account the three different tissues. For the purpose of comparing bulk compliance measurements to existing measurements there will be no knowledge of the boundaries or relative composition of the different tissues. These characteristics are unique for

each ear. Therefore the ear will be modeled as one tissue, the one that is the most compliant and therefore is responsible for much of the ear's compliance, skin. The skin's mechanical behavior has been measured in vivo in the medical literature. These properties can be used later on to validate the bulk compliance measurements.

Now that the model of the ear has been simplified from three materials to one, an appropriate geometry must be chosen. An ear canal varies in cross section, is asymmetric, and has bends. Figure 4.1 shows an ear, including the ear canal very clearly, and it can be seen that if the canal needs to be modeled as a simple shape it is most similar to a cylinder.

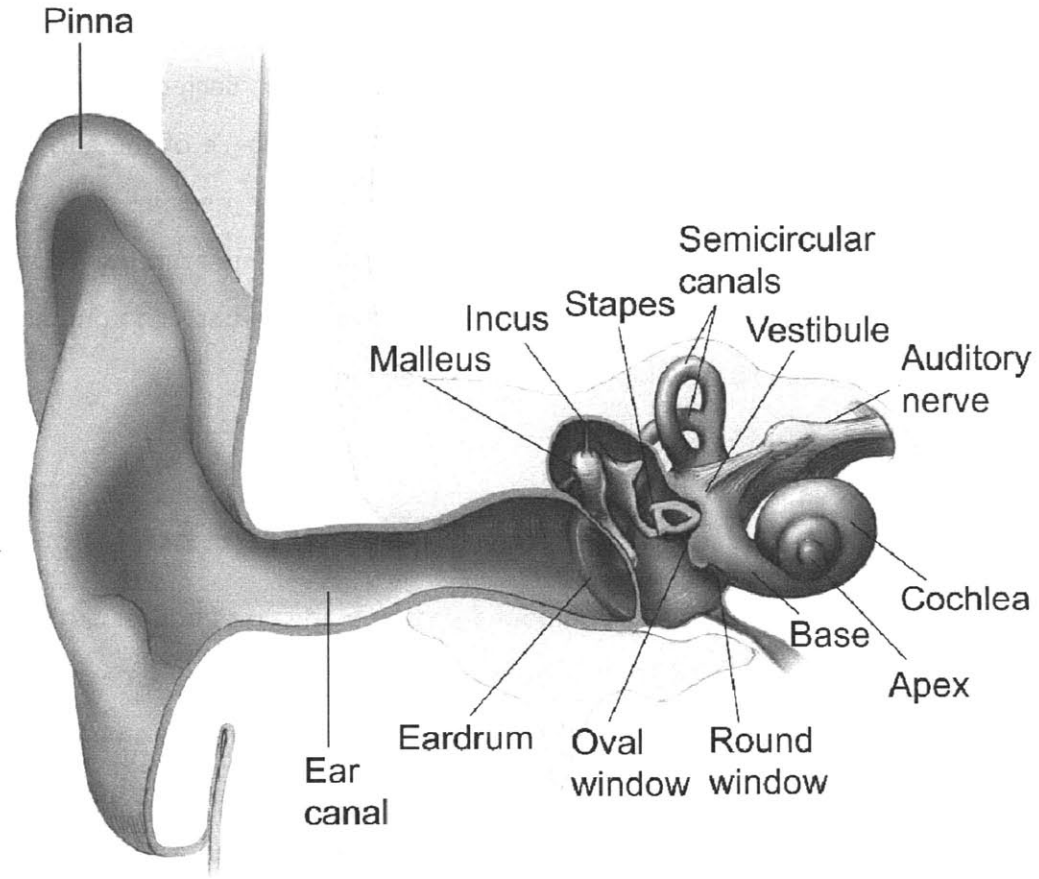

Figure 4.1: Diagram of ear, taken from NIDCD fact sheet [5]. It can be seen that the ear canal is approximately cylindrical.

The last simplification to be made to complete are model is in dimensioning this cylinder. The thickness of it will change the expected compliance dramatically if small. However, as the thickness of the cylinder grows the changes in compliance will become smaller and smaller. It will be shown that a cylinder of a couple inches of skin behaves almost as an infinite cylinder of skin.

The equations for a thick-walled cylinder are well understood and will be developed as presented in Ugarul's Advanced Strength and Applied Elasticity [42]. A differential element in an axisymmetric coordinate system shown in figure 4.2

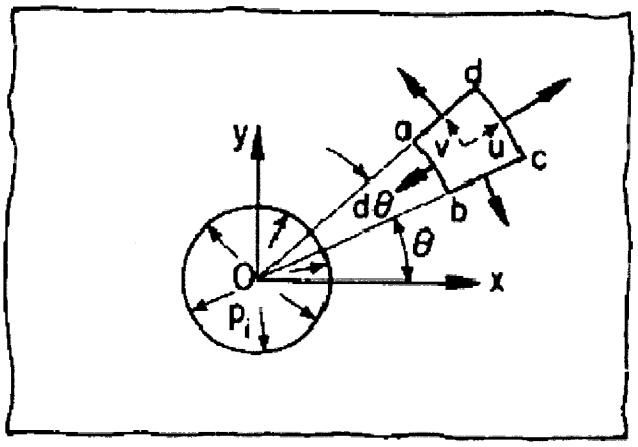

Figure 4.2: Differential element in an axisymmetric coordinate system.

In this polar coordinate system in the absence of axial loading ($\sigma_z=0$), and body forces the equation of equilibrium, given by stresses σ_r and σ_ϑ.

$$\frac{d\sigma_r}{dr} + \frac{\sigma_r - \sigma_\theta}{r} = 0, \tag{11}$$

In this equation it is also assumed that the shearing stress, $\tau_{\vartheta r}$, must be zero by symmetry arguments. There will be radial displacement, u, caused by the internal pressure, and there can be no tangential displacement, v, again because of symmetry. Taking into account the behavior of both displacements the strains of interest are given by

$$\varepsilon_r = \frac{du}{dr}, \quad \varepsilon_\theta = \frac{u}{r}, \quad \gamma_\theta = 0. \tag{12-14}$$

A compatibility equation can derived by substituting $u=r\varepsilon_\vartheta$, into equation 12

$$\frac{du}{dr} - \varepsilon_r = \frac{d}{dr}(r\,\varepsilon_\theta) - \varepsilon_r = 0. \tag{15}$$

Using the product rule and rearranging the result can be simplified to

$$r\frac{d\varepsilon_\theta}{dr} + \varepsilon_\theta - \varepsilon_r = 0. \tag{16}$$

The last relation needed to constrain the system of equations is given by Hooke's Law,

$$\frac{du}{dr} = \frac{1}{E}(\sigma_r - \nu\sigma_\theta). \tag{17}$$

$$\frac{u}{r} = \frac{1}{E}(\sigma_\theta - \nu\sigma_r). \tag{18}$$

When these equations can be solved for σ_r and σ_ϑ, and the results are substituted into equation (11) the following 2nd order equidimensional differential equation is generated,

$$\frac{d^2u}{dr^2} = \frac{1}{r}\frac{du}{dr} - \frac{u}{r^2}. \tag{19}$$

The general solution to this differential equation is given by

$$u = c_1 r + \frac{c_2}{r}. \tag{19}$$

When the boundary condition of the stress at the inner, *a,* and outer radius, *b,* is equal to the internal, p_i, and external pressure, p_o, respectively is enforced the following expression is the result.

$$u = \frac{1-\nu}{E}\frac{(a^2 p_i - b^2 p_o) r}{(b^2 - a^2)} + \frac{1+\nu}{E}\frac{(p_i - p_o) a^2 b^2}{(b^2 - a^2) r} \quad . \tag{20}$$

This expression was first derived by G. Lamé. For the purposes of this paper this result can be simplified by noting that , $p_o=0$, and that the outer radius approaches infinity.

$$u = \frac{1+\nu}{E}\frac{(p_i - p_o)}{r} \quad . \tag{21}$$

This linear model is of the appropriate complexity given the use it will be put to. The assumption of an infinite outer radius can be justified by investigating stabilization of this formula as the outer radius grows. The graph in figure 4.3 shows the displacement at the site of the inner radius with the following values substituted into equation (20), $r=a=1$, $p_o=0$, $p_i=1$, $E=1$, and $v=1$.

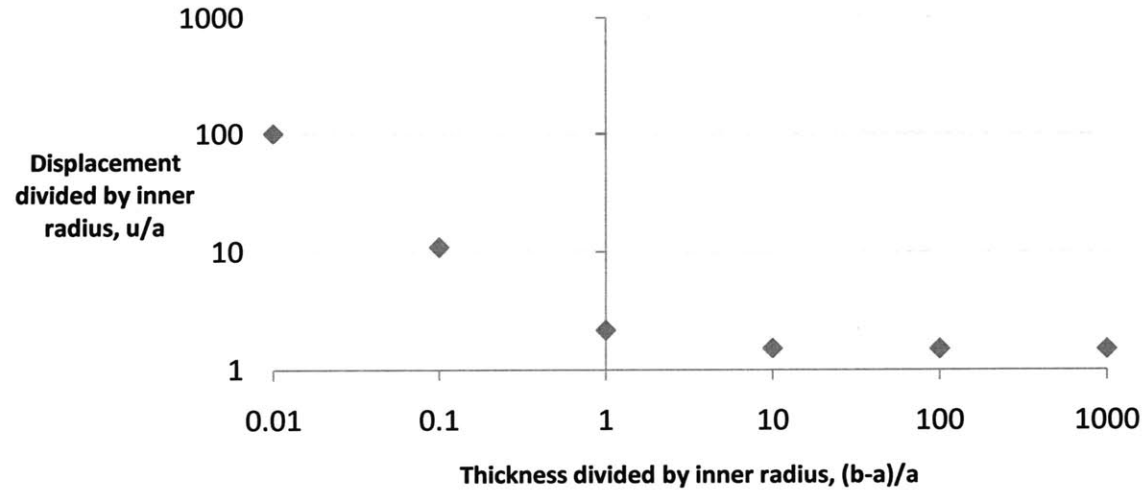

Figure 4.3: Dimensionless graph shows tendency of displacement divided by inner radius to stabilize as ratio of thickness divided by inner radius grows.

When the ratio of thickness over inner radius reaches 10, the infinite cylinder simplification is justified. For example, modeling a 10 mm ear canal as infinite is equivalent to modeling it as 10 cm thick cylinder of skin. The thick walled cylinder model was also used to evaluate some preliminary data in which balloons were used to measure the young's modulus of latex tubing, which is the subject of the next section.

4.2 Early Latex Cylinder Compliance Data and Modeling

In order to validate the technique of inflating a balloon inside of an object to measure its compliance, the compliance of a similar, simple object with known properties, latex tubing will be measured. If a reasonable measurement of the young's modulus of the tubing can made, the ear data can be treated with more confidence. The same thick-walled cylinder model shown in equation (20) initially developed for the ear canal can be used to predict theoretically how much volume the tube will expand at a given pressure.

A latex tube sleeve the length of a balloon was cut. The balloon was put inside the sleeve and inflated with water while measuring the pressure. An image of the balloon inside the sleeve is shown in figure 4.4.

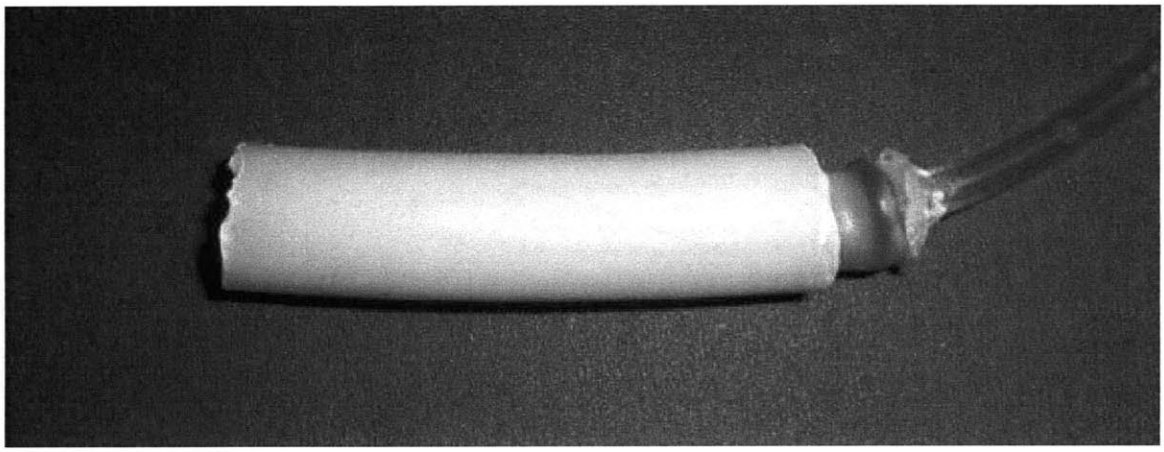

Figure 4.4: Balloon inside of latex tubing sleeve.

The balloons used for this experiment were longer than the ear canal. In these measurements this extra length would improve the data. The compliance of the balloon and sleeve, which is expected to be less than the compliance of either individually, was treated with the following model.

$$\frac{1}{C_{total}} = \frac{1}{C_{sleeve}} + \frac{1}{C_{balloon}}. \tag{22}$$

This model assumes that the volume increase in the balloon and the sleeve is equal. One of the inaccuracies of this model was that there is a cap at the end of the balloon that can expand without interference from the sleeve. That inaccuracy is mitigated later on in the ear compliance measurements, but not in these measurements. The theoretical compliance of the sleeve was calculated by utilizing measurements of its geometry, Durometer, and the model in equation (20). The Durometer needed to be converted to a Young's modulus, which was done by making use of a table in Gent's

"Engineering with Rubber" [42]. The compliance model for the latex sleeve is linear as shown in the figure 4.5.

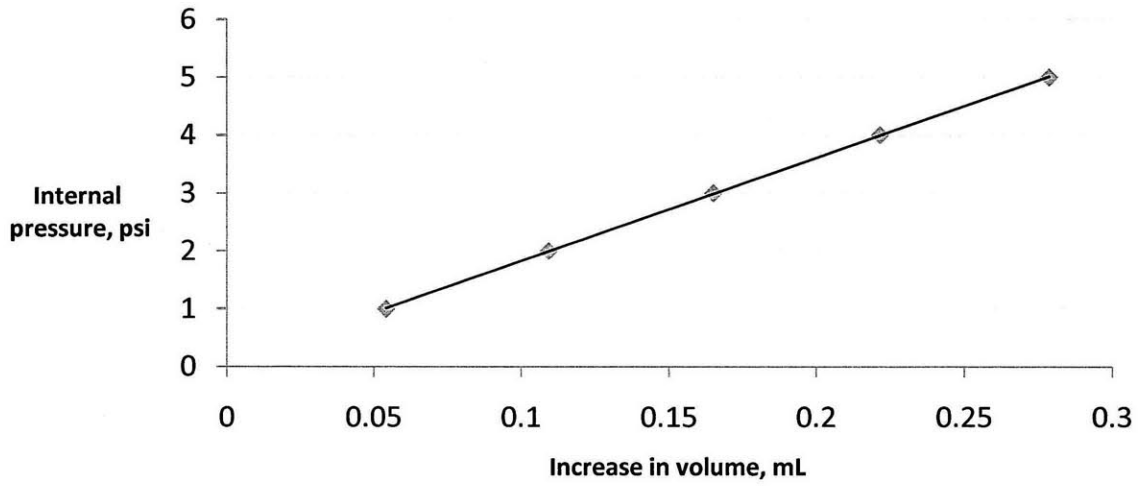

Figure 4.5: Modeled compliance of latex sleeve. Model is very linear over range of interest.

The model is very linear over this region. However, it is linear in displacement not volume, so over a large displacement more non linear behavior would be expected. The compliance of the balloon and the balloon in the latex sleeve is also very linear in the region of interest, as shown in figure 4.6.

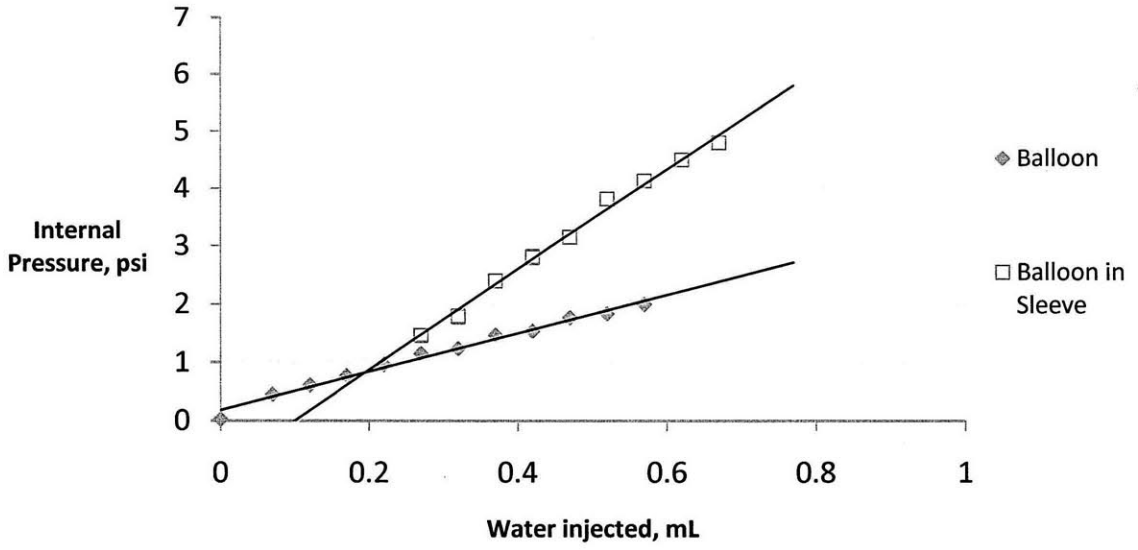

Figure 4.6: Compliance graphs for balloon in free expansion and constrained by latex sleeve.

The slope changes abruptly when the balloon comes in contact with the sleeve, which along with the linearity was encouraging. However, the compliance of the sleeve that the model gives for these measurements (0.12 psi/mL) was significantly higher than the theoretical (.047 psi/mL). It was hypothesized that this difference was from areas of the balloon that were allowed to freely expand. In order to test this hypothesis two other experiments were done where the balloon was inflated inside of a steel tube and inside of a latex sleeve with a hard stop at the end.

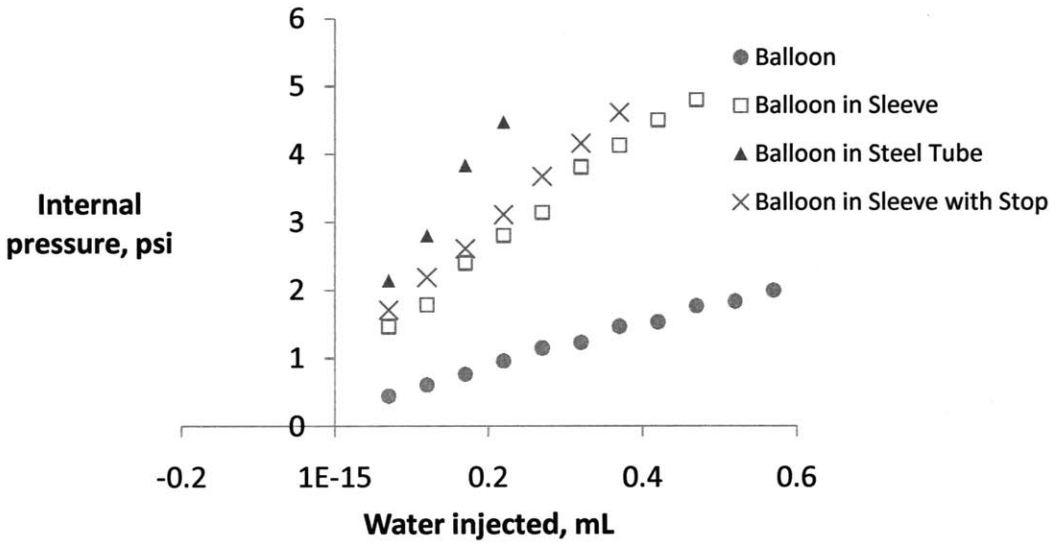

Figure 4.7: Compliance graphs for balloon in free expansion and constrained by steel tube

The compliance of the balloon inside the steel tube was not negligible (.066 mL/psi). The hard stop had a small effect on the compliance .12 versus .11 ml/psi. The compliance of the balloon cap was on the order of the compliance of latex tubing. To successfully measure the compliance of the ear, this effect must be controlled for data taken in the ear.

4.3 Compliance Experimental Setup

The experimental setup used for measuring the bulk compliance of the ear was very simple. The apparatus consisted of an ear-shaped balloon that could be filled with water by a syringe connected to a pressure sensor. This setup in a model ear is shown in figure 4.8.

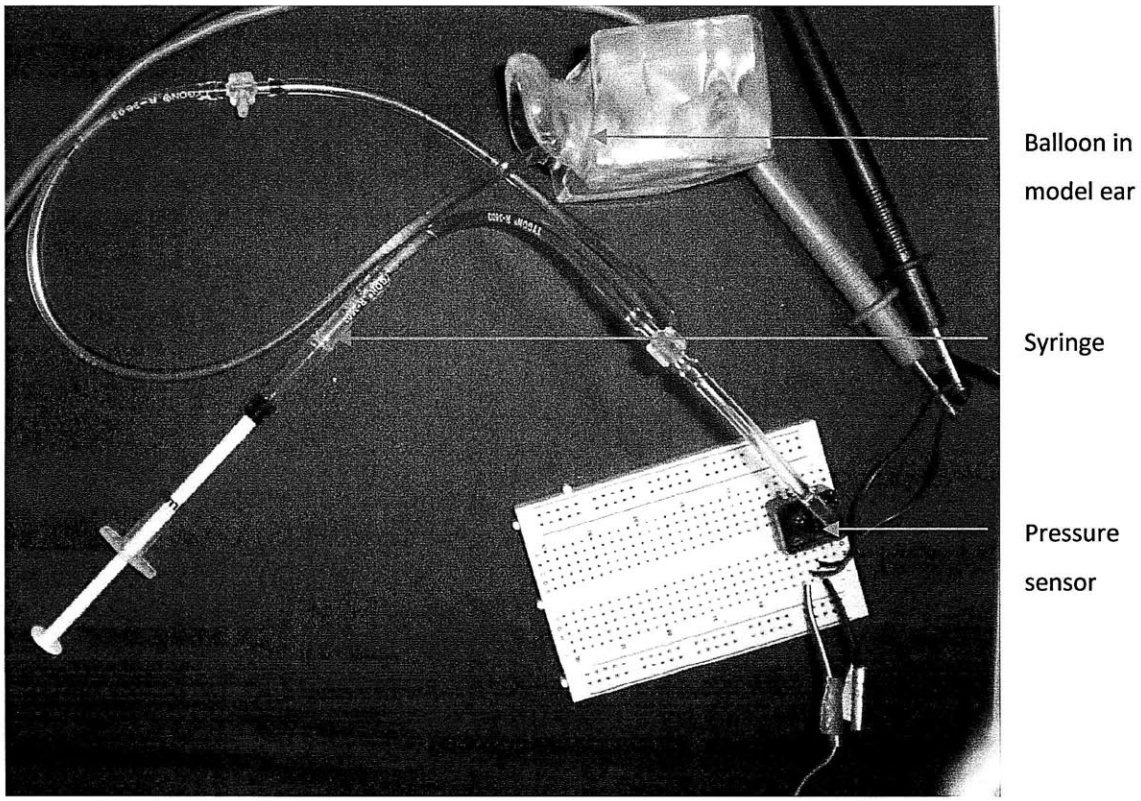

Figure 4.8: Bulk compliance measurement experimental setup. The balloon, model ear, syringe, and pressure sensor are labeled above. The multimeter and power supply are not shown.

The balloon needed to be modified in order to be used to measure bulk compliance. As noted in section 4.2 the free expansion of the cap can add an undesired compliance into the system. In order to eliminate this compliance a layer of cyanoacrylate was deposited between layers of urethane in the cap of the balloon. A balloon with this feature as well as a hard plastic base is shown in figure 4.9

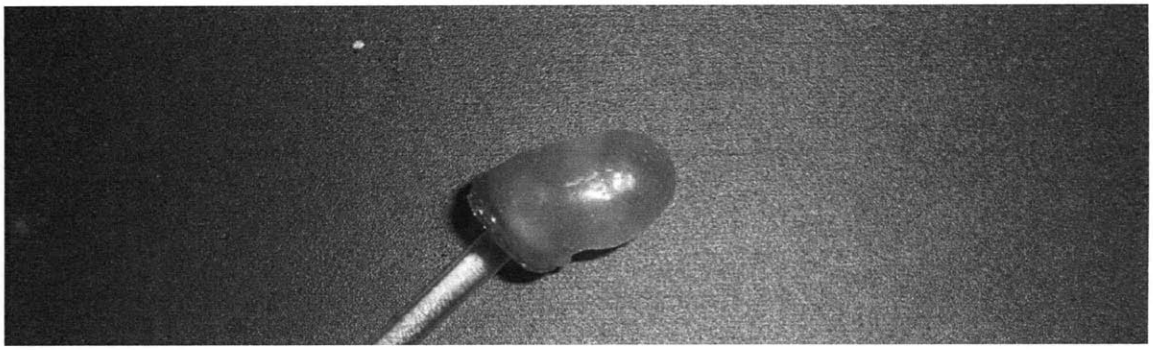

Figure 4.9: Balloon with hard plastic base and cap.

This simple modification in conjunction with a rigid plastic base eliminates areas of the balloon that can freely expand, improving the measurement of the compliance of the ear.

A simple but difficult problem that arose when assembling the system was the need to eliminate air bubbles. Air bubbles would add an additional undesired compliance and a safety concern. The highest pressure the balloon needs to be inflated to 4psi is less than the pressure an ear is exposed to 10 ft underneath the surface of a pool. Even if the balloon were to burst, the water could only store very little energy. Air on the other hand would store a significant amount of energy and could create unsafe pressures in the ear if the balloon popped. Air bubbles were present in the syringe, pressure sensor, the balloon. Each of these components required a unique solution in order to remove the air bubbles.

The air bubble in the syringe was the first dealt with and most easily eliminated. The setup for eliminating this air bubble is shown in figure 4.10.

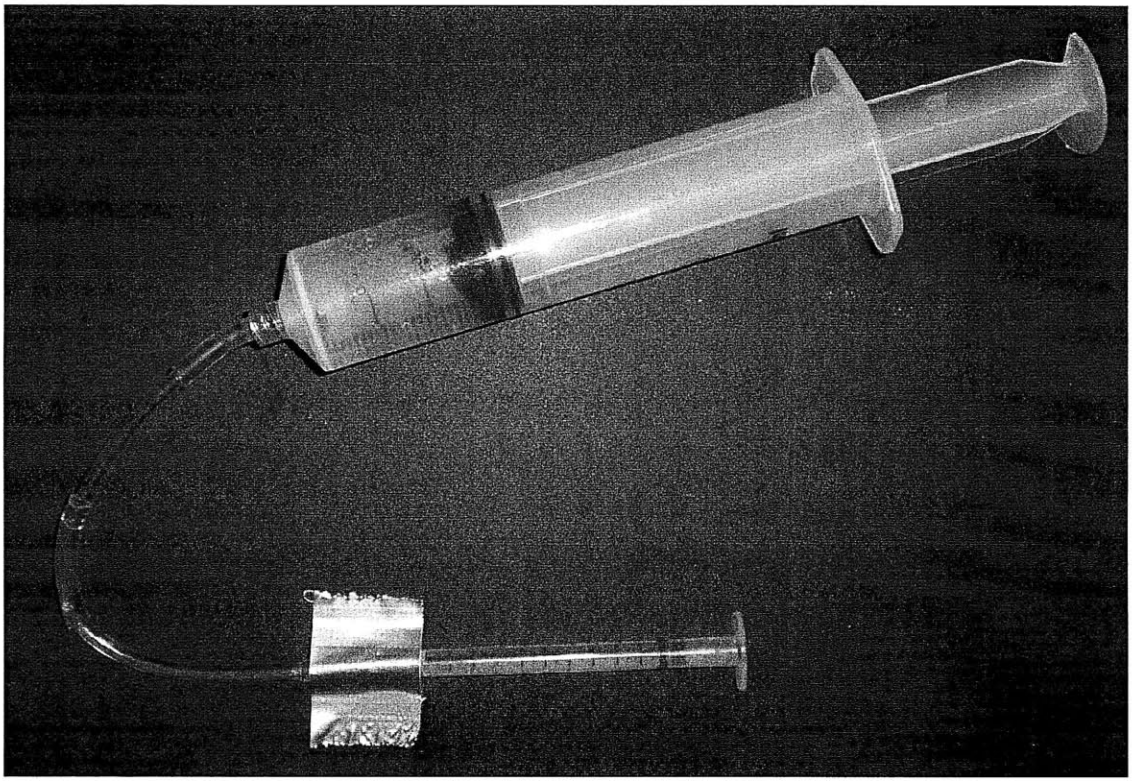

Figure 4.10: Large syringe is used to fill the small syringe to eliminate air bubbles.

The plunger of the syringe to be used was removed, and another larger syringe was used to fill the experimental syringe up, after which the plunger was replaced.

The air bubble in the balloon was also eliminated by making use of a syringe. A syringe with a long thin tube was used to fill the balloon, so that a coaxial flow could be established. The setup for eliminating this air bubble is shown in figure 4.11.

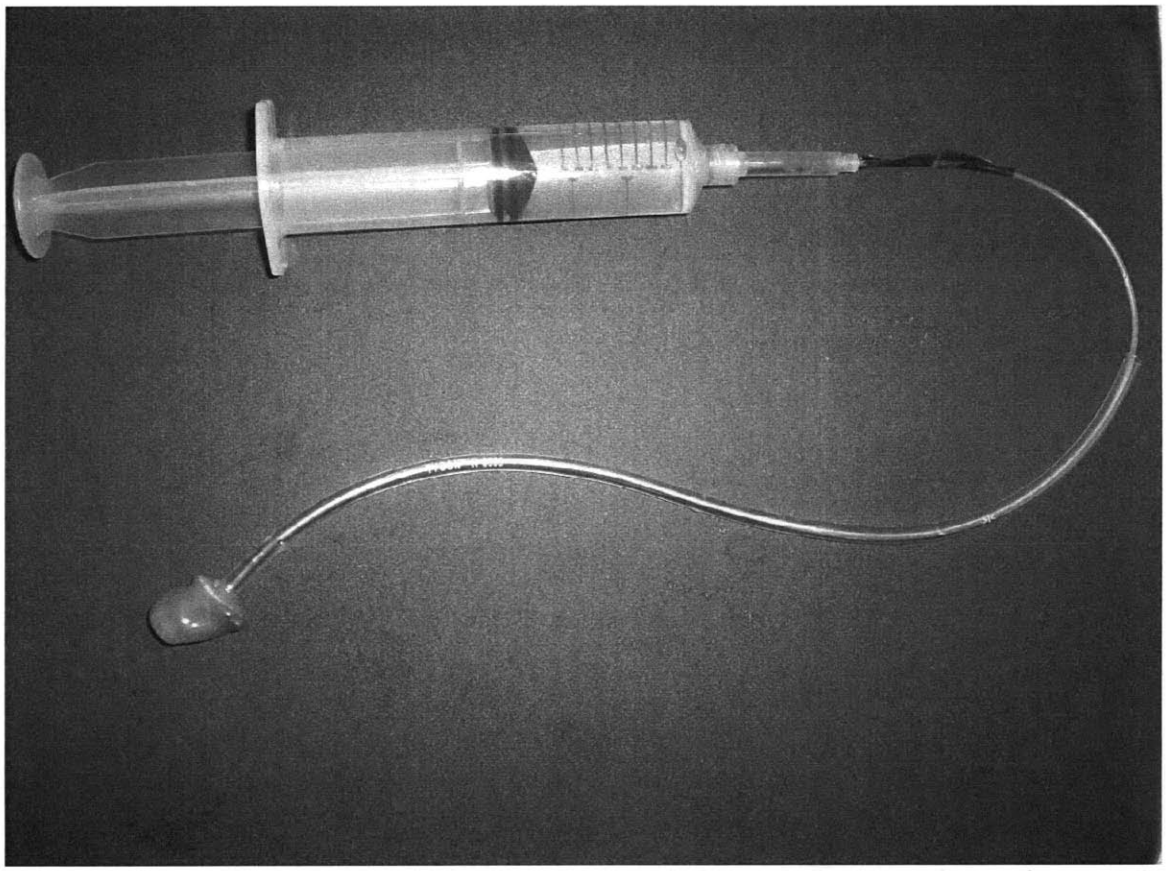

Figure 4.11: Large syringe with long probe tube is used to fill the balloon in order to eliminate air bubbles.

Water can flow into the balloon through the center channel and push the air through the outer channel. To further eliminate bubbles the balloon was compressed and then filled back up slowly with the syringe.

Finally the bubble in the pressure sensor needed to be eliminated. This bubble required a different approach because it was actually protecting the sensor from water which is conductive enough to short circuit a capacitive pressure sensor. A non conductive incompressible fluid bubble was needed to replace the air bubble. For this need a 10 cst silicone oil was used. This silicone oil was inserted into the pressure sensor with a syringe. In the next section that data generated with this approach is presented.

4.4 Compliance and Jaw Movement Data

The first compliance data is taken with a balloon without a hard cap. Three runs were taken inside and outside of a human ear. The balloon was prevented from moving axially by hand. The rigid plastic base was manually held flat with respect to features of my ear by my thumb and index finger. The pressure volume plot for the data take in vitro for the ear is shown in figure 4.12.

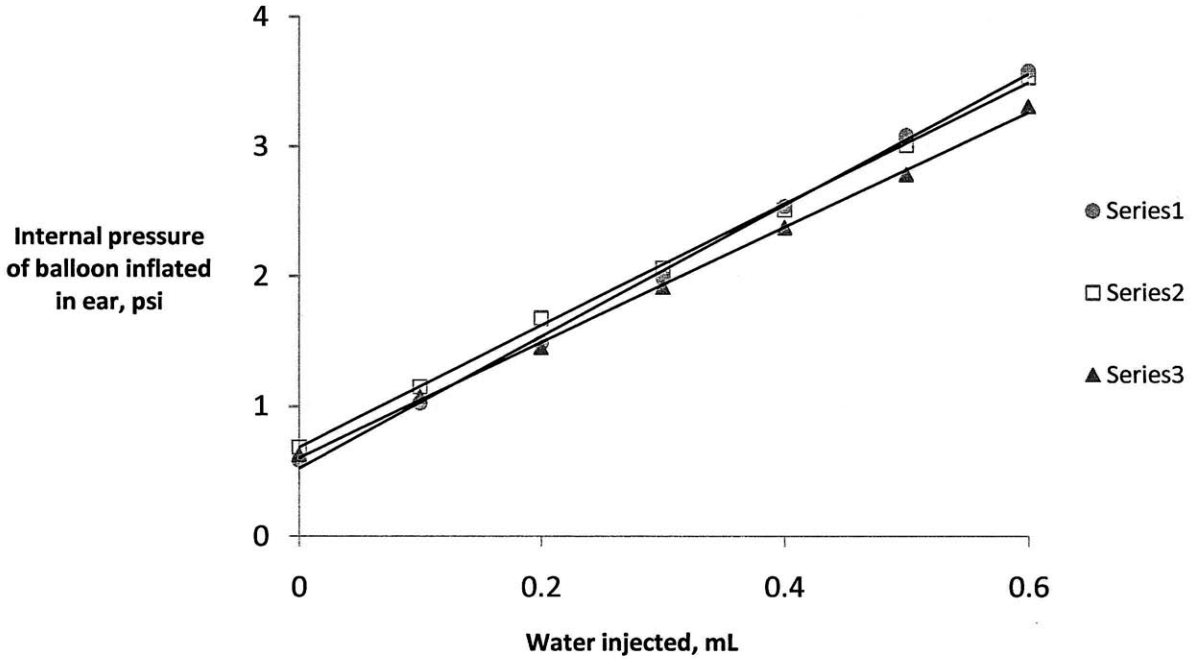

Figure 4.12: Internal pressure plotted as a function of volume of water injected for a balloon without hard cap in ear. (Average slope 4.73 psi/mL)

The data is very repeatable and linear, as is the data for the balloon inflated outside of the ear shown in figure 4.13.

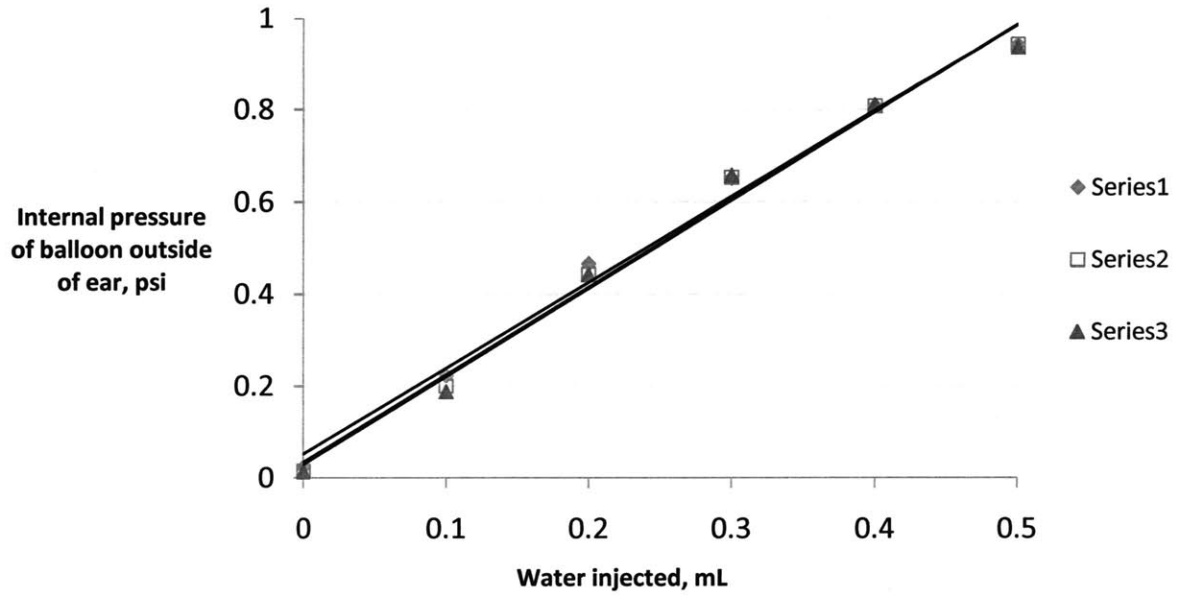

Figure 4.13: Internal pressure plotted as a function of volume of water injected for a balloon without hard cap outside of ear. (Average slope 1.9 psi/mL)

Equation (22) was used to calculate the compliance of the ear as 0.35 mL/psi. It was suspected that significant error was introduced by the unrestricted expansion of the cap of the balloon. In order to investigate the significance of this extra compliance, another set of tests was done with a balloon that had a layer cyanoacrylate between two layers of urethane.

Another modification needed to be made to the experimental procedure in order to take the next generation of data. One issue with taking the first set of measurements was popped balloons. The balloons took a long time to make, and could easily pop at pressures between 2.5 and 4 psi when repeatedly loaded. In order to ensure balloons were not popped as often in future experiments in which a lower compliance was expected the water was injected in .05 mL increments instead of .1 mL increments and the number of data points was reduced to 5 from 6. This kept the maximum pressure in near 2.7 psi. The same data for the tests with the improved balloon and procedure is shown in figure 4.14 below.

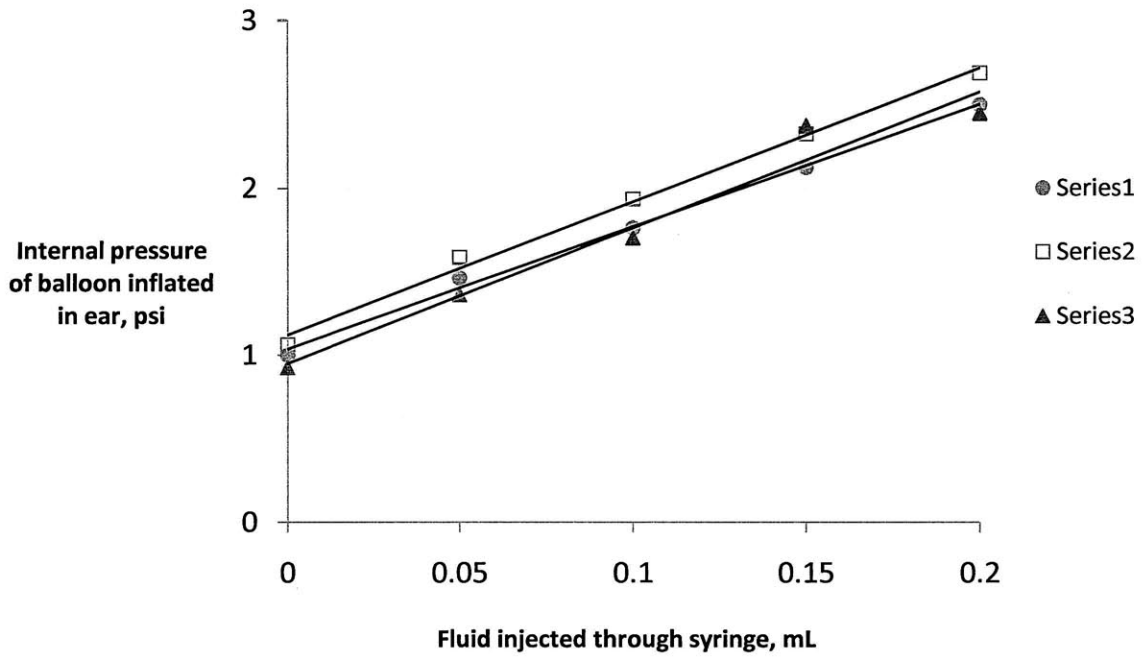

Figure 4.14: Internal pressure plotted as a function of volume of water injected for a balloon with a hard cap in ear. (Average slope 7.8 psi/mL)

Again both the in and out of ear data is very repeatable and linear. And the hard cap decreased the compliance measured of both data sets as expected. The out of ear data is shown in figure 4.15 below.

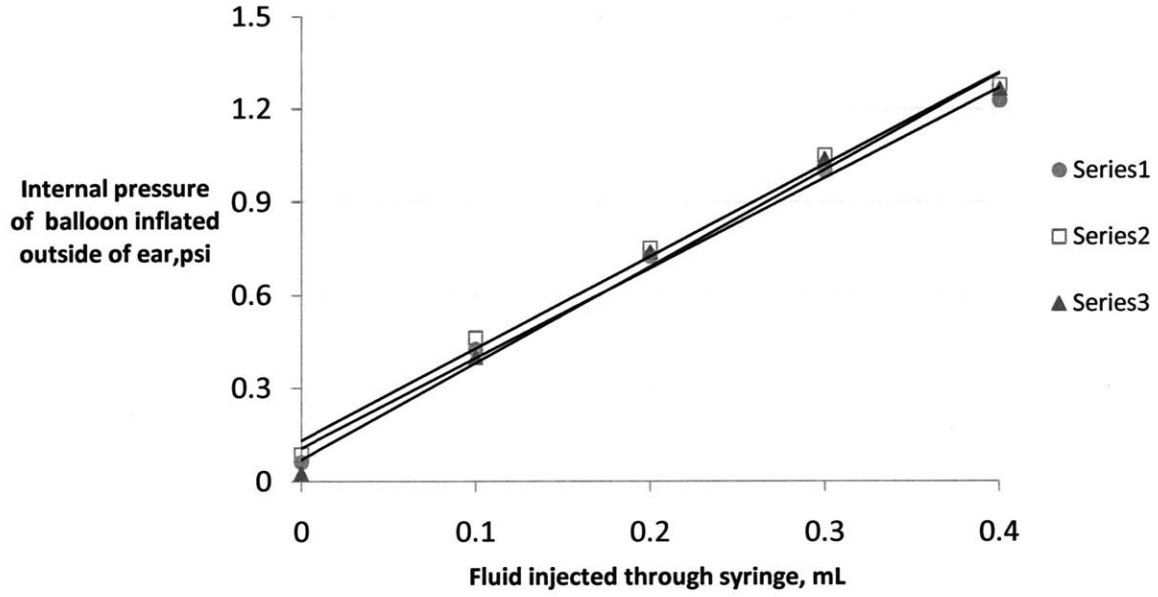

Figure 4.15: Internal pressure plotted as a function of volume of water injected for a balloon with hard cap outside of ear. (Average slope 3.0 psi/mL)

Equation (22) was used to calculate the compliance of the ear as 0.21 mL/psi. The expectation that significant compliance was introduced by the unrestricted expansion of the cap of the balloon proved true.

A final set of data that was gathered was the change in pressure when the jaw was closed from an open position at a starting pressure of 1.875 psi. For the balloon with and without a hard cap an average drop of 0.175 and 0.225 psi respectively was seen for five data points. These values for pressure translate into 0.22 and 0.52 mL. Given Pirazanski's data [16], it is expected that the TMJ associated change in canal shape would vary widely between individuals. In the next section the data will be non-dimensionalized and compared to literature values.

4.5 Non-Dimensionalization and Comparison to Existing Data

In order to compare the compliance measurements to literature values a model of the ear as thick walled cylinder of skin developed in section 4.1 is used. Using this model the compliance measurement can be used to calculate a Young's modulus. The data for the balloon with and without a hard cap gave a value for 0.88 and 0.53 MPa, respectively, for the young's modulus of skin. Diridollou [43] compiled a table of values in shown in figure 4.16.

Reference	Sites	Order of magnitude (MPa)	Device
Grahame & Holt (1969) [20]	Forearm	18–57	Suction
Sanders (1973) [41]	Dorsal side forearm	0.1–0.02	Torsion
Alexander & Cook (1976) [23]	Upper back–male	140–180	Suction
	Upper back–female	180–200	Suction
	Forearm male	320–420	Suction
	Forearm–female	520–540	Suction
Agache *et al.* (1980)	Dorsal site of the		
Lévêque *et al.* (1980, 1984) [25–27]	forearm	0.42–0.85	Torsion
Escoffier (1989) [28]	Forearm anterior		
Barel *et al.* (1998) [35]	part	1.1–1.32	Torsion
	Forearm–male	0.14	Suction
	Forearm–female	0.16	Suction
	Forehead–male	0.23	Suction
	Forehead–female	0.27	Suction
Agache (1992); Panisset	Forearm anterior		
(1992) [39, 40]	part	0.25	Suction
Our study	Forearm–male	0.11	Suction
	Forearm–female	0.12	Suction
	Forehead–male	0.21	Suction
	Forehead–female	0.25	Suction

Figure 4.16: Table of Young's modulus taken from Diridollou's paper [43].

The values for Young's modulus for skin in the literature vary by a couple of orders of magnitude from 0.1 to 540 MPa, depending on type of test and test location. The older values are much higher than recent values taken with improved techniques. Diridollou's data is shown in figure 4.17 below.

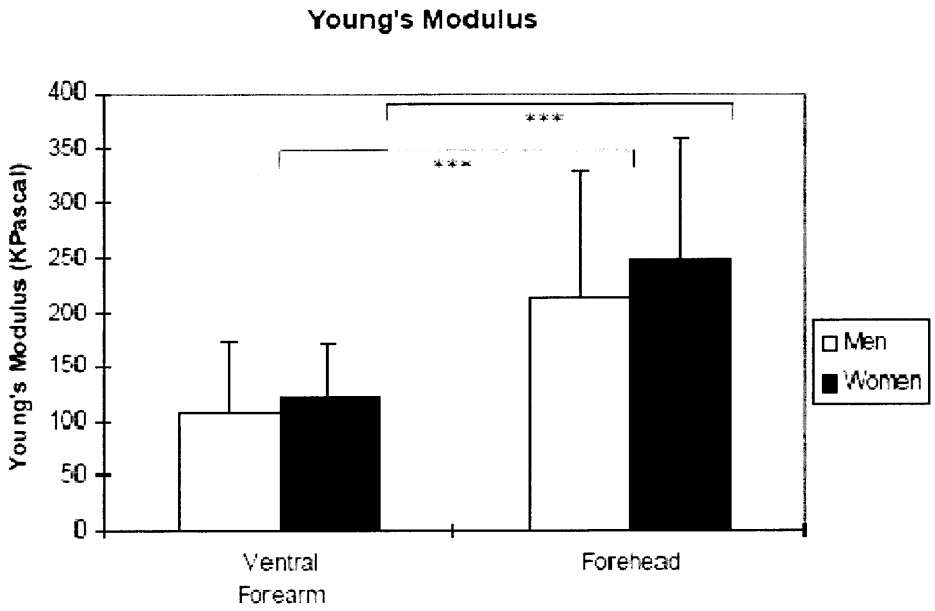

Figure 4.17: Data from Diridollou's paper on young's modulus of skin for men and women with standard deviation shown by error bar taken [43].

Given the approximate nature of the model used to calculate the Young's modulus for the ear from the compliance data and the variation in the literature value for the Young's modulus of skin, value of 0.88 MPa is very reasonable.

Another way to non-dimensionalize the compliance that does not rely on the assumption of a thick walled cylinder of skin, would be to make a lesser assumption that the compliance is proportional to surface area. This approach does not generate values that can be compared to the literature, but may form a basis of comparison for 3-D compliance imaging and other methods. The calculated bulk compliances divided by an approximate surface area for the ear with and without a hard cap are 0.82 and 1.4 mm/psi respectively.

5. Summary and Conclusions

5.1 Accomplishments

The problems with impression based hearing aids have been presented. In particular, the inability of current methods to routinely manufacture hearing aid shells that are comfortable and perform well have been investigated. Specifically, attention is paid to the inability of current methodology to take compliance and jaw movement into account.

A potential cost effective technique for scanning the ear canal, absorption based imaging has been presented. A one dimensional calibration was made, and qualitative 3-D data is shown. The imaging technique was implemented with much lower cost equipment then would be needed by other 3-D techniques such as interferometry.

A stitching simulation was done to show that stitching together six to ten 3-D models of the ear was well within the ability of current methodology. A technique for the laboratory manufacture of brushed on fluorescent balloons was presented that are suitable to be used by this imaging technique to measure the dynamics of the ear. The bulk compliance of a human ear in vitro was measured with a laboratory fabricated balloon.

5.2 Future Work

An FDA approved fluorescent urethane mixture was fabricated in a laboratory setting. For a consumer product the material would need to be used in an industrial setting and approved by the FDA. It has been shown that a simple 3-D shape can be measured with

this technique but for final product the imaging technique needs to establish that it can capture a complex 3-D canal geometry in a balloon.

The largest uncertainty that has not been dealt with is taking the dynamic data from ears and translating it into an improved hearing aid. Eventually this data needs to be taken in a trial of 5 to 50 people to show that this additional information can be used to improve hearing aid fit and performance.

Acknowledgements

First I would like to thank Doug for everything. He is a brilliant, kind, supportive advisor. I would also like to thank Davide, Federico, Sean, and Wenxian. They have been a pleasure to work with. I'd also like to thank my family, Emily, Jaime, and Jacob for supporting me when I needed it. Finally I'd like to thank the Deshpandhe Center for funding my work.

References

[1] U.S. DEPARTMENT OF HEALTH AND HUMAN SERVICES, Centers for Disease Control and Prevention, and National Center for Health Statistics: "Summary Health Statistics for U.S. Adults: National Health Interview Survey, 2008." DHHS Publication No. (PHS) 2010-1570, Series 10, No. 242 Provisional Report 8/2009. Hyattsville, Maryland.

[2] Fabry, D., 2002, "Hearing aid physical fit: The next revolution?" Hear J., 55(8) pp 46-50.

[3] Kirkwood, D. H., 2003, "The bright promise of direct ear scanning" Hear J., 56(9) pp 4.

[4] Kochkin, S., 2003, "MarkeTrak V: "Why hearing aids are in the drawer": The consumers' perspective" Hear J., 53(2) pp 34-41.

[5] U.S. DEPARTMENT OF HEALTH AND HUMAN SERVICES, National Institutes of Health, National Institute on Deafness and Other Communication Disorders: "NIDCD Fact Sheet Noise-Induced Hearing Loss" Publication No. 08-4233, Updated December 2008, Bethesda, MD

[6] Kirkwood, D. H., 2008, "Economic turmoil threatens to reverse recent growth in the hearing aid market " Hear J., 61(12) pp 9-12.

[7] Kochkin, S., 2005, "MarkeTrak VII: Hearing Loss Population Tops 31 Million" Hear R., 07/1/2005.

[8] National Institutes of Health, National Institute on Deafness and Other Communication Disorders: "Hearing Aids" NIH Pub. No. 99-4340, updated April 2007. Hyattsville, Maryland.

[9] Strom, K. E., 2005, "The HR 2005 Dispenser Survey " Hear Rev., 06/01/2005.

[10] Johnson et al, 2005, "The "Hearing Aid Effect" 2005: A Rigorous Test of the Visibility of New Hearing Aid Styles" Hear J., 14 pp 169-175.

[11] Johnson, E. E., 2008 , "Practitioners give high marks for user benefit to open-canal mini-BTEs " Hear J., 61(3) pp 19-28.

[12] Johnson, E. E., 2008, "Despite having more advanced features, hearing aids hold line on retail price " Hear J., 61(4) pp 42-48.

[13] Richard Corte et all, "Changing with the Times: Applying Digital Technology to Hearing Aid Shell Manufacturing. " Hear Rev., 03/03/2006

[14] Stuart et all, 1999 , "The effect of venting on in-the-ear, in-the-canal, and completely in-the-canal hearing aid shell frequency responses: real-ear measures." Journal of Speech, Language, and Hearing Research, 42(4) pp 804-813.

[15] Sullivan R. F., 2007, "Scan/print vs. invest/pour shell-making technologies for CIC hearing aid fittings" Hear J., 60(2) pp 21-28.

[16] Pirzanski C. et all, . F., 2005, "Ear canal dynamics: Facts versus perception" Hear J., 58(10) pp 21-28.

[17] Smith et all, "Study finds compliant eartips can be used instead of custom earmolds" Hear J., 61(2) pp 27-36

[18] Lanman, Douglas; Taubin, Gabriel "Build Your Own 3-D Scanner: 3D Photography for Beginners" SIGGRAPH 2009 Course Notes, August 2009.

[19] Blais, Francois, 2004, "Review of 20 years of range sensor development" J. Electron. Imaging, Vol. 13, 231

[20] Chen et all, 2000, "Overview of three-dimensional shape measurement using optical methods" Opt. Eng. Vol. 39 pp. 10-22

[21] Scharstein, Daniel; Szeliski, Richard, 2002, "A Taxonomy and Evaluation of Dense Two-Frame Stereo Correspondence Algorithms" International Journal of Computer Vision, Volume 47 pp. 7-42.

[22] Yang et all, 2004, "Improved Real-Time Stereo on Commodity Graphics Hardware" Computer Vision and Pattern Recognition Workshop.

[23] Salvi et all, 2003, "Pattern codification strategies in structured light systems" Pattern Recognition, Vol. 37 pp. 827-849.

[24] Oliveira et all, 1992, "A look at ear canal changes with jaw motion" Ear and Hearing., 13(6) pp 464-466.

[25] Coppeta, J., Rogers, C., 1998, "Dual Emission Laser Induced Fluorescence for Direct Planar Scalar Behavior Measurements" Experiments in Fluids, Volume 25, Issue 1, pp. 1-15.

[26] Ayala, H., Hart, D. P., Yeh, O., Boyce, M. C., 1998, "Wear of Oil Containment Elastomer in Abrasive Slurries" Wear, Volume 220, pp. 9-21.

[27] Joffe, A. Y., Sayenko, V. F., Denisov, N. A., Dets, S. M., Buryi, A. N., 1999, "Early Diagnosis of Gastric Cancer with Laser Induced Fluorescence", Proceedings of SPIE, Volume 3567, pp. 10-17.

[28] Georgiev, N., Alden, M., 1997, "Two-Dimensional Imaging of Flame Species Using Two-Photon Laser-Induced Fluorescence" Applied Spectroscopy, Volume 51 Number 8, pp. 1229-1237.

[29] Kovacs, A., 1995, "Visualization of Fuel-Lubricant on the Cylinder Surface in the Combustion Chamber of SI Engines" Lubrication Science, Volume 7 Number 2, pp.149-162.

[20] Thirouard, B., Hart, D. P., 1998, "Investigation of Oil Transport Mechanisms in the Piston Ring Pack of a Single-Cylinder Diesel Engine, Using Two-Dimensional Laser Induced Fluorescence" SAE Transactions, Journal of Fuels and Lubricants, Volume 107, pp. 2007-2015.

[31] Hidrovo, C., D.P. Hart, "Dual Emission Laser Induced Fluorescence Technique (DELIF) for Oil Film Thickness and Temperature Measurement" ASME/JSME Fluids Engineering Division Summer Meeting, July 23-28, 2000, Boston, MA

[32] Guilbault, G. G., 1990, "Practical Fluorescence" Second Edition, Marcel Dekker, Inc., New York.

[33] Hidrovo, C. H., 2001, "Development of a Fluorescence Based Optical Diagnostics Technique and Investigation of Particle Ingestion and Accumulation in the Contact Region of Rotating Shaft Seals" Ph.D Thesis.

[34] Paul J. Bed, Member, IEEE, and Neil D. McKay, "A Method for Registration of 3-D Shapes" IEEE TRANSACTIONS ON PARERN ANALYSIS AND MACHINE INTELLIGENCE, VOL. 14, NO. 2, FEBRUARY 1992

[35] Advanced Polymers, " Medical Balloons, Compliant" 2007. 10, 26, 2009. http://www.advpoly.com/Products/MedicalBalloons/Compliant.aspx

[36] Shah, Tilak M, "Dip Molding of Polyurethane and Silicone for Latex-Free, Nonallergenic Products" MDDI, April 2001.

[37] Devco Design and Development. 10, 26, 2009. http://www.devco-design.com/bl-mold.htm

[38] Balloon Hq., "How Latex Balloons Are Made: General Overview" 10, 26, 2009 http://www.balloonhq.com/faq/making.html#general

[39] Polytech. 10, 26, 2009 http://www.polytechsynergies.com/dipmachineofferings.html

[40] Freeman Videos, "Vacuum Degassing and Pressurizing" 10, 26, 2009 http://freemanvideos.com/moldmaking/vacuum-degassing.html

[41] SK Fenster; AC Ugural, 1975, Advanced strength and applied elasticity, American Elsevier Pub. C

[42] Gent, Alan N. Engineering with Rubber - How to Design Rubber Components (2nd edition).. Hanser Publishers.

[43] S. Dirridollou et. all "Sex and site-dependent variations in the thickness and mechanical properties of human skin in vivo" International Journal of Cosmetic Science Volume 22 pg 421-435 2000.